# DMP1 REGULATES OSTEOCYTE FUNCTION VIA WNT/B-CATENIN SIGNALING PATHWAY

A Dissertation

by

SHUXIAN LIN

Submitted to the Office of Graduate and Professional Studies of
Texas A&M University
in partial fulfillment of the requirements for the degree of

DOCTOR OF PHILOSOPHY

| | |
|---|---|
| Chair of Committee, | Jian Q. Feng |
| Committee Members, | Paul Dechow |
| | Kathy Svoboda |
| | Chunlin Qin |
| | Fen Wang |
| Head of Department, | Kathy Svoboda |

May 2014

Major Subject: Biomedical Sciences

# ABSTRACT

DMP1, dentin matrix protein 1, was cloned from a rat dentin cDNA library 20 years ago. Initially, this non-collagenous matrix protein was thought to be dentin specific and gained little interest in other scientific communities except the dental research area. Research that identified DMP1 mutations in humans and deletion in mice lead to the discovery of a novel disease: autosomal recessive hypophosphatemic rickets (ARHR). Functional studies reveal that DMP1 is essential for the maturation and functions of osteoblast and osteocyte via two possible mechanisms: 1) as a transcriptional factor that directly regulates osteo-/odonto-specific genes; and 2) as an extracellular matrix (ECM) protein, which controls bone and dentin mineralization. However, both theories appear controversy. Besides, the mechanism by which ARHR patients or *Dmp1*-null mice develop osteomalacia is largely unknown.

In this study, we initially targeted DMP1 either in the nucleus only by replacing the endogenous signal peptide with the NLS signal peptide (named $^{NLS}$DMP1), or targeted it in the ECM by using its own signal secretive peptide with the same recombinant DMP1 protein (named $^{SP}$DMP1). The $^{NLS}$DMP1 transgene, when expressed in the *Dmp1*-null osteoblast and osteocyte *in vivo*, failed to rescue the *Dmp1*-null phenotype, whereas the $^{SP}$DMP1 transgene fully rescued the skeletal abnormalities of *Dmp1*-null mice, indicating that DMP1 functions as an ECM protein *in vivo*.

In a separate research, we revealed an elevated β-catenin expression level in *Dmp1*-KO osteocytes, besides, the targeted expression of β-catenin in the osteocyte recaptured the osteomalacia phenotype, similar to that in *Dmp1*-KO mice. Furthermore, the targeted expression of DKK1 (a potent inhibitor of Wnt/β-catenin) in *Dmp1*-KO osteoblasts by crossing *Dmp1*-KO and 2.3 Col 1-*Dkk1* mice, resulting in consequent blockade of Wnt/β-catenin signaling, significantly improved the rachitic/osteomalacic phenotype. The results of this study will expand our understanding of how the osteocytes regulate bone development and mineralization during the early postnatal period. In addition, this study has clinical relevance, as a high Pi diet alone fails to fully restore the

osteomalacic status in patients, and normalizing the Wnt/β-catenin signaling may benefit these patients.

# DEDICATION

This work was done in God's glory. Thanks God for your bearing my burdens and healing my hearts all the time. Also to my parents who have always given me their love and support throughout my Ph.D. study.

ACKNOWLEDGEMENTS

I would like to thank my committee chair, Dr. Jerry Feng, and this dissertation could not have been written without the mentoring from him. During my Ph.D. program, Dr. Feng not only served as my supervisor, but also set high standards in our lab by being an outstanding scientist who never ends his exploration in this field. I am proud as one of his students, and will take over his spirit and attitude in the scientific study in my whole research life. I would also to convey thanks to Dr. Zhi Chen, who taught me both experimental skills and knowledge of stomatology during my undergraduate period, and helped me to apply for the State Scholarship awarded by China Scholarship Council for Ph.D. training in the USA. Deepest thanks also go to my committee members, Dr. Svoboda, Dr. Dechow, Dr. Qin, and Dr. Wang, for their guidance and support throughout the course of this research. I also want to express the gratitude to Dr. Opperman, Dr. Louis-Bruno and Dr. Groppe who taught me molecular biology of skeletal development. I sincerely thank Dr. Bob Lu, Dr. Hua Zhang, Dr. Qi Zhang for their assistances in both project execution and research analysis. Special thanks also go to my coworkers Ying Liu, Yong Jiang, Zhengguo Cao and Baozhi Yuan.

Last but not the least, I would also like to convey my appreciation to Priscilla Hooks and Gerald Hill for their great help in the animal breeding issue. Thanks also go to my friends and colleagues and the department faculty and staff for making my time at Baylor College of Dentistry, Texas A&M University a great experience. Finally, special thanks to NIH for the support to fund my research.

# NOMENCLATURE

| | |
|---|---|
| ADHR | Autosomal dominant hypophosphatemic rickets |
| ARHR | Autosomal recessive hypophosphatemic rickets |
| ALP | Alkaline phosphatase |
| AB | Alveolar bone |
| APC | Adenomatous polyposis coli |
| BSP | Bone sialoprotein |
| BSEM | Backscattered scanning electron microscopy |
| BrdU | 5-Bromo-2'-deoxyuridine |
| μCT | Microcomputed tomography |
| Cont | Control group |
| CA-β | Constitutive activated β-catenin |
| Ca | Calcium |
| CKO | Conditional knockout |
| Ck1 | Casein kinase 1 |
| DMP1 | Dentin matrix protein 1 |
| nuDMP1 | Nuclear isoform of DMP1 |
| Dn | Dentin |
| pDn | Predentin |
| DSPP | Dentin sialophosphoprotein |
| DKK1 | Dickkopf-related protein 1 |
| Dvl | Disheveled |
| ECM | Extracellular matrix |
| ERK | Extracellular signal-regulated kinase |
| ER | Endoplasmic reticulum |
| En | Enamel |
| FGF23 | Fibroblast growth factor-23 |
| Fzd | Frizzled |

| | |
|---|---|
| GP | Growth plate |
| GRP-78 | Glucose-regulated protein-78 |
| GnRH | Gonadotropin-releasing hormone |
| Gsk3β | Glycogen synthase kinase 3β |
| Het | Heterozygous |
| HE | Hematoxylin & Eosin |
| Hyp | loss-of-function mutation of *Phex* |
| IWR | Compound inhibitors of Wnt response |
| KO | Conventional knockout |
| LacZ | β-Galactosidase |
| LEF | Lymphoid enhancing factor |
| LRP5/6 | Low-density lipoprotein receptor-related protein 5/6 |
| MEPE | Matrix extracellular phosphoglycoprotein |
| MAPK | Mitogen-activated protein kinase |
| MEK | Mmitogen-activated protein kinase kinas |
| M1V Mut | Met1Val mutation |
| NCPs | Non-collagenous proteins |
| NLS | Nuclear localization signal peptide |
| OSX | Osterix |
| OPN | Osteopontin |
| OCN | Osteocalcin |
| Ocy | Osteocyte |
| Ob | Osteoblast |
| PHEX | Phosphate-regulating neutral endopeptidase, X-linked |
| PTHR | Parathyroid receptor |
| PL | Periodontal ligament |
| P | Pulp |
| Pi | Phosphorus |
| PTH | Parathyroid hormone |

| | |
|---|---|
| RGD | Arginine-glycine-aspartic acid |
| Runx2 | Runt-related transcription factor 2 |
| RBC | Red blood cell |
| SIBLINGs | Small integrin-binding ligand, N-linked Glycoprotein |
| SEM | Scanning electron microscopic |
| SOST | Sclerostin |
| SP | Secretory signal peptide |
| SF | Significant difference |
| SR | Sirius red staining |
| SHH | Sonic hedgehog |
| SAPK | Stress-activated protein kinase |
| TCF | T cell factor |
| WT | Wild type |
| XLH | X-linked dominant hypophosphatemic rickets |

TABLE OF CONTENTS

Page

ABSTRACT ..... ii

DEDICATION ..... iv

ACKNOWLEDGEMENTS ..... v

NOMENCLATURE ..... vi

TABLE OF CONTENTS ..... ix

LIST OF FIGURES ..... xi

LIST OF TABLES ..... xiv

CHAPTER I INTRODUCTION AND LITERATURE REVIEW ..... 1

Specific Aims ..... 1
Review of the Literature ..... 3

CHAPTER II CONSTITUTIVE NUCLEAR EXPRESSION OF DMP1 FAILS TO RESCUE THE *DMP1*-NULL SKELETAL PHENOTYPE ..... 13

Overview ..... 13
Synopsis ..... 13
Introduction ..... 14
Experimental Procedure ..... 16
Results ..... 22
Discussion ..... 26

CHAPTER III NUCLEUS-TARGETED DMP1 FAILS TO RESCUE DENTAL DEFECTS IN DMP1 NULL MICE ..... 30

Synopsis ..... 30
Introduction ..... 30
Materials and Methods ..... 32
Results ..... 34
Discussion ..... 37

CHAPTER IV A KEY PATHOLOGICAL ROLE OF WNT/B-CATENIN IN HYPOPHOSPHATEMIC RICKETS ..... 39

Synopsis ..... 39
Introduction ..... 40
Subjects and Methods ..... 42
Results ..... 47
Discussion ..... 52

CHAPTER V CONCLUSION ..... 56

Important Roles of Osteocytes ..... 56
Signaling Involved in the Biological Regulation of DMP1 ..... 57
Pathogenesis of the Inherited Hypophosphatemic Rickets/Osteomalacia ..... 59

REFERENCES ..... 60

APPENDIX A FIGURES ..... 80

APPENDIX B TABLES ..... 128

LIST OF FIGURES

Page

Figure 1-1 Photographs and radiographs of patients with hypophosphatemic rickets osteomalacia ..... 80

Figure 1-2 Schematic structure of the human DMP1 gene and ARHR mutations..... 81

Figure 1-3 Defective osteocytes are responsible for abnormal bone formation in the *Dmp1* knockout mice..... 82

Figure 1-4 SEM images of the acid-etched, resin-casted osteocyte-canalicular system. 84

Figure 1-5 Roles of DMP1 in control of osteocyte maturation..... 85

Figure 1-6 Proposed models for DMP1 control genes critical for osteogenesis..... 86

Figure 1-7 Schematic representation of ostoecytes and their connections..... 87

Figure 2-1 *Dmp1* is expressed in postnatal osteoblasts and responsible for regulating osteoblast proliferation and differentiation ..... 88

Figure 2-2 Transfection of Ad-CMV-$^{NLS}$DMP1 or Ad-CMV-$^{SP}$DMP1 greatly changed expressions of bone markers in MC3T3 cells..... 90

Figure 2-3 $^{NLS}$DMP1 expressed in the nuclei and $^{SP}$DMP1 mainly secreted in the matrix ..... 91

Figure 2-4 $^{NLS}$DMP1 revealed no cure of rachitic phenotypes in *Dmp1*-null mice, however $^{SP}$DMP1 fully rescued the defects..... 92

Figure 2-5 Targeting DMP1 in the *Dmp1*-KO nuclei did not rescue deficiencies of mineralization in *Dmp1*-null mice, however re-expressing DMP1 in the matrix greatly recovered these defects. ..... 94

Figure 2-6 IHC analysis shown the targeted expression of $^{NLS}$DMP1 transgene revealed no rescue of the maturational defects in ostecytes..... 95

Figure 2-7 The targeted expression of $^{NLS}$DMP1 transgene (line #97) in either the Dmp1 HET or the KO background had no effect ..... 96

Figure 2-8 The *in vivo* working model..... 98

Figure 3-1 Tooth phenotypes in an M1V Mut ARHR patient ..... 99

Figure 3-2 Nucleus-targeted Dmp1 expressed in the pre-odontoblasts and odontoblassts, showing no morphological improvement of *Dmp1*-null tooth. ..... 100

Figure 3-3 Nucleus-targeted Dmp1 had no rescue of the dental abnormalities of *Dmp1*-null mice ..... 101

Figure 3-4 *Dmp1*-null mice developed typical periodontitis ..... 103

Figure 3-5 Nucleus-targeted Dmp1 had no improvement of periodontal structures ..... 104

Figure 3-6 Nucleus-targeted Dmp1 showed no effect on tooth eruptional delay ..... 106

Figure 3-7 Statistic analysis of root morphology and osteoclast numbers, radiographs of Line #97 ..... 107

Figure 4-1 A sharp reduction of SOST expression in the 3-wk-old cortical bone of *Dmp1*-null mice ..... 108

Figure 4-2 Wnt/β-catenin signaling is up regulated in the osteocyte of *Dmp1*-null mice. ..... 109

Figure 4-3 Constitutive stabilization of β-catenin in osteocyte lead to abnormal bone structures at age of 3-week-old ..... 110

Figure 4-4 Constitutive stabilization of β-catenin in osteocyte recaptured osteomalacia phenotype and displayed deformed osteocytes ..... 112

Figure 4-5 Immunohistochemistry staining of DMP1, DKK1, and β-catenin ..... 114

Figure 4-6 Normalizing the Wnt/β-catenin activity greatly improves the bone morphology ..... 114

Figure 4-7 The abnormal bone homestasis in *Dmp1*-null metaphysis is improved by *Dkk1*-Tg ..... 116

Figure 4-8 Osteomalacia phenotype in *Dmp1*-null mice is greatly restored by *Dkk1*-Tg ..... 118

Figure 4-9 Osteocyte maturation defect in *Dmp1*-null mice is greatly improved by *Dkk1*-Tg ..... 120

Figure 4-10 *Hyp*-mice displayed increased β-catenin level and *Dkk1*-transgene shown a morphological rescue in *Hyp*-mice ..... 122

Figure 4-11 Injection of anti-β-catenin compound drug improves the rickets/osteomalacia deficience in *Dmp1*-null mice.....124

Figure 4-12 The pathogenesis of the inherited hypophosphatemic ricket/osteomalacia in *Dmp1*-null or *Hyp*-mice .....126

Figure 5-1 Signaling pathways underlying the osteocyte maturation and function process that regulated by DMP1 .....127

LIST OF TABLES

Page

Table 1-1 Characteristics of ARHR patients and mice models ..... 128

Table 2-1 Three independent lines and their DMP1 expressions ..... 129

Table 2-2 RNA expression levels after transfection ..... 130

Table 2-3 Bone histomorphometry findings in the femurs of 3-week-old mouse ..... 131

Table 4-1 Hypophosphatemia phenotype in *Dmp1*-null mice is partially rescued by *Dkk1*-Tg ..... 132

# CHAPTER I

# INTRODUCTION AND LITERATURE REVIEW

## Specific Aims

Rickets is a softening of bones in children due to deficiency or impaired metabolism of vitamin D, phosphorus or calcium, potentially leading to fractures and disturbance of normal ossification, marked by bending and distortion of the bones, nodular enlargements on the ends and sides of the bones, delayed closure of the fontanelles, and muscle pain. Rickets is among the most frequent childhood diseases in many developing countries. The adult equivalent of rickets is named as osteomalacia, which contains inadequate or delayed mineralization of osteoid in mature cortical and spongy bone. Hypophosphatemic rickets/osteomalacia is a group of disorders characterized by rickets associated with hypophosphatemia, resulting from dietary phosphorus deficiency, defects in renal tubular function, or, most frequently, inherited gene mutations. Studies demonstrated several gene mutations will result in hypophosphatemic rickets, such as, mutations in Phex gene lead to x-linked dominant hypophosphatemic rickets (XLH) (1), Fgf23 mutant results in autosomal dominant hypophosphatemic rickets (ADHR) (2), and homozygous mutation in *Dmp1* that cause autosomal recessive hypophosphatemic reickts (ARHR) (3). This study works on the ARHR that is attributed to *Dmp1* mutations in humans or *Dmp1* deletion in mice. We propose to investigate the underlying mechanism, especially the signaling pathway, which plays a key pathological role during the development of hypophosphatemice rickets/osteomalacia. Furthermore, for the consideration of translational medicine of this study, we will try to rescue the rickets/osteomalacia in *Dmp1*-null mouse model using drugs, which target the identified signaling pathway. Our focus is on how DMP1 regulates osteocyte maturation and function that respond to bone morphology and mineralization defects in the hypophosphatemice rickets/osteomalacia mice. The results of this study will also cast light on the understanding of how the osteocytes regulate

bone development and mineralization during the early postnatal period. The specific aims are listed as the following:

Specific Aim 1: To investigate whether DMP1 works as a co-transcription factor that will be transported into the nucleus to regulate related gene expression. We will first test DMP1 function *in vitro* by generating two different constructs that lead to different subcellular location of DMP1. The $^{SP}$DMP1 construct contained a signal peptide that directed the extracellular transport of DMP1. We then generated transgenic mice that express DMP1 in the nucleus ($^{NLS}$DMP1) for an *in vivo* study. We hypothesize that $^{NLS}$DMP1 neither regulates osteocytes maturation nor rescues rickets/osteomalacia phenotype.

Specific Aim 2: To investigate whether the expression of canonical Wnt/β-catenin signaling is changed in Dmp1 deletion induced ARHR mouse models, and to further understand which kind of bone cells are responsible for canonical Wnt/β-catenin signaling. We will examine the expression pattern of Wnt/β-catenin signaling in *Dmp1*-null mice. We hypothesize that in ARHR mice the deletion of *Dmp1* leads to an up-regulation of canonical Wnt/β-catenin signaling mainly in osteocytes.

Specific Aim 3: To rescue the rickets/osteomalacia phenotype in Dmp1-null mice by down-regulating the β-catenin expression. We will cross our Dmp1-KO mice with Dkk1-Tg mice. Their offspring will be evaluated for the morphology and mineralization of bone, cartilaginous development, serum biochemistry, maturation and function of bone cells. We hypothesize that re-regulating β-catenin in *Dmp1* knockout mice using the Dkk1 transgene may rescue the rickets/osteomalacia phenotype via reinvigorating osteocyte maturation.

Specific Aim 4: To further confirm that increased function of Wnt/β-catenin signaling in the osteocytes that may cause its maturational and functional defects, leading to osteomalacia. We have specifically induced β-catenin expression in the osteocyte both *in vitro* and *in vivo*. Gene expression and mineral formation, morphology and mineralization of bone, serum biochemistry, maturation and function of osteocytes were evaluated. We hypothesize that it is the evaluated expression of Wnt/β-catenin

signaling in osteocytes that will cause their maturational and functional defects, leading to rachitic phenotype.

Specific Aim 5: To address the clinical translation of our studies. A compound-drug that inhibits Wnt/β-catenin signaling will be used to treat Dmp1-null rickets mice. Mice will be collected and evaluated after treatment. We hypothesize this compound, named as "IWR", can greatly improve the rickets/osteomalacia phenotypes of *Dmp1*-null mice.

Together these aims will further our understanding of how DMP1 regulates osteocyte maturation, and the pathological role of canonical Wnt/β-catenin signaling during the development of rickets/osteomalacia phenotype. These results will help explain why a high Pi diet alone fails to fully restore the osteomalacic status in patients and the restoration of phosphate homeostasis by FGF-23 antibodies only partially rescued the bone formation rate and osteomalacia. Moreover, they also provide a new comprehensive and a possible clinic therapy for patients with hypophosphatemic reickts/osteomalacia.

**Review of the Literature**

The extracellular matrix (ECM) of bone and dentin contains numerous non-collagenous proteins (NCPs). One of the categories of NCPs is termed the "Small Integrin-Binding Ligand, N-linked Glycoprotein (SIBLINGs) family" based on the similarities of the intron/exon properties, conserved protein biochemical properties (such as unstructured and acidic), and specific peptide motifs (e.g., phosphorylation and integrin-binding RGD). There are five members in this SIBLINGs family: Dentin matrix protein 1 (DMP1), bone sialoprotein (BSP), osteopontin (OPN), enamelin, matrix extracellular phosphoglycoprotein (MEPE), and dentin sialophosphoprotein (DSPP) (4). DMP1 was originally identified by cDNA cloning from the rat dentin matrix (5) and was initially believed to be dentin specific but was later observed in bone matrices at a much higher level (6,7). Studies suggested that DMP1 initiates its expression at E15.5 and

resides mainly in osteoblasts during embryonic development. However, DMP1 is predominantly expressed in the osteocytes during postnatal development (8,9).

The *Dmp1* gene was mapped to the long (q) arm of chromosome 4 at position 21 (4q21) in humans and to 5q21 in mice. *Dmp1* is encoded by 6 exons with 80% of its coding information in exon 6. There are two promoter control domains: a proximal one located between the -2.4 kb and the +4 kb region, and a distal one between the -2.4 kb and -9.6 kb region. The proximal domain controls the early stages of DMP1 expression, and the distal domain controls the later stages (10). AP-1, JunB, Runx2, Msx1/2, Tcf/Lef, C/EBP, and YY-1 are essential transcription factors for bone and tooth tissue-specific regulation. The potential response elements for these transcription factors have been identified in the mouse *Dmp1* promoter (11).

***DMP1 mutation/deletion leads to autosomal recessive hypophosphatemia***

*In vivo* animal studies showed that DMP1 has potential functions in non-mineralized tissues such as in brain (12), kidney (13) and salivary tissues (14), although this matrix protein is mainly expressed in mineralized tissues and plays an important role during osteogenesis (15). For example, DMP1 is thought to actively promote and control the mineralization of collagen fibers and crystal growth within osteoids and predentin when these tissues are converted to mature bone and dentin (15). In addition, DMP1 is considered to regulate and support the maturational process converting osteoblasts to osteocytes and preodontoblasts to odontoblasts (16). Importantly, *DMP1* mutations in humans or the deletion of *Dmp1* in mice lead to autosomal recessive hypophosphatemic rickets (ARHR)/osteomalacia (3). It is noteworthy that, unlike other genetic disease cases in which human mutations are identified first and then animal studies such as gene knockouts are performed, it is the *Dmp1*-null mouse research results (17,18) that have triggered searches for *DMP1* mutations in humans.

*Autosomal recessive hypophosphatemia*

Rickets is the softening of bones in children because of a deficiency or impaired metabolism of vitamin D, phosphorus or calcium. This disease not only interrupts child development but also can potentially lead to fractures and disturbance of normal ossification. Rickets due to nutrition deficiency is more common in children in developing countries. The adult equivalent of rickets is known as "osteomalacia", a disease characterized by inadequate or delayed mineralization of osteoids in mature cortical and spongy bones. Hypophosphatemic rickets/osteomalacia is a group of disorders characterized by hypophosphatemia, which mainly results from disorders of renal phosphate wasting (Unlike the situation with calcium, there is no rickets due to phosphorus deficiency, since one's daily diet is rich in this element). There are several inherited gene mutations responsible for deficiencies in reabsorption of the renal tubule that result in hypophosphatemia. For example, mutations in the *PHEX* gene lead to x-linked dominant hypophosphatemic (XLH) rickets (1), *FGF23* mutations result in autosomal dominant hypophosphatemic rickets (ADHR) (19), and homozygous inactivating mutations in *DMP1* cause autosomal recessive hypophosphatemic rickets (ARHR)/osteomalacia (3,20,21). Comparisons of patients having XLH, the most common hypophosphatemic rickets, it has shown that fewer than 10 cases of kindred ARHR have been identified worldwide due to the autosomal recessive nature of the *DMP1* mutations (3,20-23) (Fig. 1-1). Molecular genetic analysis of these cases revealed the following changes: 1) the deletion of nucleotides 1484-1490 in exon 6 (1484-1490del) resulting in a frameshift that replaced the 18 conserved C-terminal residues with 33 unrelated residues, or another deletion in the same exon leading to a frameshift replacing 335 conserved amino acids with 53 unrelated ones; 2) a mutation in the start codon (1A→G) causing a methionine to valine change (M1V); 3) a homozygous 1-bp deletion in exon 6 (362delC) led to the placement of a premature stop codon after 120 unrelated amino acids; 4) a biallelic nucleotide substitution at nucleotide 98 in exon 3 (98G→A) introduced a premature termination codon (PTC) at codon 33, which replaced the wild type tryptophan residue (W33X); and 5) a mutation at the splice acceptor

junction of exon 6 (IVS5-1G→A) and intron 2 (55-1G→G) is predicted to alter pre-mRNA splicing, which results in a shift in the open-reading frame if the final message is stable (Fig. 1-2).

Based on the reported cases, the primary clinical symptoms of ARHR include: lower limb deformities (bowed legs or knock-knees), waddling gait, short stature or stunted growth, tooth abscesses or early loss of teeth, bone and muscle pain, biochemical abnormalities (hypophosphatemia with normal levels of serum calcium and parathyroid hormone). More severely afflicted patients may also suffer from nerve deafness, facial and dental abnormalities, learning disabilities, joint pain, and contracture and immobilization of the spine. Patients diagnosed with ARHR display symptoms in their early childhood that are likely to have a wide spectrum of severity, depending on the site and size of the mutations and the severity and chronicity of the associated phosphate depletion (24) (Table 1-1).

*Dmp1*-null mice do not have apparent abnormalities during prenatal bone development. However, they are severely impaired after birth with a chondrodysplasia-like phenotype characterized by short and widened long bones having flared and irregular metaphyses and delayed malformed ossification centers in postnatal development (18). Compared with human patients, *Dmp1*-null animals displayed significantly lower serum phosphorus levels than the wild type controls. This difference is due to the increased urinary phosphate excretion associated with increased FGF23 levels. Furthermore, the levels of 1,25-dihydroxyvitamin D [$1,25(OH)_2D_3$] were inappropriately normal, whereas the serum PTH level significantly increased in the *Dmp1*-null mice (3,16,25). Bone histological studies demonstrated that the *Dmp1*-null mice displayed severe osteomalacia bone changes with significant reduction in bone mineralization. Furthermore, the *Dmp1*-null mice had increased osteoid and more porous cortical bone. Under higher-magnification back-scattered scanning electron microscopic (SEM) images, the minerals, which are evenly distributed around the osteocyte lacunae in normal condition, were either absent or sparsely located in regions surrounding the *Dmp1*-null osteocytes. The scanning transmission electron microscopic images indicated

a much lower content of mineral, calcium, and phosphorus in the *Dmp1*-null mineralized matrix (3,16,25) (Fig. 1-3, a-b).

*Osteocyte maturational defects in Dmp1-null mice*

Numerous studies have consistently suggested the key pathological cause responsible for the ARHP phenotype in *Dmp1*-null mice is the maturational and functional defects of the osteocytes (3,16,25) (Fig. 1-3, c).

The osteocytes reside in lacunae within the mineralized bone matrix and send their dendritic processes (ranging from 40–100 per cell) through tiny tunnels called "canaliculi" to form the osteocyte lacunocanalicular network (26). As the osteocytes mature, numerous cellular projections form and elongate. Next, their cell volume and ultrastructure, such as the endoplasmic reticulum and the Golgi apparatus, are reduced, and a well-organized lacunocanalicular system is built up (26). Compared to the well-established smooth inner wall of the lacunae and canaliculi, *Dmp1*-null osteocytes display bulky and coarse microstructural features, as well as abnormally enlarged and round-shaped osteocytes accompanied by a reduction in dendrite numbers (3,16,25).

An early transfection study of MC3T3-E1 cells that expressed excessive DMP1, displayed accelerated differentiation of osteoblasts and an earlier onset of mineralization, suggesting that DMP1 plays an important role during the osteoblast differentiation, as well as osteocyte maturation and function (27). It was later reported that patients with *DMP1* mutations or mice with *Dmp1* deletion did not display any gross abnormalities during the embryonic period or at birth (28). However, they generally appeared to have the ARHP phenotype during their early postnatal development, when DMP1 is highly produced by osteocytes and secreted into the mineralized matrix. Further analysis indicated that *Dmp1* deletion leads to defects primarily in the osteocytes (3,16,25), cells that account for more than 95% of bone cells (Fig. 1-4).

There is general agreement that dramatic decreases in protein expression and metabolic activity occur during the maturation of osteoblasts into osteocytes (29). However, the analysis of *Dmp1*-null mice showed sharp increases of osteoblastic marker

expression levels, such as runt-related transcription factor 2 (RunX2), osterix (OSX), Collagen I (Col I), alkaline phosphatase (ALP), bone sialoprotein (BSP), and osteocalcin (OCN). In addition, the early osteocyte marker E11/gp38 is widely and increasingly expressed throughout the whole cortical bone layer in the *Dmp1*-null mice. In contrast, sclerostin (SOST), mainly expressed in mature osteocytes, is greatly reduced. These studies indicated that osteocyte differentiation is likely regulated by DMP1 (3,16,25). There is strong evidence showing that the osteocytes, the terminally differentiated cells, regain the ability to divide and proliferate in *Dmp1*-null mice (3,16,18,25,30) (Fig. 1-5).

***DMP1 regulates osteocyte biology and bone development***

As previously mentioned, DMP1 is essential for osteogenesis by regulating the maturational process of osteoblasts to osteocytes and bone mineralization during postnatal development. As a key regulator, DMP1 performs several functions in osteocyte biology and bone development as described below.

*DMP1 directly promotes hydroxyapatite formation in vitro*

The initial finding linking DMP1 with mineralization was based on the close association of the DMP1 expression and the in vitro "bone nodule" formation in primary rat calvarial cell cultures (8). Soon after, He and colleagues (31) reported that the specific acidic clusters in DMP1 molecules can provide the molecular design necessary for controlling the formation of oriented calcium phosphate crystals and that the self-assembly of acidic clusters into a beta-sheet template of DMP1 is likely required for the role of DMP1 in biomineral induction. Gajjeraman *et al.* also showed that both full-length recombinant DMP1 and native DMP1 C-terminal fragments isolated from rat bone accelerated the nucleation of hydroxyapatite in the presence of type I collagen, whereas the N-terminal domain of DMP1 (amino acid residues 1-334) inhibited hydroxyapatite nucleation (32). Further analysis of the three DMP1 fragments within the mineralized tissues [N-terminal, C-terminal, and a chondroitin-sulfate-linked N-terminal fragment (DMP1-PG)] implies that both the C-terminal and N-terminal fragments are

promoters of hydroxyapatite formation and growth, while DMP1-PG is an inhibitor (33). These findings appear controversial although they indicate that distinct forms of DMP1 may work collectively to control the mineralization process in different ways. However, the direct role of DMP1 in mineralization described above is mainly based on *in vitro* culture studies with little *in vivo* evidence.

*DMP1 signaling*

*DMP1 signals via cell surface integrin*

*In vitro* studies have shown that DMP1 promotes cell attachment through the RGD motif in a cell- and tissue-specific manner, suggesting a possible interaction of this protein with specific cells and activating signaling pathways. This speculation is strengthened by the observation that exogenous DMP1 added to the exposed dental pulp may act as a morphogen trigger and/or promoter of the differentiation of undifferentiated ectomesenchymal cells in the pulp toward the odontoblast lineage. A further *in vitro* analysis demonstrated that either the full-length DMP1 or the 57-kDa fragment can activate phosphorylated extracellular signal-regulated kinase (p-ERK). The difference between them is that the effect of the 57-kDa fragment lasted longer than that of the full-length protein (34). More recently, two separate studies confirmed that the matrix DMP1 has the ability to activate the ERK-MAPK (extracellular signal-regulated kinase-mitogen-activated protein kinase) pathways via interaction with cell surface αvβ3 integrin. It also further stimulates the translocation of phosphorylated JNK to the nucleus, as well as a concomitant up-regulation of transcriptional activation by phosphorylated c-Jun, such as *Runx2* activation (35,36) (Fig. 1-6, a).

*DMP1 works as a transcriptional factor*

As mentioned above, DMP1 is generally considered to be an extracellular matrix protein. However, some *in vitro* studies showed the expression of DMP1 in the nuclei of several cell lines: MC3T3-E1, C3H10T1/2, and 17IIA11 (37,38). These studies suggest that DMP1 could function as a transcriptional factor. Moreover, Narayanan *et al*.

reported a functional nuclear localization signal (NLS) peptide at the carboxyl terminal of DMP1 and thought that this signal peptide could bring DMP1 into the nucleus (37). They then found a specific domain in the N-terminal of DMP1 that interacted with the glucose-regulated protein-78 (GRP-78) receptor leading to the internalization and nuclear localization of full-length DMP1 (39). Recently, Siyam *et al.* reported finding two DMP1 subpopulations in non-synchronized cells: one in the nucleus and one in the cytoplasm (38). Nevertheless, this transcriptional factor theory is mainly supported by the *in vitro* cell line studies with little *in vivo* evidence. Importantly, Lu and colleagues reported that the 57 kDa C-terminal fragment of DMP1 is sufficient to fully rescue the rachitic abnormalities found in the *Dmp1*-null mice (25). However, more *in vivo* studies are required to support this transcriptional factor theory (Fig. 1-6, b).

*Pathophysiologic regulation*

Recent findings showed that osteocytes embedded in the mineralized bone matrix are far more important than previously described in the literature (Fig. 1-7). These studies imply that osteocytes are multifunctional cells that connect to themselves, to cells on the bone surface and to the vasculature, and they play a key regulatory role in bone and mineral homeostasis under normal and pathological conditions during postnatal development (29). As a crucial protein mainly produced by osteocytes, DMP1 is responsible for the pathophysiologic development of the heritable disorders of rickets and osteomalacia by impacting the regulatory effect of osteocytes (24).

*Regulating the axis of FGF23-renal phosphorus reabsorption-serum phosphorus level*

Prior studies demonstrated that serum FGF23, which is released from bone, targets the kidneys and decreases the expression of the sodium/phosphate cotransporters: NaPi-IIa and NaPi-IIc. These co-transporters are required for renal phosphate reabsorption, and a decrease in co-transporter expression will lead to an increase of the urinary excretion of phosphate and a decrease of serum phosphate levels (40). Additionally, FGF23 also down-regulates the production of 1-α hydroxylase, resulting in

a decreased conversion of $1,25(OH)_2D_3$ to the active vitamin D metabolite, $1,25(OH)_2D_3$. This reduced production leads to a decreased expression of NaPi-IIb, a third sodium/phosphate co-transporter, and therefore affects phosphate absorption in the intestine (41). It is generally agreed that the functional axis of the FGF23 renal and intestinal phosphorus reabsorption serum phosphorus level is the key systematic pathological mechanism responsible for the development of inherited hypophosphatemic rickets/osteomalacia. Studies of *Dmp1*-null mice and *DMP1* mutations in patients showed that FGF23 is significantly up-regulated in osteocytes, which is released into circulation through the connection between osteocytes and vessels, leading to an increase of FGF23 in serum and in subsequent hypophosphatemia (3). Specifically, *in situ* hybridization (measuring mRNA levels) or immunohistochemistry (measuring protein levels), revealed that the FGF23 level in control osteocytes was much lower than that in osteoblasts, indicating differential regulatory mechanisms for FGF23 in bone cells of healthy versus disease conditions. The discovery of elevated level of FGF23 in the *Dmp1*-null osteocytes indicates that bone is an endocrine organ regulating phosphate homeostasis (42) (Fig. 1-7).

*Canonical Wnt/β-catenin pathway*

In addition to controlling FGF23 levels, DMP1 may regulate hypophosphatemic rickets/osteomalacia disorder via the canonical Wnt/β-catenin signaling pathway. In normal bone development, the canonical Wnt/β-catenin pathway is required for osteogenesis and bone remodeling via regulation of early osteoblast lineage (43). However, recent studies have indicated that a high level of β-catenin may cause bone defects in rickets (44). This pathological change is likely due to a dramatic decrease in the expression levels of SOST (a potent inhibitor of the Wnt/β-catenin pathway(45)) in the *Dmp1*-KO osteocytes. In addition, the expression level of DKK1, another antagonist of the Wnt signaling pathway (46), is low in *Dmp1*-null mice. As a result, the canonical Wnt/β-catenin signaling is abnormally upregulated in *Dmp1*-null mice. A pilot study by

Lin *et al.* showed that normalization of the β-catenin level by overexpressing DKK1 significantly improved the osteomalacia phenotype of *Dmp1*-null mice (Fig. 1-7).

***Summary***

DMP1 was cloned 20 years ago (5). Since then, great progress has been made, including gene regulation, biochemical characterization, cell/tissue localization and function, as well as identification of DMP1 mutations in ARHR patients. It is now clear that the full-length DMP1 is not biologically active and is cleaved into the 37 kDa N-terminal and the 57 kDa C-terminal fragments. The latter is the key functional form of DMP1. There is strong evidence that DMP1, highly expressed in dentin and bone, is critical for mineralization, although the direct role of DMP1 on the formation of hydroxyapatite is largely based on the *in vitro* non-cell model with little *in vivo* evidence. The development of different forms of *Dmp1* transgenic mouse models such as conventional and conditional null mice, the full length and the C-terminal forms of over-expressed *Dmp1* transgenic mice, and the *Dmp1* point mutation models have started to reveal the *in vivo* functions of DMP1 in bones and teeth during development (25,28,34,47). Because DMP1 controls the maturation of both odontoblasts and osteoblasts, defects in this process result in sharp changes in dentin morphologies (such as dentin tubules) and bone (especially the osteocyte-canalicular system). Finally, studies of abnormal FGF23 production in the *Dmp1*-null osteocytes have led to the discovery of *DMP1* mutations in humans. Altogether, the accumulated data from different laboratories strongly support the theory that DMP1 is a key player in the control of osteocyte and bone biology.

# CHAPTER II

# CONSTITUTIVE NUCLEAR EXPRESSION OF DMP1 FAILS TO RESCUE THE *DMP1*-NULL SKELETAL PHENOTYPE

## Overview

It is widely believed that DMP1 functions not only as a matrix protein but also as a transcription factor. However, this study found that nuclear activities of DMP1 didn't recover the defects in *Dmp1*-null mice, whereas the secreted DMP1 fully rescued. We concluded DMP1 mainly functions as an extracellular matrix protein *in vivo*. This is the first evaluation of the biological functions of DMP1 in different subcellular locations (nuclear and extracellular matrix) *in vivo*.

## Synopsis

Dentin Matrix Protein 1 (DMP1) plays multiple roles in bone, tooth, phosphate homeostasis, kidney, salivary gland, body balance, reproductive cycles, and the development of cancer. Previous *in vivo* studies have demonstrated its key role in osteocytes. However, recent *in vitro* studies have indicated DMP1 may also be expressed in the osteoblasts, and during the differentiation and maturation of osteoblasts/osteocytes, it has two different biological roles: 1) As a matrix protein, DMP1 interacts with αvβ3 integrin and activates MAP kinase signaling; and 2) DMP1 serves as a transcription factor. This study attempted to determine whether DMP1 expressed in the osteoblasts and works as a transcription factor that regulates osteoblast functions *in vivo*. We first identified that DMP1 continues its expression in osteoblasts during postnatal development and that the deletion of *Dmp1* leads to an increase in osteoblast proliferation. Then using the adenovirus construct, we targeted the expressions of DMP1 either in the nucleus only by replacing the endogenous signal peptide with a nuclear localization signal (NLS) sequence (referred to as $^{NLS}$DMP1) or as the WT type (referred to as $^{SP}$DMP1) in the MC3T3 osteoblast for gene expression

comparisons. High levels of DMP1 in either form greatly increased cell differentiation in an identical manner. However, the targeted $^{NLS}$DMP1 transgene, driven by a 3.6 kb rat Col 1α1 promoter in the nucleus of osteoblasts and osteocytes, failed to rescue the *Dmp1*-null mouse phenotype, whereas the $^{SP}$DMP1 transgene rescued the rickets phenotype. These studies support the theory that DMP1 functions as an extracellular matrix (ECM) protein, rather than a transcription factor *in vivo*.

**Introduction**

DMP1 was originally isolated from rat dentin matrices (48) and later was found to have a broader expression profile in many tissues, such as bone, cartilage, salivary gland, kidney, pituitary gland, and blood vessels, as well as cancer tissues, such as those in lung and breast (6,7,12,13,49-54). This acidic phosphorylated extracellular matrix protein belongs to the Small Integrin-Binding Ligand, N-linked Glycoprotein (SIBLING) family (55,56). Like other SIBLING family members, the *Dmp1* gene is located on chromosome 4q21 in humans and 5q21in mice (49,55). The mutation in this gene results in autosomal recessive hypophosphatemic rickets (ARHR) in humans (3,20-23,57), which is similar to that found in *Dmp1-null* mice (3). Additionally it is known that DMP1 must be cleaved to the $NH_2$-terminal and COOH-terminal fragments, among which the C-terminal appears to be a key functional domain of DMP1 (25,30,47,58,59).

DMP1 has been considered as an extracellular matrix (ECM) protein since its discovery. An early *in vitro* mechanism study showed that DMP1 facilitates the biomineralization of collagen fibers and the crystal growth (60). Although the phosphorylated bovine DMP1 expressed in marrow stromal cells showed an inhibitory effect on hydroxylapatite formation and growth (61), however, these authors also showed that the recombinant full-length non-phosphated DMP1 and the phosphated C-terminal work as the hydroxylapatite nucleator. Furthermore, studies found in the C-terminal of DMP1 there is a RGD motif, which can bind to the integrin receptors. Based on this structure, Wu *et al.* (35), Eapen *et al.* (36) and our lab (34) carried out different kinds of mechanistic studies, and each of these studies independently demonstrated that

DMP1 activates the MAP kinase signaling pathway using the full-length or the C-terminal fragment of recombinant DMP1 in different mesenchymal cell lines, including osteoblast cell lines. All of these groups concluded that DMP1 functions as an extracellular matrix (ECM) protein and controls cell function via the αvβ3-integrin-MAP kinase signaling pathway.

Recently, a prevailing theory suggests it has dual functional roles that, in addition to functions as ECM protein during biomineralization, it also works as a transcription factor in osteoblast and odontoblast. This transcription factor theory of DMP1 is mainly based on two lines of evidence: there is a functional NLS sequence in the C-terminal of DMP1 which enables its role as a transcription factor that regulates the *in vitro* osteoblast and odontoblast function (37); the N-terminal of DMP1 can specifically bind to the glucose-regulated protein-78 (GRP-78) receptor on the cell membrane and then triggers the internalization of full-length DMP1 via the endocytosis process (39). In addition, two laboratories showed evidence of DMP1 in the nucleus both *in vivo* (based on the immunostaining images) (62) and *in vitro* [DMP1 in the cell (38)]. Briefly, DMP1 is first internalized and transported into the nucleus to function as a transcription factor in osteoblasts, and later DMP1 gets phosphorylation in the nuclei, which triggers its exportation in to the matrix where it initiates the nucleation of hydroxyapatite formation and promotes the maturation and differentiation of osteoblasts/osteocytes (37).

However, this dual function theory is debatable. It was challenged by the identification of a *DMP1* mutation in several ARHR patients, named as Met1Val (M1V) mutation, which had a biallelic nucleotide substitution in *DMP1* start codon (ATG to GTG, or A1→G). This mutation resulted in the disruption of the ER signal sequence in *DMP1* (3), since Farrow and coworkers transfected the construct of M1V DMP1 into UMR-106 cells (osteosarcoma-derived cell lines) and demonstrated that the M1V DMP1 did not move to the trans-Golgi network for secretion, instead, it filled the entire cytoplasm (57), suggesting DMP1 may mainly function as a ECM protein. Furthermore, Kucka and coworkers (52) reported that gonadotropin-releasing (GnRH) hormone induces a 600-fold increase in the *Dmp1* expression in the primary pituitary cells of

cycling female rats, and a 30-fold increase in *Dmp1* expression in the male pituitary cells. Their Western blot data clearly revealed a DMP1 signal in the medium of female pituitary cells after GnRH treatment, while no DMP1 signal was identified in the lysate, indicating DMP1 had been secreted after GnRH induction and little was internalized. In addition, the immunohistochemistry studies by Kucku *et al.* (8) showed DMP1 in the cytoplasm but not in the nucleus, and the co-localization of DMP1 with other secreted hormones (such as FSHβ) further supported the theory that DMP1 is a secreted ECM protein rather than a nuclear protein.

To further explore the role of DMP1 in bone biology, we firstly identified the expression of DMP1 in postnatal osteoblasts and osteocytes, and its role in regulating osteoblasts *in vivo*. We further generated two constructs, which either carried its original endoplasmic reticulum (ER)-entry signal sequence of DMP1 (referred to as $^{SP}$DMP1) or replace this secretory signal sequence with NLS sequence (referred to as $^{NLS}$DMP1). Results of *in vitro* cell transfection showing the similar regulation of these two constructs -- there are up-regulated mRNA levels of bone sialoprotein (*Bsp*) and alkaline phosphatase (*Alp*). However, the expression levels of osteopontin (*Opn*), osteocalcin (*Ocn*), dentin sialophos-phoprotein (*Dspp*), and sclerostin (*Sost*) were significantly reduced. However, evaluations of *in vivo* transgenic mice models revealed contrary results -- $^{NLS}$DMP failed to rescue *Dmp1*-null phenotype, whereas $^{SP}$DMP1 successfully reversed the defects. These findings suggest that 1) the transcription factor hypothesis based on the *in vitro* data may reflect a non-physiological event in an extremely high concentration, and 2) DMP1 mainly functions as an ECM protein during postnatal bone development.

## Experimental Procedure

### *Adenovirus constructs*

The full-length murine *Dmp1* cDNA was cloned into an adenovirus CMV construct (Ad-CMV victor) by Baylor College of Medicine (Vector Development Lab) with the endogenous signal peptide (MKTVILLVFLWGLSCAL, $^{SP}$DMP1) or with its

signal peptide replaced by a nuclear localization signal peptide (PPKKKRKV, $^{NLS}$DMP1).

***Cell culture and adenovirus infection***

MC3T3 cells were cultured in a 12-well plate with α-modified Eagle's medium (α-MEM) supplemented with 10% fetal bovine serum (Invitrogen, Carlsbad, CA, USA). Infection was performed when the cells reached at least an 80% confluence level. Vectors in α-MEM with a concentration of $1X10^9$ viral particles/well was added, and then incubated in a $CO_2$ incubator for 30 min before adding the culture medium. The infection efficiencies were tested under a fluorescent microscope, which showed the highest efficiencies after 48 hours. All the cells were cultured at 37°C in a humidified 5% $CO_2$ atmosphere.

***Quantitative real-time PCR***

Total RNA was extracted from the infected MC3T3 cells using Trizol reagent (Invitrogen, San Diego, CA, USA) according to the manufacturer's protocol, then reverse-transcribed into cDNA, followed by real-time PCR analysis, as in our previous studies (16). The genes analyzed included *Dmp1, Bsp, Alp, Opn, Ocn, Dspp, and Sost* with GAPDH as an internal control. The details of the primer sequences were as follows: the *Dmp1* forward primer, 5'- AGT GAG TCA TCA GAA GAA AGT CAA GC-3', and reverse primer, 5'- CTA TAC TGG CCT CTG TCG TAG CC-3'; *Bsp* forward primer, 5'-GAG ACG GCG ATA GTT CC-3', and reverse primer, 5'-AGT GCC GCT AAC TCA A-3'; *Alp* forward primer, 5'-CTT GCT GGT GGA AGG AGG CAG G-3', and reverse primer, 5'-CAC GTC TTC TCC ACC GTG GGT C-3'; Opn forward primer, 5'-TTT ACA GCC TGC ACC C-3', and reverse primer, 5'-CTA GCA GTG ACG GTC T-3'; Ocn forward primer, 5'-CTC TGT CTC TCT GAC CTC ACA G-3', and reverse primer, 5'-GGA GCT GCT GTG ACA TCC ATA C-3'; *Dspp* forward primer, 5'-AAC TCT GTG GCT GTG CCT CT-3', and reverse primer, 5'-TAT TGA CTC GGA GCC ATT CC -3'; *Sost* forward primer, 5'-AGC TCC TTC AGA GGG CTG AT-3', and

reverse primer, 5'-GAG GCA GGC ATT TCA GTA GC-3'; and GAPDH forward primer, 5'-GGT GTG AAC CAC GAG AAA-3', and reverse primer, 5'-TGA AGT CGC AGG AGA CAA-3'.

### *Generation and characterization of the $^{NLS}$Dmp1 transgenic mice*

To generate the *Col1α1*-$^{NLS}$*Dmp1* transgene, the full-length mouse *Dmp1* cDNA with its ER-entry signal sequence replaced by a nuclear localization signal (NLS) sequence, and a SV40 polyadenylation signal sequence were cloned into a mammalian expression vector (63) (graciously provided by B. Kream and A. Lichtler, University of Connecticut Health Center, Farmington, CT, USA) containing the 3.6-kb rat type 1 collagen promoter plus a 1.6-kb intron 1 at the EcoRV and SalI sites, which give rise to the Col1α1-$^{NLS}$*Dmp1* transgene. This transgene was released from the vector backbone by SacII and SalI, then purified for pronuclear injection. Transgenic founders with a C57B/L6 background were generated at the UT Southwestern Medical Center (Dallas, TX, USA). A total of nine independent transgenic lines were obtained and partially characterized by radiographs, μCT and H&E stain. Except for one line displaying an increase in femur trabecular bone volume, the rest of the transgenic mouse lines showed no apparent differences from the control mice (data not shown). Three independent lines, including the line with a high trabecular bone volume, were crossed to *Dmp1*-null mice for in-depth rescue studies (see Table 2-1).

### *Target expression of the $^{NLS}$Dmp1 transgene into the Dmp1-null mice*

The *Dmp1-null* mice with a C57B/L6 genetic background using the lacZ knock-in target approach were described previously (28). To target *Dmp1* in the nucleus, the *Dmp1-null* mice were crossed with 3 different $^{NLS}$DMP1 lines with line #95 (whose expression level is 6-fold higher than that of the WT *Dmp1*) for a full characterization using multiple approaches. Since no apparent phenotypic differences between the wild type (WT) and heterozygous (Het) *Dmp1* mice were found, the Het *Dmp1* mice were used as controls. All of the mice were fed with autoclaved Purina rodent chow (Ralston

Purina, St. Louis, MO, USA) containing 1% calcium, 0.67% phosphorus, and 4.4 IU of vitamin D/g. All the animal procedures were performed in accordance with the National Institutes of Health Guide for the Care and Use of Laboratory Animals and approved by the Institutional Animal Care and Use Committee of Texas A&M Baylor College of Dentistry.

***PCR genotyping***

Genomic DNA was extracted from a tail biopsy and used for genotyping by PCR analysis. Primers p01 (5'-GAG TGC GAT CTT CCT GAG GCC GAT ACT GTC-3') and p02 (5'-CGC GGC TGA AAT CAT CAT TAA AGC GAG TGG-3') were used for targeting LaccZ (490 bp); primers p03 (5'-GCC CCT GGA CAC TGA CCA TAG C-3') and p04 (5'-CTG TTC CTC ACT CTC ACT GTC C-3') were used for identification of endogenous Dmp1 (400bp); primers p05 (5'-CAG CCG TTC TGA GGA AGA CAG TG-3' from Dmp1 cDNA) and p06 (5'-TGT CCA AAC TCA TCA ATG TAT CT-3' from the SV40 polyadenylation signal) were used to detect the transgenic $^{NLS}$DMP1 (337 bp), respectively.

***Protein extract and western blot***

To determine whether the $^{NLS}$DMP1 was expressed in the bone cells, total cell lysates were extracted from the HET and *Dmp1*-null primary calvarial cells with and without the transgene. The concentration of cell lysis was determined with the BCA kit (Pierce, Rockford, IL, USA). Ten μg of the total proteins of each group were then subjected to 10% DS-PAGE gel, followed by blotting onto a polyvinylidene difluoride membrane. The membranes were subsequently immunoblotted with the anti-DMP1-C-terminal antibody (47) at the concentration level of 0.2 μg IgG/ml. Alkaline phosphatase-conjugated anti-rabbit IgG (Sigma-Aldrich, St. Louis, MO, USA) was employed at a dilution of 1:5000 as the secondary antibody. Following this procedure, the membranes were incubated in chemiluminescent substrate CDP-star (Ambion, Grand

Island, NY, USA) for 5 min and exposed to Kodak film (Perkin Elmer, Waltham MA, USA) to visualize the bands.

***Histology***

For the decalcified bone analysis, the animals were injected twice with 5-Bromo-2'-deoxyuridine (BrdU, 100 ug/g mouse, i.p.; Sigma-Aldrich, St. Louis, MO, USA). The first injection of BrdU was made after 24 hours, and the second was 2 hours before the mouse was sacrificed). For fixation, perfusion was performed using freshly prepared 4% paraformaldehyde in phosphate-buffered saline (pH 7.4). Next, the specimens were decalcified and embedded in paraffin, as described previously (7). Sections were cut in 4.5 μm slices, mounted on slides and dried. These slides were used for immunohistochemistry, Hematoxylin & Eosin (HE), safranin-O, TRAP, and BrdU staining (BrdU staining kit, Invitrogen, Grand Island, NY, USA), as previously reported (3). The antibodies used for the immunohistochemistry were listed as the following: anti-DMP1-C-terminal polyclonal antibody (59), anti-E11 antibody (64), anti-sclerostin polyclonal antibody (R&D Biosystems, Minneapolis, MN, USA), and anti-osterix monoclonal antibody (Abcam, Cambridge, MA, USA) and anti-decorin monoclonal antibody (65). For the undecalcified bones, the specimens were dehydrated in ascending concentrations of ethanol (from 70% to 100%) and embedded in methyl methycrylate (MMA, Buehler, Lake Bluff, IL), then cut in 6-mm-thick slices using a Leica 2165 rotary microtome (Ernst Leitz Wetzlar). The undecalcified specimens or sections were stained by Masson goldner trichrome staining (3), Von Kossa staining and Alizarin red/alcian blue staining (28).

***β-Galactosidase (lacZ) expression assay***

The method of β-Galactosidase staining was described previously (17). The fresh fixed 3-week-old heterozygous mouse long bone was rinsed with phosphate-buffered saline after 15 min fixation, and then the specimens were stained for 48 hours in freshly prepared X-gal solution (1mg/ml) at 37 °C. The stained samples were washed with

phosphate-buffered saline again, followed by re-fixation, decalcification, and embedded in paraffin for sectioning and counterstaining.

***High-resolution radiography, microcomputed tomography (μCT) and scanning electron microscopy (SEM)***

After the muscle tissue was removed, radiographs of the bone specimens were taken using a Faxitron model MX-20 Specimen Radiography System with a digital camera (Faxitron X-Ray Corp., Lincolnshire, IL, USA). Long bone μCT analyses were performed using the Scanco μCT35 (μCT35; Scanco Medical, Bassersdorf, Switzerland). By means of serial tomographic imaging at an energy level of 55 kV and intensity of 145 μA, the cortical thickness data were obtained at the midshaft of the bone. Thus, 100 cross sections of slices above the midshaft of the femur were analyzed at the threshold of 283. The MMA-embedded samples were cut and the surfaces polished using 1 μm and 0.3 μm alumina alpha micropolish II solution (Buehler), followed by acid etching with 37% phosphoric acid for 2 to 10 seconds, 5% sodium hydrochloride for 5 minutes and then gold-coated with gold and palladium. The specimens were scanned by a FEI/Philips XL30 field-emission environmental SEM (Hillsboro, OR, USA), as described previously (25).

***Serum biochemistry***

A common cardiac puncture method was used to collect blood from the 6-week-old mice under anesthesia. The serum phosphorus was measured using the phosphomolybdate–ascorbic acid method, and the serum FGF23 level was determined with a full-length FGF23 ELISA kit (Kainos Laboratories, Tokyo, Japan), as previously described (3).

***Statistical analysis***

The data analysis was performed with a one-way ANOVA for multiple-group comparison. If significant differences were found with the one-way ANOVA, the

Bonferroni method was used to determine which groups were significantly different from the others. The quantified results are represented as the mean ± standard error of the mean (SE). We considered $P<.05$ as the statistical significance level.

## Results

### *Identify the expression and function of DMP1 in osteoblasts in vivo*

DMP1 was previously reported having *in vivo* biological functions mainly related to its expression in osteocytes during postnatal development (8,9,28). Recent *in vitro* studies also suggested DMP1 may also be expressed in the osteoblasts to regulate their function (62,66). To further identify the expression of DMP1 *in vivo*, we studied the postnatal Dmp1 expression profile using the x-gal staining approach, in which the lacZ signal reflects endogenous *Dmp1* since the lacZ reporter is used to replace exon 6 of *Dmp1* (17). Different stages of *Dmp1*-HET bones were used for this study, and we not only confirmed that the *Dmp1*-lacZ signal is mainly expressed in the osteoblast at E16.5 (Fig. 2-1, a, insert), but also identified a strong *Dmp1-lacZ* signal in both osteocytes (Fig. 2-1, a, left) and osteoblasts, with abundant blue osteoblasts in the metaphysis region of 3 week-old mice (Fig. 2-1, a).

To test the role of DMP1 in osteoblast *in vivo*, we then re-examined the phenotype of the ectopic bone mass in the *Dmp1*-null metaphysis (Fig. 2-1, b). The safranin O stain images showed a lack of cartilage residue in the *Dmp1*-null metaphysis (Fig. 2-1, c), compared to the control trabeculae, in which there were numerous cartilage remnants (Fig. 2-1, c). However, the mineralization in these expanded *Dmp1*-null metaphyses was poor, based on the von Kossa stain images (Fig. 2-1, d). Besides, there were increased mesenchymal-derived cells in the *Dmp1*-null metaphysic as found by toluidine staining (Fig. 2-1, e). We also evaluated the molecular changes in the *Dmp1*-null metaphysis and documented high levels of BrdU, *Runx2*, parathyroid receptor (*Pthr*), and OSX compared to the control (Figs. 2-1, f-i). These results support the theory that, in addition to its role in osteocytes, DMP1 also regulates osteoblasts by slowing down cell proliferation and accelerating cell differentiation.

***The overexpression of $^{SP}$DMP1 or $^{NLS}$DMP1 greatly changed the osteoblast activities in vitro in a similar manner***

One of ways to test the dual function of DMP1 (as an ECM protein and a transcription factor) is generating two different forms of DMP1 to ensure its different subcellular localizations: $^{SP}$DMP1, the secreted DMP1 form containing its own endoplasmic reticulum (ER) entry signal sequence, and $^{NLS}$DMP1, the endogenous ER entry signal sequence was replaced by a nuclear localization signal sequence to ensure the nuclear localization of DMP1, using the adenovirus CMV (Ad-CMV) approach (Fig. 2-2, a, left). Both constructs, plus an empty Ad-CMV construct (as a control), were used to infect MC3T3 (a pre-osteoblast cell line) for 48 hours. Quantitative real-time PCR was then performed to examine the mRNA expression levels of the targeted *Dmp1* in the infected cells. As expected, there was significantly higher expression of *Dmp1* mRNAs in both forms, compared to the control (Fig. 2-2, a, right; Table 2-2). Further analyses of the common markers linked to mineralization revealed an identical response pattern in both experimental groups compared to the control. For example, *Bsp* and *Alp* sharply increased, whereas *Ocn*, *Opn*, *Dspp* and *Sost* were significantly reduced in both infected groups (Figs. 2-2, b; Table 2-2). These findings indicated that the $^{NLS}$DMP1 transgene exhibits the same biological response as that of the $^{SP}$DMP1 when highly expressed *in vitro,* in agreement with a previous report (37).

***Specifically targeting DMP1 in the nuclei of osteoblasts and osteocytes or secreting it into the matrix***

To test the *in vivo* function of both the $^{NLS}$DMP1 and $^{SP}$DMP1 transgenes, we generated transgenic mice containing these transgenes in the osteoblasts and osteocytes using a 3.6 kb *Col 1α1* promoter (Fig. 2-3, a). Three independent lines among nine partially characterized lines of $^{NLS}$DMP1 transgenic mice (see Table. 2-1) were crossed to the *Dmp1-null* mice separately, with line #2095 being fully characterized. The immunohistochemistry revealed that in the *Dmp1*-HET control, endogenous DMP1 was expressed in the bone matrices surrounding the osteocyte and its dendrites with little

signal found in the nuclei (Fig. 2-3, c), whereas in the $^{NLS}$*DMP1* transgenic mouse with the HET background, DMP1 was detected in both the bone matrix (the endogenous) and the nuclei (the transgene) of the osteoblasts and osteocytes (Fig. 2-3, c, arrows). As anticipated, there was no positive signal in the *Dmp1*-null bone matrix, whereas the $^{NLS}$DMP1 was highly expressed in the nuclei of osteoblasts and osteocytes but not in the bone matrix, compared to a expression in matrix and cytoplasm of DMP1 in the KO+$^{SP}$DMP1 group (Fig. 2-3, c). The Western blot of the cell lysates from the primary calvarial cells further confirmed a high level of $^{NLS}$DMP1 with a size of 115-KDa in the cell lysate of both HET and KO animals with $^{NLS}$*DMP1* transgene (Fig. 2-3, b).

***The Dmp1-null mice displayed hypophosphatemic rickets whith high levels of cell proliferation in the prehypertrophic zone was rescued by $^{SP}$DMP1 but not $^{NLS}$DMP1***

The key *Dmp1*-null phenotype is short limbs due to a defect in endochondral bone formation. In this study, we asked whether overexpression of the $^{NLS}$DMP1 transgene accelerates skeleton growth in the WT background. Interestingly, none of the three lines tested showed an apparent change in skeleton length and size except that there was an increase in the trabecular bone volume in the bone marrow was observed in line #2095 (Fig. 2-5, b), similar to our previous report that adding the $^{SP}$DMP1 transgene in the WT background does not accelerate *in vivo* skeleton formation or mineralization (25).

We previously demonstrated that the short stature of the *Dmp1*-null mice was secondary to the hypophosphatemia caused by the elevated FGF23 (3). This heightened FGF23 decreased Pi levels, which inhibited cell apoptosis in the hypertrophic chondrocytes (67), leading to a sharp reduction in bone growth with severe skeleton deformities (18). We hypothesized if DMP1 functioned as a transcription factor, their subcellular activity could rescue the abnormal serum FGF23 concentration. Our results suggested matrix DMP1 may be the key factor since $^{SP}$DMP1 fully normalized the serum levels of FGF23 and Pi at the age of 6 weeks; whereas, $^{NLS}$DMP1 failed to correct this affected serum biochemical changes (Figs. 2-4, a-b). We also compared the x-ray images

of mice at the ages of 3 weeks, 6 weeks and 1 year and attempted to determine which form of DMP1 may correct the remodeling defect in the *Dmp1*-KO mice, as many phenotypes are linked to the bone remodeling process and it becomes worse with age (18). Again, the representative radiographs (Fig. 2-4, e) demonstrated no apparent improvement in the KO+$^{NLS}$DMP1 animals, but the KO+$^{SP}$DMP1 group appeared to be rescued.

Unexpectedly, we also identified an expansion of the proliferating zone in the *Dmp1*-null mice with or without expression of $^{NLS}$DMP1 using Safranin O stain, an abnormity we and others hadn't systematically reported previously (Fig. 2-4, f). The BrdU images showed high levels of cell proliferation in the KO growth plate (Fig. 2-4, g). The quantitation data confirmed that these new findings have significantly different between the control and the KO groups (Figs. 2-4, c-d). However these abnormalities were greatly rescued after re-expression of $^{SP}$DMP1 as the figures and charts showed (Figs. 2-4, c-g). Our further analysis indicated several molecular markers important for chondrocyte differentiation greatly increased in the null chondrocytes, including *Runx2* (Fig. 2-4, h, *in situ*), sonic hedgehog (*Shh,* Fig. 2-4, i, *in situ*), SOX9 (Fig. 2-4, j, IHC), and osterix (OSX, Fig. 2-4, k, IHC) (68). As a whole, we demonstrated an up-regulation of chondrocyte proliferatiion and their function in the proliferating zone of *Dmp1*-null growth plate, which contributed to the expanded growth plate in the *Dmp1*-null mice. Meanwhile, we found that the *$^{NLS}$Dmp1* transgene in the null osteoblast-osteocyte had no apparent rescue effect on the rickets phenotype but $^{SP}$DMP1 did.

***Expression of $^{SP}$DMP1 in osteoblasts-osteocytes had an apparent rescue effect on mineralization while expression of $^{NLS}$DMP1 did not***

To test whether the $^{NLS}$DMP1 or the $^{SP}$DMP1 rescues mineralization defects, we stained bone (using Alizarin red) and cartilage (with alcian blue). The deformed skeleton in the *Dmp1*-null mice was essentially the same as it in KO+$^{NLS}$DMP1 group (Fig. 2-5, a), on the contrary, bone in the KO+$^{SP}$DMP1 was as normal as the HET controls (Fig. 2-5, a). Further μ-CT analysis displayed porous cortical bone in the KO and KO+$^{NLS}$DMP1

cross sectioned images (Fig. 2-5, b), and statistical analyses of bone histomorphometry showed significant changes compared to the age-matched HET and KO+ $^{SP}$DMP1 groups (Table 2-3). Additionally, the Goldner stain images (Fig. 2-5, c) also revealed no apparent rescue effect on the osteomalacia phenotype in KO+ $^{NLS}$DMP1 group. Interestingly, the expression of $^{SP}$DMP1 led to an almost full rescue of these deficiencies (Figs. 2-5, a-c).

Previously we reported that the mineralization defect in the Dmp1-*null* mice was directly linked to the pathological changes in the osteocyte morphologies, including an enlarged cell body and reduction of the dendrite number (16,69). In this study, we re-analyzed the SEM image data and found great improvement of cell morphology after re-expression of $^{SP}$DMP1 in *Dmp1*-null mouse but not in the KO+$^{NLS}$DMP1 mouse (Fig. 2-5, d), indicating that secreting DMP1 into the matrix is important for the osteocyte morphologies or functions. In accordance, analyses of mineralization-related markers indicated the secreted DMP1 but not the nuclear targeted DMP1 restored the expression pattern of 1) decorin (Fig. 2-6, a, an inhibitory factor for mineralization); 2) OSX (Fig. 2-6, b, a critical transcription factor for osteoblast function); 3) E11/gp38 (Fig. 2-6, c, E11, a marker linked to the newly formed osteocytes or immature osteocytes), or 4) sclerostin (Fig. 2-6, d, SOST, an inhibitory matrix protein against Wnt/β-catenin signaling, mainly expressed in the mature osteocytes). Collectively, the overexpression of the $^{NLS}$DMP1 in the null osteoblast and osteocyte failed to rescue osteomalacia, which challenges the dual-function hypothesis.

**Discussion**

DMP1, a key molecule controlling osteocyte function (3) and bone remodeling (70), also plays critical roles in many tissues such as cartilage, kidney, body balance, salivary, pituitary, and blood vessels (6,7,12,13,49-52). Moreover, in this report, we identified DMP1 expression in osteoblasts and its regulation of osteoblast proliferation/differentiation *in vivo*. Recent studies suggested it might also have dual function (as a transcription factor and an ECM protein) in osteogenesis (37,39).

However, the conclusion from our study did not support the hypothesis that the full-length DMP1 could act as a transcription factor, instead, the matrix expression of DMP1 had a more crucial role in bone biology.

The controversy in this study is that our *in vitro* study suggested DMP1 may function as a transcription factor in regulating osteoblasts, however, the *in vivo* study didn't agree with this data. Instead, the *in vivo* data indicated secreted DMP1 plays a more important role, since the $^{NLS}$DMP1 failed to rescue the rachitic phenotype in *Dmp1*-null mice but $^{SP}$DMP1 transgene did. Therefore, we propose that the dual-function hypothesis may reflect a non-physiological phenomenon in an extremely high *in vitro* concentration, and DMP1 actually does function as an ECM protein in both osteoblasts and osteocytes during postnatal development. Furthermore, this difference may be related to the variance between *in vivo* and *in vitro* studies. Generally, *in vivo* studies are more complicated and sometimes even lead to different conclusions when the results are compared to *in vitro* findings. For example *in vivo* cell growth is three-dimensional and affected by both local and systemic factors, especially the osteogenic cells, which are also significantly influenced by biomechanical stimulation (71).

We previously generated the $^{SP}$DMP1 transgene, which was driven by the 3.6 kb *Col 1α1* promoter (highly active in osteoblasts and osteocytes); however, it did not have an apparent effect on the WT mice but fully rescued the *Dmp1*-null mice (25,30,72), suggesting that the dosage effect of DMP1 *in vivo* is limited although it is essential for postnatal skeleton and tooth formation. As a result, the same approach and promoter were used to generate $^{NLS}$DMP1 mouse lines in this study. However, line #2095 of $^{NLS}$DMP1 transgenic mice displayed an ectopic trabecular bone formation (Fig. 2-5, b). Thus, we also evaluated another line (#2097) (Fig. 2-7) and their offspring displayed no extra bone formation, compared to line #2095. These results suggest the extra bone formation in the line #2095 was more likely resulted from the processes or the operations conducted during the generation of this transgenic line rather than a functional role of nuclear activities of DMP1.

The previous work of DMP1 was mainly focused on its role in osteocytes, since DMP1 is highly expressed in the osteocytes during postnatal development (8,9,28), In this work, we showed the continuous expression of a high level of *Dmp1-lacZ* in osteoblasts in the metaphysis during early postnatal development (Fig. 2-1, a). Furthermore, we demonstrated that the deletion of *Dmp1* leads to the acceleration of bone cell proliferation (from BrdU analysis) and osteoblast differentiation (from expression of *Runx2*, parathyroid receptor, and OSX) compared to the control, resulting in an expanded metaphysis, although the mineralization was poor (Fig. 2-1). In addition, the re-expression of DMP1 rescued the metaphysis phenotype (Fig. 2-4, e) (25,30) and the differentiation of osteoblasts (Figs. 2-6, a-d), supporting the novel role of DMP1 in osteoblasts (reducing osteoblast cell proliferation and accelerating the differentiation of osteoblasts into osteocytes).

Recent mechanistic studies suggest DMP1 is first internalized by the osteoblast/odontoblast via GRP-78-mediated endocytosis and works as a transcription factor in the nucleus to regulate the expression of osteoblast-/odontoblast-specific genes. Later during osteoblast maturation, DMP1 is phosphorylated in the nucleus, then exported into the matrix where it acts as an ECM molecule to regulate biomineralization (37,39). However, our current findings suggest that it was unlikely for the nuclear DMP1 to be transported out and secreted into the ECM during osteogenesis. First of all, both our *ex vivo* and *in vivo* analysis of $^{NLS}$DMP1 showed there was no detectable DMP1 in the culture medium and bone matrix after its transportation in the nucleus. Besides, if the nuclear DMP1 can be exported into the ECM, we would expect that $^{NLS}$DMP1 can at least partially rescue the defects of *Dmp1*-null mice; however, none of the KO+$^{NLS}$DMP1 mice showed rescue. Moreover, the M1V mutant DMP1 is presumed to enter the nuclei, since only the secretory sequence was interrupted but the NLS in the C-terminal still made function (3,37). In accordance with the results observed from mouse model, the ARHR patient with a M1V mutation had typical rachitic symptoms (3). Additionally, another transgenic DMP1 with mutations in D213 that only lead to the unsuccessful traditional processing of DMP1 but no influence in the other domains

including the secretory sequence and the NLS sequence, also failed to rescue the rachitic phenotype of *Dmp1*-null mice (47,73,74). In addition, we previously reported that the C-terminal fragment of DMP1 was sufficient to completely rescue the *Dmp1*-null mouse skeletal and dental abnormalities (25,30).

In summary, the *in vitro* over-expression of $^{SP}$DMP1 (the secreted form) or $^{NLS}$DMP1 (the nuclear form) greatly changed osteoblast differentiation in an identical manner. However, *in vivo* studies using genetic rescue approaches to target DMP1 either in the *Dmp1*-null nucleus or in the null extracellular matrix demonstrate that DMP1 functions as an ECM protein, rather than as a transcription factor, which challenges the dual-function theory. Based on new findings and the publications from our lab and others (18,34,35), we propose that DMP1 is secreted into the extracellular matrix (Fig. 2-8, a), where this ECM molecule binds to αvβ3 integrin, leading to activation of the MAP kinase signaling pathway in the cell. The deletion of *Dmp1* results in two novel phenotypes: 1) an increase in osteoblast cell proliferation, along with an inhibition in osteoblast differentiation into osteocytes, which causes abundant, but poorly mineralized intramembranous bone formation in the metaphysis (reflecting the direct role of DMP1 in osteoblasts); and 2) an increase in prechondrocyte activity (an indirect role likely due to hypophosphatemia) (Fig. 2-8, b).

# CHAPTER III

# NUCLEUS-TARGETED DMP1 FAILS TO RESCUE DENTAL DEFECTS IN DMP1 NULL MICE

## Synopsis

Dentin Matrix Protein 1 (DMP1) is essential in odontogenesis. In this study, we examined whether full-length DMP1 could function as a transcription factor in the nucleus and regulate odontogenesis. We first demonstrated that a patient with the DMP1 M1V mutation, which presumably causes a loss of the secretory DMP1 but does not affect the nuclear translocation of DMP1, shows a typical rachitic tooth defect. Furthermore, we generated a transgenic mouse in which the endoplasmic reticulum (ER) entry signal sequence of DMP1 was replaced by a nuclear localization signal (NLS) sequence (referred to as "$^{NLS}$DMP1"). Although the $^{NLS}$DMP1 was localized in the nuclei of the preodontoblasts and odontoblasts, we found that it failed to rescue the dental and periodontal defects as well as the delayed tooth eruption in *Dmp1*-null mice. We concluded that the full-length DMP1 plays no apparent role in the nuclei in odontogenesis.

## Introduction

Dentin Matrix Protein 1 (DMP1), a member of the small integrin-binding ligand N-linked glycoprotein (SIBLINGs) family (55), plays essential roles in osteogenesis and odontogenesis. DMP1 mutations in humans and its deletion in mice result in autosomal recessive hypophosphatemic rickets (ARHR), characterizing by rickets/osteomalacia, hypophosphatemia, and elevated circulating fibroblast growth factor 23 (FGF23) (3). The teeth of *Dmp1*-null mice display enlarged pulp cavities and root canals, increased thickness of the predentin zone with a reduced dentin wall, hypomineralization of dentin, abnormalities in the ultrastructure of dentinal tubules, delayed development of the third molar, breakdown of periodontal structures, and other consequences (17,34,72,75).

Several lines of evidence support the finding that DMP1 acts as an extracellular matrix (ECM) protein. First, the initial 16 amino acid residues of DMP1 deduced from its cDNA is a typical endoplasmic reticulum (ER) signal sequence, and this protein is found abundantly in the matrix (28,48). Second, the DMP1 protein sequence contains some specific acidic clusters that control the formation of oriented calcium phosphate crystals (7,31). Gajjeraman and others further confirmed that both the full-length DMP1 and the COOH-terminal fragment could accelerate the nucleation of hydroxyapatite crystals (32,33,61). Lastly, studies from our lab and others demonstrated that DMP1 has the ability to activate the extracellular signal-regulated kinase (ERK)-mitogen-activated protein kinase (MAPK) pathways via the αvβ3 integrin, leading to the translocation of phosphorylated JNK into the nucleus and the concomitant up-regulation of transcriptional activation by phosphorylated c-Jun (34-36).

However, *in vitro* studies indicated that DMP1 also might function as a transcription factor in the nucleus. George et al. first reported that the DMP1 protein sequence contained a functional nuclear localization signal (NLS) sequence, which was thought to be responsible for the nuclear import of full-length DMP1 in pre-odontoblast-like cells (37). They further demonstrated that the extracellular full-length DMP1 could be internalized via endocytosis mediated by glucose-regulated protein-78 (GRP-78), an endoplasmic reticulum (ER) chaperone protein found on the plasma membrane of preodontoblasts and subsequently transported into the nucleus. Once in the nucleus, DMP1 regulates the transcription of odontoblast-specific genes such as DSPP (37,39). These investigators proposed that during the maturation of the pre-odontoblast/odontoblast, this nuclear DMP1 would be phosphorylated by casein kinase II, leading to its exportation into the extracellular matrix where it promotes hydroxyapatite formation (37). However, the role of nuclear DMP1 has been challenged by the identification of several patients who presumably have normal nuclear localization of DMP1 due to a biallelic nucleotide substitution in the DMP1 start codon (ATG to GTG, or A1→G), but who display hypophosphatemic rickets (3). Therefore,

whether DMP1 can enter the nucleus and function as a transcription factor *in vivo* needed to be studied further.

This study was aimed at determining the nuclear DMP1 in odontogenesis had an *in vivo* function. Our human studies revealed that an ARHR patient, with a M1V mutation at the DMP1 start codon, manifested typical rachitic dental defects. Animal studies showed that the targeted expression of $^{NLS}$DMP1 in the *Dmp1*-null nucleus failed to rescue the *Dmp1*-null dental defects, suggesting that DMP1 plays no apparent role in the nuclei during odontogenesis.

## Materials and Methods

### *Human subjects*

The study protocol and patient consents were reviewed and approved by the Institutional Review Boards at the University of Ottawa. Dental radiographs were obtained from the previously described individual (3).

### *Generation of Col1α1-$^{NLS}$DMP1 transgenic mice*

For the generation of the Col1α1-$^{NLS}$DMP1 transgene, the full-length mouse *Dmp1* cDNA with its ER-entry signal sequence (30) replaced by an NLS sequence ($^{NLS}$DMP1). Together with a SV40 polyadenylation signal, the NLS sequence was cloned into the EcoR V and Sal I sites of a mammalian expression vector (63) downstream of the 3.6 kb rat type I collagen promoter plus a 1.6 kb intron 1. The Col1α1-$^{NLS}$DMP1 transgene was then released from the vector backbone by Sac II and Sal I and purified for pronuclear injection. Transgenic founders with a C57B/L6 background were generated at the UT Southwestern Medical Center, Dallas, TX, USA. Genotyping was conducted as previously (34,72).

### *Targeted expression of the $^{NLS}$DMP1 in Dmp1-null mice*

Three of five independent transgenic lines were separately crossed with *Dmp1*-null (*Dmp1*$^{-/-}$) mice to introduce the Col1α1-$^{NLS}$DMP1 transgene into the *Dmp1*$^{-/-}$ mice

(referred to as "*Dmp1*$^{-/-}$; Col1α1-$^{NLS}$DMP1"). All three transgenic lines had similar rescue effects on the *Dmp1*-null dental defects, so only the data obtained from line #95 are presented. The littermate *Dmp1*-heterozygous (*Dmp1*$^{+/-}$) mice were used as control mice since there was no phenotypic difference between these *Dmp1*$^{+/-}$ and wild-type (WT) mice. The mice were fed with Purina rodent chow (5010, Ralston Purina, St. Louis, MO, USA) containing 1% calcium, 0.67% phosphorus, and 4.4 IU of vitamin D/g. All the animal procedures were performed in accordance with the National Institutes of Health Guide for the Care and Use of Laboratory Animals and approved by the Institutional Animal Care and Use Committee of Texas A&M University Baylor College of Dentistry (Dallas, TX, USA).

***Histology***

The animals were sacrificed and fixed in freshly made 4% paraformaldehyde/PBS (pH 7.4), followed by decalcification and paraffin embedding. Sections (4.5 μm) were cut for histochemistry staining and immunohistochemistry staining as previously described (3). Toluidine Blue and Sirius Red (also called "Direct Red 80") were obtained from Sigma (Sigma, St. Louis, MO, USA). The antibodies used for immunohistochemistry were anti-DMP1-C-terminal polyclonal antibody (59), anti-DSP monoclonal antibody (76) and anti-Biglycan monoclonal antibody (77).

***High-resolution radiography, microcomputed tomography (μ-CT) and resin casted scanning electron microscopy (SEM)***

The mouse mandibles were dissected free of muscle. High-resolution radiographs were taken using a plain x-ray radiography system (Faxitron MX-20DC12 system, Faxitron Bioptics) with a digital camera (Faxitron X-Ray Corp., Lincolnshire, IL, USA). μ-CT analysis was performed with the Scanco μCT35 (Scanco Medical, Bassersdorf, Switzerland) as described previously (34). For SEM analysis, the samples were embedded in methyl methacrylate and cut to expose the dental pulp and root canals; the surface was then polished using alumina alpha micropolish II solution (Buehler), acid

etched, and then scanned by a FEI/Philips XL30 field-emission environmental SEM (Hillsboro, OR, USA) as described previously (25).

***Statistical analysis***

Data analysis was performed with one-way ANOVA for multiple-group comparison. If significant differences were found with one-way ANOVA, the Bonferroni method was used to determine which groups were significantly different from others. The quantified results were presented as the mean ± SEM. $p<.05$ was considered statistically significant.

## Results

***A patient with a DMP1 M1V mutation displayed deformed teeth***

We previously reported that a DMP1 M1V mutation was identified in an ARHR patient (3). The DMP1 in this patient had a start codon mutation (A→G) resulting in the substitution of the initial methionine with valine. As a result, there was no signaling peptide (Fig. 3-1, a). Further analysis revealed that the M1V mutant DMP1 protein was wholly retained within the cells as the 94-kDa full-length DMP1 without cleavage, consistent with the change of translational initiation (at an internal methionine) that results in the loss of the ER-entry signal peptide (3,57). Dental radiographs (Fig. 3-1, b, upper panel) showed enlarged pulp cavities and root canals as well as thinner dentin, compared to an age-matched control (Fig. 3-1, b, lower panel). These dental defects were very similar to those of other *DMP1* mutation kindreds (22) and *Dmp1*$^{-/-}$mice (17,72).

***$^{NLS}$DMP1 did not rescue the dental defects of Dmp1$^{-/-}$ mice***

To understand whether DMP1 plays a role in the nuclei *in vivo*, we generated *Col1α1*-$^{NLS}$DMP1 transgenic mice, which not only mimic the M1V mutation that leads to the suppression of its secretion, but also ensure its nuclear transportation by using an NLS sequence to replace its ER-entry signal sequence. Three of five independent lines

were then crossed with the *Dmp1*$^{-/-}$ mice to introduce $^{NLS}$DMP1 into the *Dmp1*$^{-/-}$ background. All three transgenic lines showed a similar phenotype, although only the results obtained from line #95 were presented. Immunohistochemistry staining of DMP1 revealed that in the control *Dmp1*$^{+/-}$ mice, endogenous DMP1 was detected in the dentinal matrix and alveolar bone matrix, as well as the cytoplasm and dendrites of odontoblasts (Figs. 3-2, a-c), compared to no signal in the *Dmp1*$^{-/-}$ mice (Figs. 3-2, a-c). Notably, $^{NLS}$DMP1 was identified in the nuclei, cytoplasm, and dendrites of the preodontoblasts and odontoblasts, but not in the dentinal matrix of the *Dmp1*$^{-/-}$; Col1α1-$^{NLS}$DMP1 mice (Fig. 3-2, a-c).

Next, a series of experiments were performed to assess whether the targeted expression of the $^{NLS}$DMP1 had rescue effects on the *Dmp1*-null dental defects. The representative radiographs demonstrated that, similar to the *Dmp1*$^{-/-}$ teeth, the teeth of the *Dmp1*$^{-/-}$; Col1α1-$^{NLS}$DMP1 mice teeth displayed significantly thinner dentin and shorter roots (Fig. 3-2, d; Figs. 3-7, a-b, $P<0.01$), enlarged pulp cavities and root canals (Fig. 3-2, d). Histological analysis further confirmed that, like the *Dmp1*$^{-/-}$ mice, the *Dmp1*$^{-/-}$; Col1α1-$^{NLS}$DMP1 mice teeth manifested a reduced thickness of the dentin walls and an increased thickness of the pre-dentin zone (Figs. 3-3, a-c), indicating there was a partial failure of pre-dentin to dentin maturation. At 6 weeks of age, the expanded pre-dentin remained, and the interglobular dentin, which originated from the incompletely calcified dentinal matrices between the calcified globules, were found in both the *Dmp1*$^{-/-}$ and *Dmp1*$^{-/-}$; Col1α1-$^{NLS}$DMP1 mice (Fig. 3-2, c). In addition, larger collagen fibers (Fig. 3-3, d) and high levels of biglycan (Fig. 3-5, c) were present in the dentin or pre-dentin in both the *Dmp1*$^{-/-}$ and *Dmp1*$^{-/-}$; Col1α1-$^{NLS}$DMP1 mice, compared to the control mice. Furthermore, DSPP, which is predominantly expressed in the odontoblast and is essential to dentin mineralization (78,79), was considerably decreased in both the *Dmp1*$^{-/-}$ and *Dmp1*$^{-/-}$; Col1α1-$^{NLS}$DMP1 mice (Fig. 3-3, e). Scanning electron microscopy analysis showed that fewer dentinal tubules and branches in both *Dmp1*$^{-/-}$ and *Dmp1*$^{-/-}$; Col1α1-$^{NLS}$DMP1 mice (Fig. 3-3, f). Consistently, study of another independent mouse line (Line #97) (Fig. 3-7, d) showed the same result that $^{NLS}$DMP1 did not improve the

*Dmp1*$^{-/-}$ dental defects. All of these data demonstrated that the $^{NLS}$DMP1 transgene failed to rescue the defects during odontoblast differentiation and dentinal mineralization in *Dmp1*$^{-/-}$ mice.

### $^{NLS}$*DMP1 did not cure the defects of periodontal structures in Dmp1*$^{-/-}$ *mice*

We previously reported that *Dmp1*$^{-/-}$ mice developed an early-onset periodontal defect (17,34,72) and analyzed whether $^{NLS}$DMP1 rescued the periodontal defects in *Dmp1*$^{-/-}$ mice. These mice displayed typical combined periodontal-endodontic lesions or tooth exfoliation at 1 year of age (Fig. 3-4, a), which was predominantly due to the loss of the periodontal attachment (Figs. 3-4, b-c). Sirius Red staining further confirmed that the collagen content had decreased in the PDL (Fig. 3-5, arrows) and that the collagen fibers appeared to be thinner in polarized light image, suggesting the presence of more reticular fibers (Fig. 3-5, b) in both the *Dmp1*$^{-/-}$ and *Dmp1*$^{-/-}$; Col1α1-$^{NLS}$DMP1 mice, compared to the control mice. Biglycan staining also showed reduced biglycan protein in the PDL of the *Dmp1*$^{-/-}$ and *Dmp1*$^{-/-}$; Col1α1-$^{NLS}$DMP1 mice (Fig. 3-5, c). Furthermore, the alveolar bone was hypomineralized and not well organized in the *Dmp1*$^{-/-}$ and *Dmp1*$^{-/-}$; Col1α1-$^{NLS}$DMP1 mice (Figs. 3-5, d-e). Collectively, these observations indicated that $^{NLS}$DMP1 did not rescue the periodontal defects of the *Dmp1*$^{-/-}$ mice.

### $^{NLS}$*DMP1 did not prevent the delay of tooth eruption in Dmp1*$^{-/-}$ *mice*

Unexpectedly, we also discovered a delayed tooth eruption in the *Dmp1*$^{-/-}$ mice. At the age of 10 days, the first molars had not fully erupted and were still partially embedded in the bony crypts in both the *Dmp1*$^{-/-}$ and the *Dmp1*$^{-/-}$; Col1α1-$^{NLS}$DMP1 mice (Figs. 3-6, a-b). The development of the bony crypt for the third molars was also delayed in the *Dmp1*$^{-/-}$ and *Dmp1*$^{-/-}$; Col1α1-$^{NLS}$DMP1 mice (Figs. 3-6, a-b). By the age of 3 weeks, these third molars had still not fully erupted compared to the control mice (Fig. 3-6, c). Furthermore, TRAP staining showed that there was a significant decrease in osteoclast number in both *Dmp1*$^{-/-}$ and *Dmp1*$^{-/-}$; Col1α1-$^{NLS}$DMP1 mice (Fig. 3-6, d; Fig. 3-7, c). These findings suggested that the delayed tooth eruption in the *Dmp1*$^{-/-}$ mice

might be due to a decrease in osteoclast formation and that $^{NLS}$DMP1 did not rescue this defect.

**Discussion**

DMP1 is actively expressed in the mandibular odontoblasts, osteoblasts and osteocytes. *In vitro* studies suggested that the DMP1 C-terminal contains NLS signals and can function as a transcription factor during osteogenesis/odontogenesis (37). In this study, we investigated the potential nuclear function of the full-length DMP1 *in vivo* in odontogenesis using a clinical case and mutant mouse models. Our results showed that (1) *DMP1* mutations (M1V, resulting in a loss of the ER-entry signal peptide but with the intact DMP1 preserved in the cell) led to enlarged pulp/root canals and thin dentin; (2) the nucleus-targeted DMP1 failed to rescue the tooth and periodontal structure defects in *Dmp1*-null mice; and (3) *Dmp1*-null mice unexpectedly developed delayed tooth eruption, which was not rescued by the nucleus-targeted DMP1 either. Thus, the current studies do not support the hypothesis that the full-length DMP1 has any nuclear function *in vivo*.

We previously reported that the reexpression of secretory full-length DMP1 under the control of a 3.6 kb Col1α1 promoter completely rescued the skeletal defects and serum biochemical abnormalities of *Dmp1*$^{-/-}$ mice by the age of 7 weeks (25). However, when the same 3.6 kb Col1α1 promoter was used to drive the expression of nucleus-targeted $^{NLS}$DMP1, the construct failed to rescue the defects of the tooth and periodontal structures or the delayed tooth eruption observed in *Dmp1*$^{-/-}$ mice. In addition, we showed that the ARHR patient with a M1V mutation, which presumably affected the secretion of DMP1 but not its nuclear localization, manifested a typical rachitic tooth defect. These mouse and human genetic studies suggest that DMP1 might not have an apparent role in the nucleus *in vivo*.

George's group proposed that DMP1 might shuttle between the nucleus and extracellular milieu (37,39), as they observed that DMP1 contains both the functional NLS and the functional nuclear export signal (NES) sequences (37). They speculated

that during osteoblast/odontoblast differentiation, the extracellular DMP1 was taken up by the cells via GRP-78-mediated endocytosis and subsequently transported into the nucleus to regulate the expression of the osteoblast-/odontoblast-specific genes (39). They also proposed that during osteoblast maturation, DMP1 was phosphorylated and exported into the extracellular matrix to regulate matrix mineralization (37). In the current study, we demonstrated that $^{NLS}$DMP1 was localized in the nuclei of *Dmp1*-null odontoblasts and that the M1V mutant DMP1 with the NLS signal in the intact molecule should be able to enter the nuclei. Therefore, both $^{NLS}$DMP1 and M1V mutant DMP1 should be exported into the ECM. However, we showed that $^{NLS}$DMP1 was neither found in the matrix nor did it rescue any dental defects of *Dmp1*$^{-/-}$ mice. Furthermore, the ARHR patient with a M1V mutation developed a typical rachitic dental defect that was similar to those of other ARHR patients (22,34).

Interestingly, our recent findings suggest that there might be a nuclear isoform of DMP1 (referred to as "nuDMP1") translated from an alternative downstream in-frame start codon (AUG210 or AUG227 for mouse Dmp1) of the same mRNA that encodes the secretory DMP1 (80,81). This nuDMP1 form lacks the ER-entry signal sequence and the 37-kDa $NH_2$-terminal sequence, but maintains the NLS sequence in its COOH-terminal. Our studies revealed that the nuDMP1 enters the nucleus and regulates cell differentiation *in vitro* (80,81). It is possible that the 37-kDa $NH_2$-terminal sequence may present a steric hindrance that interferes with the function of nuDMP1, as the 57-kDa COOH-terminal fragment of *Dmp1* transgene fully rescued the *Dmp1*$^{-/-}$ defects (25). However, the intact DMP1 form with the mutated cleavage sites (i.e., no 37-kDa $NH_2$ is removed from the COOH-terminal fragment) failed to rescue the *Dmp1*-null phenotype (47,74). Currently, we plan to test this theory by crossing the nuDMP1 transgene into the *Dmp1*$^{-/-}$ background.

In summary, we have demonstrated that the nucleus-targeted full-length DMP1 failed to rescue the dental defects in *Dmp1*$^{-/-}$ mice, suggesting that full-length DMP1 plays no apparent role in the nucleus *in vivo* during odontogenesis.

# CHAPTER IV

# A KEY PATHOLOGICAL ROLE OF WNT/B-CATENIN IN HYPOPHOSPHATEMIC RICKETS

## Synopsis

Deletion or mutation of *Dmp1* or *Phex* leads to a hypophosphatemic rachitic/osteomalacic disorder, in which increased FGF23 plays a key pathological role. However, we recently found that elevated β-catenin expression levels in *Dmp1*-null and Hyp mice (*Phex*-deficient mice) also have a role in the development of hypophosphatemic rickets/osteomalacia. To affirm this hypothesis, we first crossed *Dmp1*-null mice with *2.3 Col 1-Dkk1* transgenic mice, generating offspring that over-expressed DKK1 (a potent inhibitor of the Wnt/β-catenin signaling pathway) in the osteoblasts and osteocytes. By 3 weeks, the targeted expression of DKK1 and consequent blockade of Wnt/β-catenin signaling significantly improved the following elements of the rachitic/osteomalacic phenotype: 1) FGF23, PTH, Pi and Ca levels; 2) skeleton length (long bone and vertebrae); 3) growth plate thickness; 4) epiphysis and metaphysis phenotype; 5) cell proliferation (BrdU); 6) molecular bone markers (OSX, BSP, OPN, Col I, Biglycan); and 7) bone mineralization and formation rates. By 8 weeks, the *Dmp1*-null phenotype had further improved. Moreover, the DKK1 transgene also partially rescued the Hyp mice. Further analysis indicated this elevated Wnt/β-catenin signaling activity was responsible for the maturation defects of the osteocytes, since the constitutive expression of β-catenin specifically in the osteocytes recaptured the osteomalacia phenotype. In addition, the anti-Wnt signaling compound treatment also improved the rachitic phenotype in the *Dmp1*-null mice. Taken together, we demonstrated that an abnormally high level of Wnt/β-catenin expression in *Dmp1*-null mice and Hyp mice was a key pathological local factor responsible for defects in the osteoblast/osteocyte maturation leading to hypophosphatemic rickets/osteomalacia.

## Introduction

Dentin matrix protein 1 (DMP1) is expressed predominantly in odontoblasts in tooth and osteocytes in bone (6,8,9,48). The deletion of murine *Dmp1* causes striking defects in tooth and bone during postnatal development in mice that are similar to the *DMP1* mutations in autosomal recessive hypophosphatemic rickets (ARHR) patients (3). ARHR, together with x-linked dominant hypophosphatemic rickets (XLH, caused by *PHEX* gene mutation) (1) and autosomal dominant hypophosphatemic rickets (ADHR, resulting from *FGF23* gene mutation) (2), were considered to be heritable hypophosphatemic rickets/osteomalacia. These inherited diseases make up a group of disorders characterized by hypophosphatemia, which results from inherited gene mutation and leads to dietary phosphorus deficiency and/or disorders of renal phosphate wasting. The characteristics of inherited hypophosphatemic rachitic/osteomalacic disorder included short stature, skeletal deformities, cartilaginous defects, tooth abnormalities and changes of serum biochemistry markers. Furthermore, our recent studies suggested that DMP1 likely regulates the downsizing process in osteoblastic protein expression and metabolic activity during the maturation of osteoblasts into osteocytes (16). It is indicated that DMP1 regulates normal osteoblast-to-osteocyte maturation and its deletion would disrupt the differentiation process (16). However, other molecular and cellular mechanisms involved in DMP1 regulation are largely unknown.

It is well known that fibroblast growth factor 23 (FGF23) is a key factor in the pathogenesis of hypophosphatemic rickets/osteomalacia (3,82-85). Studies have shown that FGF23, as a potent phosphaturic hormone, is significantly up-regulated in the osteocytes and then targets the kidneys to promote renal excretion of phosphate, which led to decreased serum phosphorus levels in *Dmp1*-null mice and *Hyp* mice (3,16,84-87). However, the restoration of phosphate homeostasis by a higher phosphate diet or FGF23 antibody injection only partially rescues the bone formation rate and osteomalacia, as well as the maturational defects of osteocytes (16). As a result, it was suggested there

could be other factors or signal pathways involved in the development of the rickets/osteomalacia phenotype in these mice.

Some of our previous results implied that canonical Wnt/β-catenin signaling may be involved in the phenotype formation primarily because the serum biochemistry analyses of *Dmp1*-null mice showed that the parathyroid hormone (PTH) levels increased more than 5-fold. PTH was able to induce β-catenin stabilization through the low-density lipoprotein receptor-related protein (LRP) 6 and PTH receptor (88,89). Secondly, a dramatically decreased expression of sclerotin (SOST), an inhibitor of the Wnt/β-catenin pathway, was found in the osteocytes of *Dmp1*-null mice (16). As a target downstream of SOST, canonical Wnt/β-catenin signaling could be abnormally up-regulated in the *Dmp1*-null osteocytes. As a result, we hypothesized that there was an increased expression of β-catenin in the *Dmp1*-null osteocytes and that this ectopic activity of β-catenin might cause the disruption of the maturational progress of the late osteo-lineage (including osteoblast differentiation and osteocyte maturation), subsequently leading to defective bone mineralization and porosity.

In this study, we identified that an up-regulation of Wnt/β-catenin signaling activity in *Dmp1*-null was one of key factors affecting the osteoblast differentiation and osteocyte maturation. We then normalized the β-catenin level in both *Dmp1*-null mice and *Hyp* mice by crossing them with DKK1 transgenic mice (2.3 Col 1α1-DKK1). We evaluated the bone morphology and mineralization, osteocyte and osteoblast maturation and function, and biochemical testing; all the tests indicated a significant rescue of the osteomalacia phenotype in these mice. In addition, we also cured the osteomalacia defects of *Dmp1*-null mice using an anti-β-catenin compound injection. Altogether, these results suggested that the increased activity of the canonical Wnt signaling pathway was a key factor, except for FGF23, which was responsible for the development of hypophosphatemic rickets/osteomalacia by regulating the maturational process and biological functions of osteocytes.

## Subjects and Methods

### *Constitutive stabilization of β-catenin in osteocytes in vivo*

Two kinds of mice were used to investigate the role of increased β-catenin activity in osteocytes *in vivo*. Mice with the targeted β-catenin gene (exon 3) located within *loxP* sites (β-cat$^{ex3loxP/loxP}$) (90) were obtained from the Jackson Laboratory (Bar Harbor, ME, USA) and were crossed with *Dmp1-Cre* transgenic mice, which express Cre recombinase selectively in osteocytes under the control of a 14 kb promoter fragment of the *Dmp1* (91). Heterozygous mice with constitutively activated β-catenin specifically in the osteocytes (*Dmp1-Cre*; β-cat$^{ex3loxP/+}$, referred to as "CA-β") were generated from crossing both mouse lines, and the progeny were analyzed. The data obtained from *Dmp1-Cre* transgenic mice were pooled and used as controls (referred to as "Cont"). All of the mice were fed with autoclaved Purina rodent chow (Ralston Purina, St. Louis, MO, USA) containing 1% calcium, 0.67% phosphorus, and 4.4 IU of vitamin D/g. All animal procedures were performed in accordance with the National Institutes of Health Guide for the Care and Use of Laboratory Animals and approved by the Institutional Animal Care and Use Committee of Texas A&M University Baylor College of Dentistry (Dallas, TX, USA).

### *Dkk1 transgene in Dmp1-null or Hyp-mice*

The *Dkk1* transgene (46) was driven by the 2.3 kb Col 1α1 promoter in the transgenic *Dkk1* mice. These mice were crossed with *Dmp1*-null mice (8) and *Hyp*-mice (92). Among their offspring, WT mice were used as the control group. Other groups of mice included Dkk1-Tg with wild type background (DKK1), *Dkk1*-Tg with *Dmp1* knockout background (DKK1; KO), Dkk1-Tg with *Phex* inactivated mutation (DKK1; Hyp), *Dmp1* conventional knockout (KO); and loss-of-function mutation of *Phex* (Hyp). The genetic backgrounds of all the mice were uniform mixtures of CD1-C57BL/6J.

***Anti-β-catenin compound injection***

A compound drug that acts as an inhibitor of Wnt response (IWR-1) was kindly provided by Dr. Lawrence Lum (University of Texas Southwestern Medical Center, Dallas, TX) as a gift (93). Briefly, IWR-1 is a small molecule (M.W. 410.2) that inhibits Axin2 protein destruction. To make the injection formulation, IWR-1 was dissolved in N,N-dimethylacetamide, Cremophor EL, and sodium bicarbonate (ph=9.0) (Sigma-Aldrich, St. Louis, MO, USA). One-week-old mice were injected (i.p.) daily (7.1mg/kg) (referred to as "KO+IWR") and sacrificed at four weeks. Their littermates injected with the vehicle were used as the controls (referred to as "HET+Vehicle" or "KO+Vehicle").

***PCR genotyping***

Genomic DNA was extracted from a tail biopsy done on each mouse and used for genotyping by PCR analysis. The primers used were the following: *LacZ* (forward: 5'-GAG TGC GAT CTT CCT GAG GCC GAT ACT GTC-3' and reverse: 5'-CGC GGC TGA AAT CAT CAT TAA AGC GAG TGG-3'; 490 bp); endogenous *Dmp1* (forward: 5'-GCC CCT GGA CAC TGA CCA TAG C-3' and reverse: 5'-CTG TTC CTC ACT CTC ACT GTC C-3'; 337 bp); *Dkk1*-Tg (forward: 5'-ATT CCA ACG CGA TCA AGA ACC TG-3' and reverse: 5'-GCA AGC CAG ACA GAT CTG TAC-3'; 236 bp); *Phex* (forward: 5'-CCA AAA TTG TTC TTC AGT ACA CC-3' and reverse: 5'-ATC TGG CAG CAC ACT GGT ATG-3'; 258 bp); *Cre* (forward: 5'-CCC GCA GAA CCT GAA GAT G-3' and reverse: 5'-GAC CCG GCA AAA CAG GTA G-3'; 534 bp); β-cat$^{ex3loxP}$ (forward: 5'-AGG GTA CCT GAA GCT CAG CG-3' and reverse: 5'-CAG TGG CTG ACA GCA GCT TT-3'; 646 bp). The reagents and conditions used were as previously described (25).

***Histomorphometric and immunohistological analyses***

The animals were injected with BrdU (5-Bromo-2'-deoxyuridine, 100 ug/g mouse, i.p.; Sigma-Aldrich, St. Louis, MO, USA) once a day and injected twice before they were sacrificed. Perfusion of the mouse heart chamber with freshly prepared 4%

paraformaldehyde in PBS (pH 7.4) was used for sacrifice. The samples were further fixed in the same fixation solution for 2 days in 4°C and then stored in 0.5% paraformaldehyde/PBS. The long bones were dissected from the whole body, free of muscle, and then decalcified and embedded in paraffin as described previously (8). Sections were cut (4.5 μm) and mounted on slides and dried. After dewaxing and rehydration, they were used for histomorphometric and immunohistological analyses. The methods included Hematoxylin & Eosin (HE), Sirius Red, TRAP, BrdU (BrdU staining kit, Invitrogen, Grand Island, NY, USA), *in situ* hybridization, and immunohistochemistry staining, as formerly reported (3). The antibodies and probes used were the following: anti-Biglycan monoclonal antibody (24), anti-osterix (OSX) monoclonal antibody (Abcam, Cambridge, MA, USA), anti-osteopontin (OPN) monoclonal antibody (Santa Cruz Biotechnology, TX, USA) and anti-bone sialoprotein (BSP) monoclonal antibody (51,94) anti-E11 polyclonal antibody (64), anti-DMP1-C-terminal polyclonal antibody (59), anti-sclerostin polyclonal antibody (R&D Biosystems, Minneapolis, MN, USA), anti-dickkopf-1 (DKK1) polyclonal antibody (R&D Biosystems, Minneapolis, MN, USA), and anti-β-catenin monoclonal antibody (Sigma-Aldrich, St. Louis, MO, USA).

***Mineral deposition analysis***

To evaluate the amount of mineralization, the mice were injected (i.p.) with calcein green (5 mg/kg, Sigma-Aldrich, St. Louis, MO, USA), followed by injection of an Alizarin Red (5 mg/kg; Sigma-Aldrich, St. Louis, MO, USA) 5 days later. The mice were sacrificed 48 hours after the second label, and the bones were dissected free of muscle and then fixed in 70% ethanol for 3 days. Later, the undecalcified bones were dehydrated in ascending concentrations of ethanol (from 70% to 100%) and embedded in methyl methyacrylate (MMA, Buehler, Lake Bluff, IL) and sectioned (6 mm) using a Leica 2165 rotary microtome (Ernst Leitz Wetzlar). These sections were photographed using a Leica SP5 confocal microscope for fluorochrome labeling. The mineralization of

the same samples was analyzed with Goldner Masson's trichrome staining and photographed with a wide field light microscope, as described previously (3).

***In vivo β-galactosidase analysis***

Mice with the top-gal (95), a β-galactosidase gene under the control of the lymphoid enhancing factor (LEF)/T cell factor (TCF) (DNA-binding protein complex that acts in concert with nuclear localized β-catenin) and c-fos (β-catenin inducible promoter) were crossed with *Dmp1* conditional knockout mice (*3.6 kb Col I-Cre*; $Dmp1^{loxP/loxP}$). In the offspring with a top-gal transgene, the β-galactosidase expression was directly stimulated by a stabilized form of β-catenin, but was also dependent upon LEF/TCF in the bone. Top-gal transgenic mice without the conditional *Dmp1* knockout background were used as controls (referred to as "Top-gal+"), whereas mice with Top-gal+; *3.6 kb Col I-Cre*; $Dmp1^{loxP/loxP}$ (referred to as "Top-gal; CKO") were used as the experimental group. β-galactosidase staining was performed as previously described (91).

***High-resolution radiography, microcomputed tomography (μ-CT) and scanning electron microscopy (SEM)***

Long bone radiographs were taken using a Faxitron model MX-20 Specimen Radiography System with a digital camera (Faxitron X-Ray Corp., Lincolnshire, IL, USA). The μ-CT analysis was performed using a Scanco μCT35 (μCT35; Scanco Medical, Bassersdorf, Switzerland). The cortical porosity was obtained from analyzing the midshaft of each group. One hundred cross-sectional slices of the midshaft were analyzed at the threshold of 283. Scanning electron microscopic (SEM) images were taken using the MMA-embedded long bone as previously described (3). The samples were cut to expose the cortical surface and then polished using 1 μm and 0.3 μm alumina alpha micropolish II solution (Buehler). This step was followed by acid etching with 37% phosphoric acid for 2 to 10 seconds, 5% sodium hydrochloride for 5 minutes and

then coated with gold and palladium. The scanning electron microscopy was performed with a FEI/Philips XL30 field-emission environmental SEM (Hillsboro, OR, USA).

***Quantitative real-time PCR***

Total RNA was extracted from mouse long bones using the Trizol reagent (Invitrogen, San Diego, CA, USA) and then reverse-transcribed into cDNA using the Super Script first-strand synthesis system (Invitrogen, San Diego, CA, USA). The real-time PCR analysis of *β-catenin* and *Fgf23* was done using TaqMan Gene Expression Specific Probes (Life Technologies, NY, USA), and GAPDH (used as an internal control, forward primer, 5'-ACC ACA GTC CAT GCC ATC AC-3', and reverse primer, 5'-TCC ACC ACC CTG TTG CTG TA-3'). The SYBR Green System (Applied Biosystems, Carlsbad, CA, USA) was used as described in our previous studies (25).

***Protein extracts and western blot***

The total protein was extracted from both wild type (WT) and Hyp mouse long bones under the same conditions. The concentrations were adjusted according to the instructions for the BCA kit (Pierce, Rockford, IL, USA). Ten μg of total protein from each group at a concentration level of 0.2 μg IgG/ml was subjected to 10% SDS-PAGE gel, followed by blotting onto a polyvinylidene difluoride membrane. Anti-β-catenin-antibodies (Cell Signaling, Danvers, MA, USA) were used (1:1000) for detection. An anti-β-actin-antibody (Cell Signaling, Danvers, MA, USA) was used as an internal control. The blots were washed and incubated with a color development reagent (Ambion, Grand Island, NY, USA). The bands were assayed with a Kodak film imaging system (Perkin Elmer, Waltham, MA, USA) after 5 min exposure.

***Serum biochemistry***

Mouse blood was collected through heart punctures, and serum was obtained by precipitation and centrifugation at 6,000 rpm for 30 min. The serum FGF23, phosphorus (Pi), Calcium (Ca) and PTH levels were determined as previously described (3).

***Statistical analysis***

The data from the two experimental groups were analyzed by student's T test, while the data sets with more than two groups were analyzed using a one-way ANOVA. If significant differences were found, the Bonferroni method was used to determine which groups were significantly different from the others. The quantified results were represented in mean ± standard error of the mean (SE). We considered $P<.05$ as statistically significant.

**Results**

***Elevated Wnt/β-catenin signaling pathway activity in Dmp1-null mice***

We reported previously that the serum PTH level (3) and the expression level of SOST were notably down-regulated (16) in the *Dmp1*-null mice. As the anti-SOST immunostain (Fig. 4-1, left) indicated, SOST is normally produced primarily by osteocytes and is abundant in the osteocytic canalicular system and bone surface. There it interacts with late-osteoblast/preosteocyte and lining cells so as to regulate their status (quiescent or mature) via the canonical Wnt/β-catenin signaling pathway (96-98). SOST remarkably decreased in the osteocytes of the *Dmp1*-null mice (Fig. 4-1, left), which may have led to abnormal Wnt/β-catenin signaling activity. To further clarify this hypothesis, we first analyzed both the mRNA and protein expression levels of β-catenin in the long bones, and the results suggested a significant increase of β-catenin in the *Dmp1*-null mice (Figs. 4-2, a-b), especially in the osteocytes, compared to the controls. We then further tested whether this increased β-catenin level was transported into the nucleus and regulated gene expression. TCF*,* one of the direct downstream genes of β-catenin that serves as a transcriptional co-activator regulating gene expression, was detected using Top-gal staining of the *Dmp1* conditional knockout mice (Fig. 4-2, c) and *in situ* hybridization of the *Dmp1*-null mice (Fig. 4-2,d). The results supported the immnunohistochemical analysis that the Wnt/β-catenin signaling in the *Dmp1*-null osteocytes was elevated, compared to the controls. Taken together, *Dmp1* deletion led to the increased activity of Wnt/β-catenin signaling, which targeted the osteocytes and may

have been responsible for the development of the rickets/osteomalacia phenotype in the *Dmp1*-null mice.

***β-catenin regulated osteocyte maturation and function***

To demonstrate the hypothesis that the up-regulated Wnt/β-catenin activity in osteocytes was responsible for its maturational defect, we specifically induced β-catenin expression in the osteocytes by crossing the *Dmp1-Cre* mice with β-cat$^{ex3loxP/loxP}$ mice, which introduced a constitutive stabilization of β-catenin in the osteocytes. The offspring had a rickets-/osteomalacia-like phenotype, including short stature (Fig. 4-3, a), cortical bone porosity (Fig. 4-3, b), and hypomineralization (Figs. 4-4, a-c). The histological images suggested that, compared with the controls, the matrix of the mutant cortical bone was filled with type I collagen (Col I) and biglycan, which is a small leucine-rich repeat proteoglycan that interacted with Col I (99,100) and appeared to have an increased osteoid area. These results highly indicated that the mineralization of the cortical bone in the mutant mice was suppressed compared to the controls. Immunohistochemistry labeling of the osteogenic markers [OSX (Fig. 4-4, d) and OPN (Fig. 4-4, e) for the osteoblasts, E11 (Fig. 4-4, f) for newly formed osteocytes] demonstrated that the ectopic β-catenin levels in osteocytes led to the maturational defect (Figs. 4-4, d-f). Cell proliferation analysis (Fig. 4-3, c; Fig. 4-4, g) indicated that the osteocytes in the CA-β mice maintained their proliferation abilities, which further supported the idea that there was an interrupted maturational process. However, serum biochemistry testing showed the Pi, FGF23 and Ca levels hadn't significantly changed (Table. 4-1), but PTH had significantly up-regulated. Collectively, these data consistently supported the idea that the evaluated activity of Wnt/β-catenin signaling in osteocytes cause their maturational and functional defects, leading to an osteomalacia phenotype.

***Normalized Wnt/β-catenin activity significantly rescued the rickets/osteomalacia in Dmp1-null mice***

To further investigate whether the abnormal activity of canonical Wnt signaling could be one of the pathological reasons for the development of hypophosphatemic rickets/osteomalacia in *Dmp1*-null mice, Dkk1 transgenic mice were introduced into the *Dmp1*-null background to down-regulate the β-catenin expression. DKK1, like SOST, inhibits the Wnt/β-catenin signaling pathway. DKK1 bound to the kremen and LRP5/6 interrupted the interaction between Wnts and the LRP5/6 co-receptor (101). Using the 2.3 kb Col1α1 promoter specific to osteoblasts and osteocytes, our studies also showed that the transgenic over-expression of Dkk1 in WT mice did not cause notable early long bone deficiencies (Figs. 4-5). As a result, we crossed the *Dkk1*-Tg mice with *Dmp1*-null mice for over-expression of *Dkk1* in the *Dmp1*-null background. The representative radiographs and μ-CT analysis demonstrated an apparent improvement of the epiphysis and metaphysic structures, long bone shape, and cortical porosity in the DKK1; KO group, compared to the *Dmp1*-null group (Fig. 4-5).

The expressions of DMP1, DKK1 and β-catenin in the offspring were evaluated. As predicted, DMP1 was not detectable in the *Dmp1*-null mice (KO, Fig. 4-6, a), and DKK1 was highly expressed in the transgenic osteoblasts and osteocytes, compared to a weak expression in the WT osteocytes and an almost undetectable expression in the KO osteocytes (Fig. 4-6, b). As we anticipated, β-catenin was markedly normalized in the DKK1; KO group (Fig. 4-6, c). A series of experiments was performed to assess whether the targeted expression of the DKK1 in the *Dmp1*-null mice showed the rescue effects. A close examination of the metaphysis area revealed that the abnormal bone homeostasis, including increased bone formation (OSX, BSP, OPN, Figs. 4-7, a-d) and decreased bone absorption (TRAP, Figs. 4-7, e), also significantly rescued the *Dmp1*-null phenotype by re-regulating the Wnt/β-catenin activity with *Dkk1*-Tg. Further analysis suggested the ectopic Wnt/β-catenin activity could lead to both significantly up-regulated osteoblast proliferation activity (BrdU, Figs. 4-7, f), and significantly down-regulated osteoclast number in the primary spongiosa (TRAP, Figs. 4-7, g), since the

*Dkk1*-transgene significantly rescued these abnormal bone cell activities. Analysis of the mineral deposit (double labeling, Fig. 4-8, a) and bone mineralization (Goldner, sirius red, and biglycan staining, Figs. 4-8, b-d) indicated a prominent rescue of the osteomalacia phenotype in the DKK1; KO mice, suggesting that Wnt/β-catenin signaling is important for the pathological development of the osteomalacia phenotype in *Dmp1*-null mice. Further analysis of osteocytes, including analysis of bone markers (OSX, E11, SOST), osteocyte morphology, mineralization of the pericellular matrix, and cell proliferation, confirmed that lowering the β-catenin level in *Dmp1*-null mice resulted in well formed osteocytes with almost normal functions. In another words, it remarkably rescued the maturation defect of the *Dmp1*-null osteocyte (Fig. 4-9). This result suggested the osteocyte maturation and mineralization defects in *Dmp1*-null mice could directly or indirectly cause the elevated osteocytic Wnt/β-catenin signaling activity. However, DKK1 only partially rescued the serum biochemistry markers (including Pi and FGF23) in *Dmp1*-null mice (Table. 4-1), in accordance with the previous studies showing that the hypophosphatemia phenotype in *Dmp1*-null mice is primarily regulated by the abnormal production of FGF23 (3,102). Taken together, the genetic rescue of *Dmp1*-null via the *Dkk1* transgene indicated that except for up-regulated FGF23, which is responsible for the pathogenesis of hypophosphatemia in *Dmp1*-null mice, the osteocytic canonical Wnt signaling pathway also plays an important pathological role during hypophosphatemic rickets/osteomalacia development, especially the osteomalacia phenotype, via regulating the osteocyte maturation.

***Down-regulation of Wnt/β-catenin activity rescued the defects of Hyp mice***

XLH, another common type of hypophosphatemic rickets/osteomalacia with an incidence of 1:20,000 live births, resulted from *Phex* gene mutation (24). Cloning the *Phex* gene mutation in murine homologs generated a typical hypophosphatemic animal model named "*Hyp*" mice (1,103). Recently, Yuan *et al.* (104) identified a decrease in the 7B2 chaperone protein ("*Signe*" gene) in *Hyp* mouse osteocytes/osteoblasts that consequently diminished the 7B2•PC2 enzyme activity. The 7B2•PC2 enzyme was

demonstrated to be an important regulator of the DMP1 process due to its effects on BMP1, the only identified enzyme for DMP1 processing (105). Full-length DMP1 works as a precursor that was cleaved into functional forms – the 57 kDa C-terminal and 37 kDa N-terminal (15). As a result, DMP1 lost its biological function in *Hyp* mice. Thus, serum biochemistry analysis confirmed that, similar to the *Dmp1*-null mice, FGF 23 significantly increased in the *Hyp* mice (Fig. 4-10, a), which resulted in the abnormal production of FGF23 in bone cells (Fig. 4-10, b, >3 fold) and played an essential pathogenic role in *Hyp* mice (85,86). More importantly, β-catenin also increased (over 9 -fold) in the *Hyp* mice (Figs. 4-10, c-d), consistent with the *Dmp1*-null mice. As a result, we also crossed *Dkk1*-Tg mice with *Hyp* mice to further identify whether Wnt/β-catenin was responsible for hypophosphatemic development in the absence of functional DMP1. The results of serum biochemistry analysis suggested the hypophosphatemia phenotype wasn't effectively rescued when the canonical Wnt pathway was blocked, based on the results from the DMP1 groups (Table 4-1). However, bone morphology and histology analyses revealed an apparent improvement of the skeletal abnormalities in the DKK1; Hyp mice (Figs. 4-10, e-f). These data were consistent with the rescue results obtained from DKK1; *Dmp1*-KO mice, suggesting the osteomalacia abnormality in the *Hyp* mice was also caused by the increased Wnt/β-catenin activity.

***Injection of anti-β-catenin compound drug improved the rickets/osteomalacia deficiency in Dmp1-null mice***

Normalization of the Wnt/β-catenin expression in both the *Dmp1*-null mice and *Hyp* mice consistently showed a significant improvement of the ostomalacia phenotype but only partially restored the hypophosphatemia. The normalized expression further confirmed that Wnt/β-catenin worked as a local factor regulating the osteocyte maturation and function. To address the clinical translation of this discovery, a compound drug named "IWR," that inhibits Wnt/β-catenin signaling was used to treat the *Dmp1*-null mice. The IWR compound was designed to inhibit the Wnt-induced accumulation of β-catenin by abrogating Axin protein turnover (93,106-108). Axin

protein was part of the β-catenin destruction complex, which consists of adenomatous polyposis coli (Apc), Axin, casein kinase (Ck) 1 and glycogen synthase kinase (Gsk) 3β that promoted proteasome-mediated proteolysis of phosphorylated β-catenin (108,109). Daily IWR injections started at 1 week of age and continued for 3 weeks. The injection group, together with both WT and *Dmp1*-KO mice with vehicle injections (as controls), were collected at 4 week of age. Bone morphological and histological analysis revealed that anti-β-catenin compound (IWR) rescued the rickets/osteomalacia phenotype in *Dmp1*-null mice (Fig. 4-11, a-c). This result suggested a new clinical drug strategy for the treatment of heritable hypophosphatemic rickets/osteomalacia patients. Since the current oral supplementation of phosphorus couldn't fully cure the symptoms of these patients, especially the bone hypomineralization, the combination of an anti-β-catenin drug and dietary intake of phosphate should be developed for a better therapeutic effect.

**Discussion**

Previous studies from several groups confirmed that FGF23 influenced the serum phosphorus level, which was critical for bone and tooth malformation in mice with hypophosphatemic rickets/osteomalacia (3,16,84-86,110). In this study, we first identified the up-regulation of Wnt/β-catenin signaling activity in osteocytes. Further analysis of both ectopic activation and reasonable down-regulation of osteocytic β-catenin confirmed that Wnt/β-catenin was one of the key factors regulating osteocyte maturation and its function. Taken together, our results strongly suggested that in addition to the FGF23, the Wnt/β-catenin signaling pathway also played an important role during the pathogenesis of hypophosphatemic rickets/osteomalacia, especially the osteomalacia development via regulation of osteocyte maturation and function (Fig. 4-12).

In the canonical Wnt signaling pathway, when certain Wnts or other triggers were present, they crosslinked cell surface molecules, Lrp5/6 and Frizzled (Fzd), which mobilized Gsk3β and Ck1 to the membrane where they phosphorylated serines on Lrp5/6, promoted the formation of a signalosome, and recruited disheveled (Dvl) and

axin1/2. This released β-catenin, increased its levels and entered the nucleus to regulate bone-related genes, such as Tcf/Lef1 and axin2 (109,111-113). It was well documented that the Wnt/β-catenin pathway is necessary for osteogenesis and bone remodeling via regulation of early osteo-lineage (113-115). However, the function of canonical Wnt pathway on the terminally differentiated osteocytes making up almost 90% of the total bone cells was largely unknown. Previous evidence suggested there was a close relationship between the Wnt/β-catenin signaling pathway and osteocytes either directly or indirectly. For example, Bonewald *et al*. found that Wnt/β-catenin signaling was activated upon mechanical loading in osteocytes (116). Two major Wnt inhibiters important for regulating osteogenesis (SOST, DKK1) were postnatally produced by osteocytes (Fig. 4-1; Fig. 4-5, b) (16,117-119). In addition, a recent study showed osteocyte Wnt/β-catenin signaling was required for normal bone homeostasis via regulation of osteoclast activity (120,121), while in this study, we further investigated the role of Wnt/β-catenin signaling in regulating osteocytes. Our results strongly suggested that Wnt/β-catenin signaling regulated osteocyte maturation and function by controlling the osteoblast-osteocyte transition and that keeping a low level of β-catenin in osteocytes was essential for bone modeling and remodeling (Fig. 4-12).

We have shown that the ectopic expression of Wnt/β-catenin was negative for osteocyte maturation and function; however, it did not mean less was better. Actually, osteocytic Wnt/β-catenin signaling should be maintained at a specific level. Studies from Kramer *et al.* indicated that osteocyte-specific β-catenin-deficient mice (*Dmp1-Cre*; β-cat$^{loxP/loxP}$) displayed progressive bone loss associated with increased osteoclast number and activity, which was due to a reduction in the osteocytic OPG and increased osteocytic RANKL/OPG ratio (121). Collectively, Wnt/β-catenin signaling was more like a "valve" that could be turned on during the early osteo-lineage formation (from mesenchymal stem cell to osteoblast progenitor) as a key regulator of osteoblastogenesis and expression in early osteo-lineage, which was necessary for osteogenic differentiation and maturation (122-126). However, this "valve" would be progressively turned down to a specific level during the differentiation and maturation of osteoblast/osteocytes. This

down-regulation might be controlled by a simultaneously increased expression of several Wnt antagonists including secreted frizzled-related protein 1 (Sfrp1), DKK2 and SOST (117,119,127-130). The adjustment of Wnt/β-catenin signaling would consequently promote osteocyte maturation and was important for normal bone homestasis.

Increased serum PTH levels were found in both *Dmp1*-null and *Hyp* mice (3,131). Previously it was thought the up-regulation of serum PTH resulted from the high serum FGF23 level. Briefly, the FGF23-mediated down-regulation of $1,25(OH)_2D_3$ synthesis reduced intestinal Ca absorption and thus also the serum Ca, which stimulated PTH release. However, serum Ca levels in the *Dmp1*-null mice didn't significantly change (3). Interestingly, a recent study suggested that murine FGF23 directly inhibited PTH synthesis in a mitogen-activated protein kinase (MARK)-dependent manner (132,133). Therefore, other mechanisms might be responsible for the up-regulation of PTH. In this study, we found that none of serum biochemistry markers were considerably changed in the CA-β group except for the PTH level, suggesting the up-regulated Wnt/β-catenin signaling in osteocytes was one of the possible causes for elevated serum PTH. A study by Guo *et al.* demonstrated that a certain amount of Wnt signaling was required to enable PTH to induce peritrabecular stromal cells and subsequent bone formation (134). Furthermore, several studies confirmed that PTH activated canonical Wnt signaling through the co-receptor Lrp6 (88,89,134). Collectively, based on the current studies, we think the increased Wnt/β-catenin in the osteocytes of the hypophosphatemic mice led to a higher serum PTH level through an unknown mechanism, and this increased serum PTH further activated the canonical Wnt signaling in bone cells, forming a positive feedback loop.

For several decades, the disorder of the functional axis of the FGF23-renal phosphorus reabsorption-serum phosphorus level was well established as a major factor in the pathogenesis of inherited hypophosphatemic rickets/osteomalacia. However, the restoration of phosphate homeostasis only partially rescued the rickets/osteomalacia phenotype, suggesting that other factors or signaling pathways could work as a local pathological mechanism. This study found that Wnt/β-catenin is one of the underlying

mechanisms, which enabled a more comprehensive understanding of the pathological development and biochemical regulation of hypophosphatemia. It also has clinical relevance, as an oral phosphorus therapy alone fails to fully restore the osteomalacic status in patients, and thus, genetic therapy that normalizes the Wnt/β-catenin signaling may benefit these patients.

# CHAPTER V

# CONCLUSION

DMP1 is essential for both odontogenesis and osteogenesis. Previous *in vitro* studies suggested that, in addition to its role as an ECM protein, DMP1 could also function as a transcription factor. However, this nuclear transcription theory was debatable. Moreover, the loss-function of DMP1 *in vivo* would lead not only to the hypophosphatemia but also to the osteomalacia defect. The hypophosphatemia phenotype was well demonstrated as a result of the increased expression of FGF23 in osteocytes; however, the underlying mechanism of the osteomalacia phenotype still needs to be identified. In this study, we investigated the potential nuclear function of the full-length DMP1 in osteogenesis and odontogenesis using both *in vivo* and *in vitro* methods. Our results showed that the nucleus-targeted DMP1 failed to rescue the bone and tooth defects in *Dmp1*-null mice, indicating that DMP1 worked mainly as an ECM protein that, as we and others previously reported, functions via the extracellular signal-regulated kinases (ERK)-mitogen-activated protein kinases (MAPK) pathway. We also identified an up-regulation of the Wnt/β-catenin signaling activity in the osteocytes. Further analysis of both the ectopic activation and reasonable down-regulation of osteocytic β-catenin confirmed that Wnt/β-catenin was a key factor in regulating osteocyte maturation and function. Taken together, our results confirmed that DMP1 regulated the osteocytes via both ERK-MAPK and the canonical Wnt signaling pathways.

## Important Roles of Osteocytes

The osteocyte, defined as the terminally differentiated cells derived from osteoblasts located within the bone matrix, comprises more than 90% to 95% of all bone cells in the adult skeleton. Previously, osteocytogenesis was considered a passive process, during which osteoblasts produced a matrix/osteoid and became trapped under new osteoid over the embedded cells (135,136). However, in the last decade, there was a

virtual explosion of data on the molecular biology and function of osteocytes. Far from being the "passive placeholder in bone", this cell type has demonstrated numerous functions, such as remodeling the bone (137), producing hormones such as the parathyroid hormone (138-140) and estrogen (141,142), acting as a mechanosensory cell (143), regulating bone resorption via osteoclasts (70,144), and working as an endocrine cell via connections with the vascular system (145). More clinic observations indicated osteocytes were important for bone mineralization and maintenance. For example, the functional disorder of osteocytes leads to osteoporosis, a disease affecting 55% of Americans aged 50 or above and is responsible for millions of fractures annually (146-148). The differentiation of osteoblasts into osteocytes occurs in several stages, including osteoid osteocyte (or newly formed osteocyte), mineralized osteocyte, and mature osteocyte (26). However, the molecular and cellular mechanisms governing this maturation process and the functions of osteocytes have been largely unknown due to the lack of appropriate research techniques. Therefore, the osteocyte was one of the key cells involved in skeleton development and homeostasis, and the identification of the mechanisms underlying its differentiation and maturation process helped to further the understanding of bone biology in order to develop skeletal disease therapy.

**Signaling Involved in the Biological Regulation of DMP1**

DMP1, one of acidic phosphorylated extracellular matrix proteins specifically produced by osteocytes, was identified as a key regulator of the differentiation and maturation of osteocytes from osteoblasts (15,16). However, how this molecule regulated this process, or which signaling pathways control it were largely unknown. To date, one of the well-known mechanisms was that DMP1 could activate the ERK-MAPK pathway through the RGD integrin-binding domain in DMP1 (35,36). Recent studies also suggested DMP1 might function as a transcription factor transported into the nucleus via the functional NLS peptide in its C-terminal (37,39). In the nucleus, this protein regulated several genes that specifically control osteoblast and odontoblast differentiation. However, this nuclear theory was debatable. Our in vivo validation of the

theory indicated the nuclear-targeted DMP1 did not create biological functions that rescued the *Dmp1*-null phenotype. DMP1 functioned as an ECM protein that triggered the ERK-MAPK pathway. We also confirmed another underlying mechanism that controlled osteocyte differentiation and maturation: the canonical Wnt signaling pathway. The ectopic expression of Wnt/β-catenin in osteocytes caused the suppression of osteocyte maturation and affected function, leading to the pathogenesis of osteomalacia.

Matrix DMP1 interacted with CD44 and integrin αvβ3 receptors via its RGD integrin-binding domain, which induced the cellular mitogen-activated protein kinase kinase (MEK1/2) and extracellular signal-regulated kinase (ERK1/2) activation. The activated ERK1/2 stimulated the translocation of phosphorylated JNK [also known as "stress-activated protein kinase" (SAPK)] to the nucleus and concomitant up-regulation of transcriptional activation. The ERK-MAPK pathway was involved in several cellular activities, including gene expression, cellular differentiation, mitosis, and cell survival (34-36,149). The osteocyte producing SOST and DKK1 were identified as antagonists of the canonical Wnt/β-catenin signaling pathway via binding to Lrp co-receptors to prevent interactions with Wnts (150,151). In the absence of Wnts, excess β-catenin was quickly sequestered by a protein complex containing Axin1/2, Apc, Ck1 and Gsk3β, and then phosphorylated and degraded by ubiquitin-mediated proteolysis (111,152-160). These down-stream signals from both the ERK-MAPK and Wnt/β-catenin signaling pathways resulted in down-regulation of osteoblastic genes (*Osx*, *Col I*, Alp, *Bsp*, *Fgf23*) but also an increase of osteocytic genes (*Sost*, *Dkk1* and *Dmp1*), further promoting the osteoblast-osteocyte transition and the maturation process of the osteocytes. The decreased FGF23 production in the osteocytes kept the serum FGF23 at a specific level that targeted the kidney and enabled the reabsorption of Pi, thereby keeping a relatively high serum Pi level. By diminishing the Wnt/β-catenin signaling activity in the osteocytes, the serum PTH was also kept at a certain level. The elevated activity of ERK-MAPK signaling, together with a decreased expression of Wnt/β-catenin signaling, will: 1) promote the osteoblast-osteocyte transition and the maturation process of the

osteocyte; and 2) keep serum FGF23 and Pi at specific levels that contribute to normal skeletal development and bone homestasis (Fig. 5-1, a).

On the other hand, in the absence of DMP1, ERK-MAPK signaling was down-regulated, possibly causing the reduction of the osteocytic DKK1 and SOST. Consequently, Wnts bound to the co-receptors and activated Wnt/β-catenin signaling in the osteocyte. As a result, a decrease of osteoblastic protein expression (OSX, Col I, BSP, OPN, ALP, FGF23) in the osteocytes was suppressed, leading to a disturbed differentiation and maturation process and causing osteomalacia. In addition, the lower Pi level (due to excess FGF23) promoted the hypophosphatemia phenotype (Fig. 5-1, b).

**Pathogenesis of the Inherited Hypophosphatemic Rickets/Osteomalacia**

This study produced a more comprehensive understanding of the pathological and biochemical regulation of hypophosphatemic rickets/osteomalacia. The inherited hypophosphatemic rickets/osteomalacia phenotype includes two major characteristics: 1) lower serum Pi levels causing hypophosphatemia, growth plate expansion, short stature and developmental retardation; and 2) osteomalacia, characterized by inadequate or delayed mineralization of osteoid in mature cortical and spongy bone. For the last several decades, the disorder of the functional axis of the FGF23-renal phosphorus reabsorption-serum phosphorus level was established as the major pathogenesis for inherited hypophosphatemia (24). This study clearly demonstrated that, in addition to the phosphate waste caused by increased FGF23, the osteocytic up-regulation of Wnt/β-catenin played an important pathological role in the development of osteomalacia. Therefore, for the clinical therapy of patients, the oral phosphate therapy should be further extended, and a genetic targeting drug, which would down-regulate the Wnt/β-catenin activity in osteocytes, should be developed for a better therapeutic treatment.

REFERENCES


1. Francis1, F., Hennig1, S., Korn, B., Reinhardt, R., de Jong, P., Poustka, A., Lehrach, H., Rowe, P.S.N., Goulding, J.N., Summerfield, T., Mountford, R., Read, A.P., Popowska, E., Pronicka, E., Davies, K.E., O'Riordan, J.L.H., Econs, M.J., Nesbitt, T., Drezner, M.K., Oudet, C., Pannetier, S., Hanauer, A., Strom, T.M., Meindl, A., Lorenz, B., Cagnoli, B., Mohnike, K.L., Murken, J., and Meitinger, T. (1995) A gene (PEX) with homologies to endopeptidases is mutated in patients with X-linked hypophosphatemic rickets. The HYP Consortium. *Nat Genet* **11**(2), 130-136
2. The ADHR Consortium. (2000) Autosomal dominant hypophosphataemic rickets is associated with mutations in FGF23. *Nat Genet* **26**(3), no. 3, 345-348
3. Feng, J. Q., Ward, L. M., Liu, S., Lu, Y., Xie, Y., Yuan, B., Yu, X., Rauch, F., Davis, S. I., Zhang, S., Rios, H., Drezner, M. K., Quarles, L. D., Bonewald, L. F., and White, K. E. (2006) Loss of DMP1 causes rickets and osteomalacia and identifies a role for osteocytes in mineral metabolism. *Nat Genet* **38**(11), 1310-1315
4. Fisher, L. W., and Fedarko, N. S. (2003) Six genes expressed in bones and teeth encode the current members of the SIBLING family of proteins. *Connect Tissue Res* **44 Suppl 1**, 33-40
5. George, A., Sabsay, B., Simonian, P. A., and Veis, A. (1993) Characterization of a novel dentin matrix acidic phosphoprotein. Implications for induction of biomineralization. *J Biol Chem* **268**(17), 12624-12630
6. D'Souza, R. N., Cavender, A., Sunavala, G., Alvarez, J., Ohshima, T., Kulkarni, A. B., and MacDougall, M. (1997) Gene expression patterns of murine dentin matrix protein 1 (Dmp1) and dentin sialophosphoprotein (DSPP) suggest distinct developmental functions in vivo. *J Bone Miner Res* **12**(12), 2040-2049
7. Feng, J. Q., Zhang, J., Dallas, S. L., Lu, Y., Chen, S., Tan, X., Owen, M., Harris, S. E., and MacDougall, M. (2002) Dentin matrix protein 1, a target molecule for

Cbfa1 in bone, is a unique bone marker gene. *J Bone Miner Res* **17**(10), 1822-1831

8. Fen, J. Q., Zhang, J., Dallas, S. L., Lu, Y., Chen, S., Tan, X., Owen, M., Harris, S. E., and MacDougall, M. (2002) Dentin matrix protein 1, a target molecule for Cbfa1 in bone, is a unique bone marker gene. *J Bone Miner Res* **17**(10), 1822-1831
9. Toyosawa, S., Shintani, S., Fujiwara, T., Ooshima, T., Sato, A., Ijuhin, N., and Komori, T. (2001) Dentin matrix protein 1 is predominantly expressed in chicken and rat osteocytes but not in osteoblasts. *J Bone Miner Res* **16**(11), 2017-2026
10. Lu, Y., Zhang, S., Xie, Y., Pi, Y., and Feng, J. Q. (2005) Differential regulation of dentin matrix protein 1 expression during odontogenesis. *Cells Tissues Organs* **181**(3-4), 241-247
11. Narayanan, K., Ramachandran, A., Hao, J., and George, A. (2002) Transcriptional regulation of dentin matrix protein 1 (DMP1) by AP-1 (c-fos/c-jun) factors. *Connect Tissue Res* **43**(2-3), 365-371
12. Lv, K., Huang, H., Lu, Y., Qin, C., Li, Z., and Feng, J. Q. (2010) Circling behavior developed in Dmp1 null mice is due to bone defects in the vestibular apparatus. *Int J Biol Sci* **6**(6), 537-545
13. Rangiani, A., Cao, Z., Sun, Y., Lu, Y., Gao, T., Yuan, B., Rodgers, A., Qin, C., Kuro, O. M., and Feng, J. Q. (2012) Protective roles of DMP1 in high phosphate homeostasis. *PloS one* **7**(8), e42329
14. Ogbureke, K. U., and Fisher, L. W. (2004) Expression of SIBLINGs and their partner MMPs in salivary glands. *J Dent Res* **83**(9), 664-670
15. Qin, C., D'Souza, R., and Feng, J. Q. (2007) Dentin matrix protein 1 (DMP1): new and important roles for biomineralization and phosphate homeostasis. *J Dent Res* **86**(12), 1134-1141
16. Zhang, R., Lu, Y., Ye, L., Yuan, B., Yu, S., Qin, C., Xie, Y., Gao, T., Drezner, M. K., Bonewald, L. F., and Feng, J. Q. (2011) Unique roles of phosphorus in

endochondral bone formation and osteocyte maturation. *J Bone Miner Res* **26**(5), 1047-1056

17. Ye, L., MacDougall, M., Zhang, S., Xie, Y., Zhang, J., Li, Z., Lu, Y., Mishina, Y., and Feng, J. Q. (2004) Deletion of dentin matrix protein-1 leads to a partial failure of maturation of predentin into dentin, hypomineralization, and expanded cavities of pulp and root canal during postnatal tooth development. *J Biol Chem* **279**(18), 19141-19148
18. Ye, L., Mishina, Y., Chen, D., Huang, H., Dallas, S. L., Dallas, M. R., Sivakumar, P., Kunieda, T., Tsutsui, T. W., Boskey, A., Bonewald, L. F., and Feng, J. Q. (2005) Dmp1-deficient mice display severe defects in cartilage formation responsible for a chondrodysplasia-like phenotype. *J Biol Chem* **280**(7), 6197-6203
19. The ADHR Consortium. (2000) Autosomal dominant hypophosphataemic rickets is associated with mutations in FGF23. *Nat Genet* **26**(3), 345-348
20. Lorenz-Depiereux, B., Bastepe, M., Benet-Pages, A., Amyere, M., Wagenstaller, J., Muller-Barth, U., Badenhoop, K., Kaiser, S. M., Rittmaster, R. S., Shlossberg, A. H., Olivares, J. L., Loris, C., Ramos, F. J., Glorieux, F., Vikkula, M., Juppner, H., and Strom, T. M. (2006) DMP1 mutations in autosomal recessive hypophosphatemia implicate a bone matrix protein in the regulation of phosphate homeostasis. *Nat Genet* **38**(11), 1248-1250
21. Makitie, O., Pereira, R. C., Kaitila, I., Turan, S., Bastepe, M., Laine, T., Kroger, H., Cole, W. G., and Juppner, H. (2010) Long-term clinical outcome and carrier phenotype in autosomal recessive hypophosphatemia caused by a novel DMP1 mutation. *J Bone Miner Res* **25**(10), 2165-2174
22. Turan, S., Aydin, C., Bereket, A., Akcay, T., Guran, T., Yaralioglu, B. A., Bastepe, M., and Juppner, H. (2010) Identification of a novel dentin matrix protein-1 (DMP-1) mutation and dental anomalies in a kindred with autosomal recessive hypophosphatemia. *Bone* **46**(2), 402-409

23. Koshida, R., Yamaguchi, H., Yamasaki, K., Tsuchimochi, W., Yonekawa, T., and Nakazato, M. (2010) A novel nonsense mutation in the DMP1 gene in a Japanese family with autosomal recessive hypophosphatemic rickets. *J Bone Miner Res* **28**(5), 585-590

24. Feng, J. Q., Clinkenbeard, E. L., Yuan, B., White, K. E., and Drezner, M. K. (2013) Osteocyte regulation of phosphate homeostasis and bone mineralization underlies the pathophysiology of the heritable disorders of rickets and osteomalacia. *Bone* **54**(2), 213-221

25. Lu, Y., Yuan, B., Qin, C., Cao, Z., Xie, Y., Dallas, S. L., McKee, M. D., Drezner, M. K., Bonewald, L. F., and Feng, J. Q. (2011) The biological function of DMP-1 in osteocyte maturation is mediated by its 57-kDa C-terminal fragment. *J Bone Miner Res* **26**(2), 331-340

26. Bonewald, L. F. (2011) The amazing osteocyte. *J Bone Miner Res* **26**(2), 229-238

27. Narayanan, K., Srinivas, R., Ramachandran, A., Hao, J., Quinn, B., and George, A. (2001) Differentiation of embryonic mesenchymal cells to odontoblast-like cells by overexpression of dentin matrix protein 1. *Proc Natl Acad Sci U S A* **98**(8), 4516-4521

28. Feng, J. Q., Huang, H., Lu, Y., Ye, L., Xie, Y., Tsutsui, T. W., Kunieda, T., Castranio, T., Scott, G., Bonewald, L. B., and Mishina, Y. (2003) The Dentin matrix protein 1 (Dmp1) is specifically expressed in mineralized, but not soft, tissues during development. *J Dent Res* **82**(10), 776-780

29. Dallas, S. L., Prideaux, M., and Bonewald, L. F. (2013) The Osteocyte: An Endocrine Cell and More. *Endocr Rev* **34**(5), 658-690

30. Lu, Y., Qin, C., Xie, Y., Bonewald, L. F., and Feng, J. Q. (2009) Studies of the DMP1 57-kDa functional domain both in vivo and in vitro. *Cell Ttissues Organs* **189**(1-4), 175-185

31. He, G., Dahl, T., Veis, A., and George, A. (2003) Nucleation of apatite crystals in vitro by self-assembled dentin matrix protein 1. *Nat Mater* **2**(8), 552-558

32. Gajjeraman, S., Narayanan, K., Hao, J., Qin, C., and George, A. (2007) Matrix macromolecules in hard tissues control the nucleation and hierarchical assembly of hydroxyapatite. *J Biol Chem* **282**(2), 1193-1204

33. Gericke, A., Qin, C., Sun, Y., Redfern, R., Redfern, D., Fujimoto, Y., Taleb, H., Butler, W. T., and Boskey, A. L. (2010) Different forms of DMP1 play distinct roles in mineralization. *J Dent Res* **89**(4), 355-359

34. Jiang, B., Cao, Z., Lu, Y., Janik, C., Lauziere, S., Xie, Y., Poliard, A., Qin, C., Ward, L. M., and Feng, J. Q. (2010) DMP1 C-terminal mutant mice recapture the human ARHR tooth phenotype. *J Bone Miner Res* **25**(10), 2155-2164

35. Wu, H., Teng, P. N., Jayaraman, T., Onishi, S., Li, J., Bannon, L., Huang, H., Close, J., and Sfeir, C. (2011) Dentin matrix protein 1 (DMP1) signals via cell surface integrin. *J Biol Chem* **286**(34), 29462-29469

36. Eapen, A., Ramachandran, A., Pratap, J., and George, A. (2011) Activation of the ERK1/2 mitogen-activated protein kinase cascade by dentin matrix protein 1 promotes osteoblast differentiation. *Cells Tissues Organs* **194**(2-4), 255-260

37. Narayanan, K., Ramachandran, A., Hao, J., He, G., Park, K. W., Cho, M., and George, A. (2003) Dual functional roles of dentin matrix protein 1. Implications in biomineralization and gene transcription by activation of intracellular Ca2+ store. *J Biol Chem* **278**(19), 17500-17508

38. Siyam, A., Wang, S., Qin, C., Mues, G., Stevens, R., D'Souza, R. N., and Lu, Y. (2012) Nuclear localization of DMP1 proteins suggests a role in intracellular signaling. *Biochem Biophys Res Commun* **424**(3), 641-646

39. Ravindran, S., Narayanan, K., Eapen, A. S., Hao, J., Ramachandran, A., Blond, S., and George, A. (2008) Endoplasmic reticulum chaperone protein GRP-78 mediates endocytosis of dentin matrix protein 1. *J Biol Chem* **283**(44), 29658-29670

40. Gattineni, J., Bates, C., Twombley, K., Dwarakanath, V., Robinson, M. L., Goetz, R., Mohammadi, M., and Baum, M. (2009) FGF23 decreases renal NaPi-

2a and NaPi-2c expression and induces hypophosphatemia in vivo predominantly via FGF receptor 1. *Am J Physiol Renal Physiol* **297**(2), F282-291

41. Nashiki, K., Taketani, Y., Takeichi, T., Sawada, N., Yamamoto, H., Ichikawa, M., Arai, H., Miyamoto, K., and Takeda, E. (2005) Role of membrane microdomains in PTH-mediated down-regulation of NaPi-IIa in opossum kidney cells. *Kidney Int* **68**(3), 1137-1147
42. Quarles, L. D. (2012) Role of FGF23 in vitamin D and phosphate metabolism: implications in chronic kidney disease. *Exp Cell Res* **318**(9), 1040-1048
43. Liu, F., Kohlmeier, S., and Wang, C. Y. (2008) Wnt signaling and skeletal development. *Cell Signal* **20**(6), 999-1009
44. Zhang, R., Chen, F. M., Zhao, S. L., Xiao, M. Z., Smith, A. J., and Feng, J. Q. (2011) Expression of dentine sialophosphoprotein in mouse nasal cartilage. *Arch Oral Biol* **57**(6), 607-613
45. Ke, H. Z., Richards, W. G., Li, X., and Ominsky, M. S. (2012) Sclerostin and dickkopf-1 as therapeutic targets in bone diseases. *Endocr Rev* **33**(5), 747-783
46. Li, J., Sarosi, I., Cattley, R. C., Pretorius, J., Asuncion, F., Grisanti, M., Morony, S., Adamu, S., Geng, Z., Qiu, W., Kostenuik, P., Lacey, D. L., Simonet, W. S., Bolon, B., Qian, X., Shalhoub, V., Ominsky, M. S., Zhu Ke, H., Li, X., and Richards, W. G. (2006) Dkk1-mediated inhibition of Wnt signaling in bone results in osteopenia. *Bone* **39**(4), 754-766
47. Sun, Y., Prasad, M., Gao, T., Wang, X., Zhu, Q., D'Souza, R., Feng, J. Q., and Qin, C. (2010) Failure to process dentin matrix protein 1 (DMP1) into fragments leads to its loss of function in osteogenesis. *J Biol Chem* **285**(41), 31713-31722
48. George, A., Sabsay, B., Simonian, P. A., and Veis, A. (1993) Characterization of a novel dentin matrix acidic phosphoprotein. Implications for induction of biomineralization. *J Biol Chem* **268**(17), 12624-12630
49. Hirst, K. L., Ibaraki-O'Connor, K., Young, M. F., and Dixon, M. J. (1997) Cloning and expression analysis of the bovine dentin matrix acidic phosphoprotein gene. *J Dent Res* **76**(3), 754-760

50. MacDougall, M., Simmons, D., Luan, X., Nydegger, J., Feng, J., and Gu, T. T. (1997) Dentin phosphoprotein and dentin sialoprotein are cleavage products expressed from a single transcript coded by a gene on human chromosome 4. Dentin phosphoprotein DNA sequence determination. *J Biol Chem* **272**(2), 835-842

51. Sun, Y., Ma, S., Zhou, J., Yamoah, A. K., Feng, J. Q., Hinton, R. J., and Qin, C. (2010) Distribution of small integrin-binding ligand, N-linked glycoproteins (SIBLING) in the articular cartilage of the rat femoral head. *J Histochem Cytochem* **58**(11), 1033-1043

52. Kucka, M., Bjelobaba, I., Clokie, S. J., Klein, D. C., and Stojilkovic, S. S. (2013) Female-specific induction of rat pituitary dentin matrix protein-1 by GnRH. *Mol Endocrinol* **27**(11), 1840-1855

53. Chaplet, M., De Leval, L., Waltregny, D., Detry, C., Fornaciari, G., Bevilacqua, G., Fisher, L. W., Castronovo, V., and Bellahcene, A. (2003) Dentin matrix protein 1 is expressed in human lung cancer. *J Bone Miner Res* **18**(8), 1506-1512

54. Bucciarelli, E., Sidoni, A., Bellezza, G., Cavaliere, A., Brachelente, G., Costa, G., Chaplet, M., Castronovo, V., and Bellahcene, A. (2007) Low dentin matrix protein 1 expression correlates with skeletal metastases development in breast cancer patients and enhances cell migratory capacity in vitro. *Breast Cancer Res Treat* **105**(1), 95-104

55. Fisher, L. W., Torchia, D. A., Fohr, B., Young, M. F., and Fedarko, N. S. (2001) Flexible structures of SIBLING proteins, bone sialoprotein, and osteopontin. *Biochem Biophys Res Commun* **280**(2), 460-465

56. Kaartinen, M. T., Sun, W., Kaipatur, N., and McKee, M. D. (2005) Transglutaminase crosslinking of SIBLING proteins in teeth. *J Dent Res* **84**(7), 607-612

57. Farrow, E. G., Davis, S. I., Ward, L. M., Summers, L. J., Bubbear, J. S., Keen, R., Stamp, T. C., Baker, L. R., Bonewald, L. F., and White, K. E. (2009)

Molecular analysis of DMP1 mutants causing autosomal recessive hypophosphatemic rickets. *Bone* **44**(2), 287-294

58. Qin, C., Baba, O., and Butler, W. T. (2004) Post-translational modifications of sibling proteins and their roles in osteogenesis and dentinogenesis. *Crit Rev Oral Biol Med* **15**(3), 126-136
59. Qin, C., Brunn, J. C., Cook, R. G., Orkiszewski, R. S., Malone, J. P., Veis, A., and Butler, W. T. (2003) Evidence for the proteolytic processing of dentin matrix protein 1. Identification and characterization of processed fragments and cleavage sites. *J Biol Chem* **278**(36), 34700-34708
60. He, G., Dahl, T., Veis, A., and George, A. (2003) Dentin matrix protein 1 initiates hydroxyapatite formation in vitro. *Connect Tissue Res* **44 Suppl 1**, 240-245
61. Tartaix, P. H., Doulaverakis, M., George, A., Fisher, L. W., Butler, W. T., Qin, C., Salih, E., Tan, M., Fujimoto, Y., Spevak, L., and Boskey, A. L. (2004) In vitro effects of dentin matrix protein-1 on hydroxyapatite formation provide insights into in vivo functions. *J Biol Chem* **279**(18), 18115-18120
62. Maciejewska, I., Qin, D., Huang, B., Sun, Y., Mues, G., Svoboda, K., Bonewald, L., Butler, W. T., Feng, J. Q., and Qin, C. (2009) Distinct compartmentalization of dentin matrix protein 1 fragments in mineralized tissues and cells. *Cells Tissues Organs* **189**(1-4), 186-191
63. Braut, A., Kalajzic, I., Kalajzic, Z., Rowe, D. W., Kollar, E. J., and Mina, M. (2002) Col1a1-GFP transgene expression in developing incisors. *Connect Tissue Res* **43**(2-3), 216-219
64. Zhang, K., Barragan-Adjemian, C., Ye, L., Kotha, S., Dallas, M., Lu, Y., Zhao, S., Harris, M., Harris, S. E., Feng, J. Q., and Bonewald, L. F. (2006) E11/gp38 selective expression in osteocytes: regulation by mechanical strain and role in dendrite elongation. *Mol Cell Biol* **26**(12), 4539-4552
65. Corsi, A., Riminucci, M., Fisher, L. W., and Bianco, P. (2001) Achondrogenesis type IB: agenesis of cartilage interterritorial matrix as the link between gene

defect and pathological skeletal phenotype. *Arch Pathol Lab Med* **125**(10), 1375-1378

66. Huang, B., Maciejewska, I., Sun, Y., Peng, T., Qin, D., Lu, Y., Bonewald, L., Butler, W. T., Feng, J., and Qin, C. (2008) Identification of full-length dentin matrix protein 1 in dentin and bone. *Calcif Tissue Int* **82**(5), 401-410
67. Sitara, D., Kim, S., Razzaque, M. S., Bergwitz, C., Taguchi, T., Schuler, C., Erben, R. G., and Lanske, B. (2008) Genetic evidence of serum phosphate-independent functions of FGF-23 on bone. *PLoS Genet* **4**(8), e1000154
68. Lanske, B., Karaplis, A. C., Lee, K., Luz, A., Vortkamp, A., Pirro, A., Karperien, M., Defize, L. H., Ho, C., Mulligan, R. C., Abou-Samra, A. B., Juppner, H., Segre, G. V., and Kronenberg, H. M. (1996) PTH/PTHrP receptor in early development and Indian hedgehog-regulated bone growth. *Science* **273**(5275), 663-666
69. Burra, S., Nicolella, D. P., Francis, W. L., Freitas, C. J., Mueschke, N. J., Poole, K., and Jiang, J. X. (2010) Dendritic processes of osteocytes are mechanotransducers that induce the opening of hemichannels. *Proc Natl Acad Sci U S A* **107**(31), 13648-13653
70. Xiong, J., Onal, M., Jilka, R. L., Weinstein, R. S., Manolagas, S. C., and O'Brien, C. A. (2011) Matrix-embedded cells control osteoclast formation. *Nat Med* **17**(10), 1235-1241
71. Barron, M. J., Tsai, C. J., and Donahue, S. W. (2010) Mechanical stimulation mediates gene expression in MC3T3 osteoblastic cells differently in 2D and 3D environments. *J Biomech Eng* **132**(4), 041005
72. Lu, Y., Ye, L., Yu, S., Zhang, S., Xie, Y., McKee, M. D., Li, Y. C., Kong, J., Eick, J. D., Dallas, S. L., and Feng, J. Q. (2007) Rescue of odontogenesis in Dmp1-deficient mice by targeted re-expression of DMP1 reveals roles for DMP1 in early odontogenesis and dentin apposition in vivo. *Dev Biol* **303**(1), 191-201

73. Sun, Y., Chen, L., Ma, S., Zhou, J., Zhang, H., Feng, J. Q., and Qin, C. (2011) Roles of DMP1 processing in osteogenesis, dentinogenesis and chondrogenesis. *Cells Tissues Organs* **194**(2-4), 199-204

74. Sun, Y., Lu, Y., Chen, L., Gao, T., D'Souza, R., Feng, J. Q., and Qin, C. (2011) DMP1 processing is essential to dentin and jaw formation. *J Dent Res* **90**(5), 619-624

75. Ye, L., Zhang, S., Ke, H., Bonewald, L. F., and Feng, J. Q. (2008) Periodontal breakdown in the Dmp1 null mouse model of hypophosphatemic rickets. *J Dent Res* **87**(7), 624-629

76. Moses, K. D., Butler, W. T., and Qin, C. (2006) Immunohistochemical study of small integrin-binding ligand, N-linked glycoproteins in reactionary dentin of rat molars at different ages. *Eur J Oral Sci* **114**(3), 216-222

77. Fisher, L. W., Stubbs, J. T., 3rd, and Young, M. F. (1995) Antisera and cDNA probes to human and certain animal model bone matrix noncollagenous proteins. *Acta Orthop Scand Suppl* **266**, 61-65

78. Prasad, M., Butler, W. T., and Qin, C. (2010) Dentin sialophosphoprotein in biomineralization. *Connect Tissue Res* **51**(5), 404-417

79. Zhu, Q., Gibson, M. P., Liu, Q., Liu, Y., Lu, Y., Wang, X., Feng, J. Q., and Qin, C. (2012) Proteolytic processing of dentin sialophosphoprotein (DSPP) is essential to dentinogenesis. *J Biol Chem* **287**(36), 30426-30435

80. S. WANG, Y. H., C. QIN, R. D'SOUZA, and Y. LU. (Seattle: IADR, 2013) Nuclear DMP1 (nuDMP1) is Generated by Alternative Initiation of Translation. Available at https://iadr.confex.com/iadr/13iags/webprogram/Paper173877.html (accessed March 173823 172013)

81. Siyam, A., Wang, S. Z., Qin, C. L., Mues, G., Stevens, R., D'Souza, R. N., and Lu, Y. B. (2012) Nuclear localization of DMP1 proteins suggests a role in intracellular signaling. *Biochem Bioph Res Co* **424**(3), 641-646

82. Sitara, D., Razzaque, M. S., Hesse, M., Yoganathan, S., Taguchi, T., Erben, R. G., Juppner, H., and Lanske, B. (2004) Homozygous ablation of fibroblast

growth factor-23 results in hyperphosphatemia and impaired skeletogenesis, and reverses hypophosphatemia in Phex-deficient mice. *Matrix Biol* **23**(7), 421-432

83. Shimada, T., Kakitani, M., Yamazaki, Y., Hasegawa, H., Takeuchi, Y., Fujita, T., Fukumoto, S., Tomizuka, K., and Yamashita, T. (2004) Targeted ablation of Fgf23 demonstrates an essential physiological role of FGF23 in phosphate and vitamin D metabolism. *J Clin Invest* **113**(4), 561-568
84. Liu, S., Zhou, J., Tang, W., Menard, R., Feng, J. Q., and Quarles, L. D. (2008) Pathogenic role of Fgf23 in Dmp1-null mice. *Am J Physiol Endocrinol Metab* **295**(2), E254-261
85. Liu, S., Zhou, J., Tang, W., Jiang, X., Rowe, D. W., and Quarles, L. D. (2006) Pathogenic role of Fgf23 in Hyp mice. *Am J Physiol Endocrinol Metab* **291**(1), E38-49
86. Yuan, B., Takaiwa, M., Clemens, T. L., Feng, J. Q., Kumar, R., Rowe, P. S., Xie, Y., and Drezner, M. K. (2008) Aberrant Phex function in osteoblasts and osteocytes alone underlies murine X-linked hypophosphatemia. *J Clin Invest* **118**(2), 722-734
87. Martin, A., Liu, S., David, V., Li, H., Karydis, A., Feng, J. Q., and Quarles, L. D. (2011) Bone proteins PHEX and DMP1 regulate fibroblastic growth factor Fgf23 expression in osteocytes through a common pathway involving FGF receptor (FGFR) signaling. *FASEB J* **25**(8), 2551-2562
88. Wan, M., Yang, C., Li, J., Wu, X., Yuan, H., Ma, H., He, X., Nie, S., Chang, C., and Cao, X. (2008) Parathyroid hormone signaling through low-density lipoprotein-related protein 6. *Genes Dev* **22**(21), 2968-2979
89. Shi, C., Li, J., Wang, W., Cao, W., Cao, X., and Wan, M. (2011) Antagonists of LRP6 regulate PTH-induced cAMP generation. *Ann N Y Acad Sci* **1237**, 39-46
90. Harada, N., Tamai, Y., Ishikawa, T., Sauer, B., Takaku, K., Oshima, M., and Taketo, M. M. (1999) Intestinal polyposis in mice with a dominant stable mutation of the beta-catenin gene. *EMBO J* **18**(21), 5931-5942

91. Lu, Y., Xie, Y., Zhang, S., Dusevich, V., Bonewald, L. F., and Feng, J. Q. (2007) DMP1-targeted Cre expression in odontoblasts and osteocytes. *J Dent Res* **86**(4), 320-325

92. Sheen, C. R., Pilarowski, G. O., Wang, W., and Millan, J. L. (2012) Molecular characterisation of the Hyp deletion and an improved assay for its detection. *Bone* **50**(3), 592-595

93. Chen, B., Dodge, M. E., Tang, W., Lu, J., Ma, Z., Fan, C. W., Wei, S., Hao, W., Kilgore, J., Williams, N. S., Roth, M. G., Amatruda, J. F., Chen, C., and Lum, L. (2009) Small molecule-mediated disruption of Wnt-dependent signaling in tissue regeneration and cancer. *Nat Chem Biol* **5**(2), 100-107

94. Sun, Y., Gandhi, V., Prasad, M., Yu, W., Wang, X., Zhu, Q., Feng, J. Q., Hinton, R. J., and Qin, C. (2010) Distribution of small integrin-binding ligand, N-linked glycoproteins (SIBLING) in the condylar cartilage of rat mandible. *Int J Oral Maxillofac Surg* **39**(3), 272-281

95. DasGupta, R., and Fuchs, E. (1999) Multiple roles for activated LEF/TCF transcription complexes during hair follicle development and differentiation. *Development* **126**(20), 4557-4568

96. Atkins, G. J., Rowe, P. S., Lim, H. P., Welldon, K. J., Ormsby, R., Wijenayaka, A. R., Zelenchuk, L., Evdokiou, A., and Findlay, D. M. (2011) Sclerostin is a locally acting regulator of late-osteoblast/preosteocyte differentiation and regulates mineralization through a MEPE-ASARM-dependent mechanism. *J Bone Miner Res* **26**(7), 1425-1436

97. Moester, M. J., Papapoulos, S. E., Lowik, C. W., and van Bezooijen, R. L. (2010) Sclerostin: current knowledge and future perspectives. *Calcif Tissue Int* **87**(2), 99-107

98. Poole, K. E., van Bezooijen, R. L., Loveridge, N., Hamersma, H., Papapoulos, S. E., Lowik, C. W., and Reeve, J. (2005) Sclerostin is a delayed secreted product of osteocytes that inhibits bone formation. *FASEB J* **19**(13), 1842-1844

99. Sugars, R. V., Milan, A. M., Brown, J. O., Waddington, R. J., Hall, R. C., and Embery, G. (2003) Molecular interaction of recombinant decorin and biglycan with type I collagen influences crystal growth. *Connect Tissue Res* **44 Suppl 1**, 189-195

100. Schonherr, E., Witsch-Prehm, P., Harrach, B., Robenek, H., Rauterberg, J., and Kresse, H. (1995) Interaction of biglycan with type I collagen. *J Biol Chem* **270**(6), 2776-2783

101. Mao, B., Wu, W., Davidson, G., Marhold, J., Li, M., Mechler, B. M., Delius, H., Hoppe, D., Stannek, P., Walter, C., Glinka, A., and Niehrs, C. (2002) Kremen proteins are Dickkopf receptors that regulate Wnt/beta-catenin signalling. *Nature* **417**(6889), 664-667

102. Zhang, R., Oyajobi, B. O., Harris, S. E., Chen, D., Tsao, C., Deng, H. W., and Zhao, M. (2013) Wnt/beta-catenin signaling activates bone morphogenetic protein 2 expression in osteoblasts. *Bone* **52**(1), 145-156

103. Beck, L., Soumounou, Y., Martel, J., Krishnamurthy, G., Gauthier, C., Goodyer, C. G., and Tenenhouse, H. S. (1997) Pex/PEX tissue distribution and evidence for a deletion in the 3' region of the Pex gene in X-linked hypophosphatemic mice. *J Clin Inves* **99**(6), 1200-1209

104. Yuan, B., Feng, J. Q., Bowman, S., Liu, Y., Blank, R. D., Lindberg, I., and Drezner, M. K. (2013) Hexa-D-arginine treatment increases 7B2*PC2 activity in hyp-mouse osteoblasts and rescues the HYP phenotype. *J Bone Miner Res* **28**(1), 56-72

105. Steiglitz, B. M., Ayala, M., Narayanan, K., George, A., and Greenspan, D. S. (2004) Bone morphogenetic protein-1/Tolloid-like proteinases process dentin matrix protein-1. *J Biol Chem* **279**(2), 980-986

106. Dodge, M. E., Moon, J., Tuladhar, R., Lu, J., Jacob, L. S., Zhang, L. S., Shi, H., Wang, X., Moro, E., Mongera, A., Argenton, F., Karner, C. M., Carroll, T. J., Chen, C., Amatruda, J. F., and Lum, L. (2012) Diverse chemical scaffolds

support direct inhibition of the membrane-bound O-acyltransferase porcupine. *J Biol Chem* **287**(27), 23246-23254

107. Dodge, M. E., and Lum, L. (2011) Drugging the cancer stem cell compartment: lessons learned from the hedgehog and Wnt signal transduction pathways. *Annu Rev Pharmacol Toxicol* **51**, 289-310

108. Lu, J., Ma, Z., Hsieh, J. C., Fan, C. W., Chen, B., Longgood, J. C., Williams, N. S., Amatruda, J. F., Lum, L., and Chen, C. (2009) Structure-activity relationship studies of small-molecule inhibitors of Wnt response. *Bioorg Med Chem Lett* **19**(14), 3825-3827

109. Jho, E. H., Zhang, T., Domon, C., Joo, C. K., Freund, J. N., and Costantini, F. (2002) Wnt/beta-catenin/Tcf signaling induces the transcription of Axin2, a negative regulator of the signaling pathway. *Mol Cell Biol* **22**(4), 1172-1183

110. Yamazaki, Y., Okazaki, R., Shibata, M., Hasegawa, Y., Satoh, K., Tajima, T., Takeuchi, Y., Fujita, T., Nakahara, K., Yamashita, T., and Fukumoto, S. (2002) Increased circulatory level of biologically active full-length FGF-23 in patients with hypophosphatemic rickets/osteomalacia. *J Clin Endocrinol Metab* **87**(11), 4957-4960

111. Monroe, D. G., McGee-Lawrence, M. E., Oursler, M. J., and Westendorf, J. J. (2012) Update on Wnt signaling in bone cell biology and bone disease. *Gene* **492**(1), 1-18

112. Huang, H., and He, X. (2008) Wnt/beta-catenin signaling: new (and old) players and new insights. *Curr Opin Cell Biol* **20**(2), 119-125

113. Westendorf, J. J., Kahler, R. A., and Schroeder, T. M. (2004) Wnt signaling in osteoblasts and bone diseases. *Gene* **341**, 19-39

114. Kang, S., Bennett, C. N., Gerin, I., Rapp, L. A., Hankenson, K. D., and Macdougald, O. A. (2007) Wnt signaling stimulates osteoblastogenesis of mesenchymal precursors by suppressing CCAAT/enhancer-binding protein alpha and peroxisome proliferator-activated receptor gamma. *J Bio Chem* **282**(19), 14515-14524

115. Bodine, P. V., and Komm, B. S. (2006) Wnt signaling and osteoblastogenesis. *Rev Endocr Metab Disord* **7**(1-2), 33-39

116. Bonewald, L. F., and Johnson, M. L. (2008) Osteocytes, mechanosensing and Wnt signaling. *Bone* **42**(4), 606-615

117. Li, X., Liu, P., Liu, W., Maye, P., Zhang, J., Zhang, Y., Hurley, M., Guo, C., Boskey, A., Sun, L., Harris, S. E., Rowe, D. W., Ke, H. Z., and Wu, D. (2005) Dkk2 has a role in terminal osteoblast differentiation and mineralized matrix formation. *Nat Genet* **37**(9), 945-952

118. Winkler, D. G., Sutherland, M. K., Geoghegan, J. C., Yu, C., Hayes, T., Skonier, J. E., Shpektor, D., Jonas, M., Kovacevich, B. R., Staehling-Hampton, K., Appleby, M., Brunkow, M. E., and Latham, J. A. (2003) Osteocyte control of bone formation via sclerostin, a novel BMP antagonist. *EMBO J* **22**(23), 6267-6276

119. van Bezooijen, R. L., Roelen, B. A., Visser, A., van der Wee-Pals, L., de Wilt, E., Karperien, M., Hamersma, H., Papapoulos, S. E., ten Dijke, P., and Lowik, C. W. (2004) Sclerostin is an osteocyte-expressed negative regulator of bone formation, but not a classical BMP antagonist. *J Exp Med* **199**(6), 805-814

120. Sabbagh, Y., Graciolli, F. G., O'Brien, S., Tang, W., dos Reis, L. M., Ryan, S., Phillips, L., Boulanger, J., Song, W., Bracken, C., Liu, S., Ledbetter, S., Dechow, P., Canziani, M. E., Carvalho, A. B., Jorgetti, V., Moyses, R. M., and Schiavi, S. C. (2012) Repression of osteocyte Wnt/beta-catenin signaling is an early event in the progression of renal osteodystrophy. *J Bone Miner Res* **27**(8), 1757-1772

121. Kramer, I., Halleux, C., Keller, H., Pegurri, M., Gooi, J. H., Weber, P. B., Feng, J. Q., Bonewald, L. F., and Kneissel, M. (2010) Osteocyte Wnt/beta-catenin signaling is required for normal bone homeostasis. *Mol Cell Biol* **30**(12), 3071-3085

122. Hill, T. P., Spater, D., Taketo, M. M., Birchmeier, W., and Hartmann, C. (2005) Canonical Wnt/beta-catenin signaling prevents osteoblasts from differentiating into chondrocytes. *Dev Cell* **8**(5), 727-738

123. Day, T. F., Guo, X., Garrett-Beal, L., and Yang, Y. (2005) Wnt/beta-catenin signaling in mesenchymal progenitors controls osteoblast and chondrocyte differentiation during vertebrate skeletogenesis. *Dev Cell* **8**(5), 739-750

124. Rodda, S. J., and McMahon, A. P. (2006) Distinct roles for Hedgehog and canonical Wnt signaling in specification, differentiation and maintenance of osteoblast progenitors. *Development* **133**(16), 3231-3244

125. Glass, D. A., 2nd, Bialek, P., Ahn, J. D., Starbuck, M., Patel, M. S., Clevers, H., Taketo, M. M., Long, F., McMahon, A. P., Lang, R. A., and Karsenty, G. (2005) Canonical Wnt signaling in differentiated osteoblasts controls osteoclast differentiation. *Dev Cell* **8**(5), 751-764

126. Holmen, S. L., Zylstra, C. R., Mukherjee, A., Sigler, R. E., Faugere, M. C., Bouxsein, M. L., Deng, L., Clemens, T. L., and Williams, B. O. (2005) Essential role of beta-catenin in postnatal bone acquisition. *J Biol Chem* **280**(22), 21162-21168

127. Nie, X., Luukko, K., Fjeld, K., Kvinnsland, I. H., and Kettunen, P. (2005) Developmental expression of Dkk1-3 and Mmp9 and apoptosis in cranial base of mice. *J Mol Histol* **36**(6-7), 419-426

128. van Bezooijen, R. L., ten Dijke, P., Papapoulos, S. E., and Lowik, C. W. (2005) SOST/sclerostin, an osteocyte-derived negative regulator of bone formation. *Cytokine Growth Factor Rev* **16**(3), 319-327

129. van Bezooijen, R. L., Bronckers, A. L., Gortzak, R. A., Hogendoorn, P. C., van der Wee-Pals, L., Balemans, W., Oostenbroek, H. J., Van Hul, W., Hamersma, H., Dikkers, F. G., Hamdy, N. A., Papapoulos, S. E., and Lowik, C. W. (2009) Sclerostin in mineralized matrices and van Buchem disease. *J Dent Res* **88**(6), 569-574

130. Bodine, P. V., Billiard, J., Moran, R. A., Ponce-de-Leon, H., McLarney, S., Mangine, A., Scrimo, M. J., Bhat, R. A., Stauffer, B., Green, J., Stein, G. S., Lian, J. B., and Komm, B. S. (2005) The Wnt antagonist secreted frizzled-related

protein-1 controls osteoblast and osteocyte apoptosis. *J Cell Biochem* **96**(6), 1212-1230

131. Meyer, R. A., Jr., Meyer, M. H., and Morgan, P. L. (1996) Effects of altered diet on serum levels of 1,25-dihydroxyvitamin D and parathyroid hormone in X-linked hypophosphatemic (Hyp and Gy) mice. *Bone* **18**(1), 23-28
132. Ben-Dov, I. Z., Galitzer, H., Lavi-Moshayoff, V., Goetz, R., Kuro-o, M., Mohammadi, M., Sirkis, R., Naveh-Many, T., and Silver, J. (2007) The parathyroid is a target organ for FGF23 in rats. *J Clin Invest* **117**(12), 4003-4008
133. Krajisnik, T., Bjorklund, P., Marsell, R., Ljunggren, O., Akerstrom, G., Jonsson, K. B., Westin, G., and Larsson, T. E. (2007) Fibroblast growth factor-23 regulates parathyroid hormone and 1alpha-hydroxylase expression in cultured bovine parathyroid cells. *J Endocrinol* **195**(1), 125-131
134. Guo, J., Liu, M., Yang, D., Bouxsein, M. L., Saito, H., Galvin, R. J., Kuhstoss, S. A., Thomas, C. C., Schipani, E., Baron, R., Bringhurst, F. R., and Kronenberg, H. M. (2010) Suppression of Wnt signaling by Dkk1 attenuates PTH-mediated stromal cell response and new bone formation. *Cell Metab* **11**(2), 161-171
135. Franz-Odendaal, T. A., Hall, B. K., and Witten, P. E. (2006) Buried alive: how osteoblasts become osteocytes. *Dev Dyn* **235**(1), 176-190
136. Nefussi, J. R., Sautier, J. M., Nicolas, V., and Forest, N. (1991) How osteoblasts become osteocytes: a decreasing matrix forming process. *J Biol Buccale* **19**(1), 75-82
137. Baylink, D. J., and Wergedal, J. E. (1971) Bone formation by osteocytes. *Am J Physiol* **221**(3), 669-678
138. Belanger, L. F., and Robichon, J. (1964) Parathormone-Induced Osteolysis in Dogs. A Microradiographic and Alpharadiographic Survey. *J Bone Joint Surg Am* **46**, 1008-1012
139. Rhee, Y., Allen, M. R., Condon, K., Lezcano, V., Ronda, A. C., Galli, C., Olivos, N., Passeri, G., O'Brien, C. A., Bivi, N., Plotkin, L. I., and Bellido, T. (2011)

PTH receptor signaling in osteocytes governs periosteal bone formation and intracortical remodeling. *J Bone Miner Res* **26**(5), 1035-1046

140. Saini, V., Marengi, D. A., Barry, K. J., Fulzele, K. S., Heiden, E., Liu, X., Dedic, C., Maeda, A., Lotinun, S., Baron, R., and Pajevic, P. D. (2013) Parathyroid hormone (PTH)/PTH-related peptide type 1 receptor (PPR) signaling in osteocytes regulates anabolic and catabolic skeletal responses to PTH. *J Biol Chem* **288**(28), 20122-20134
141. Kondoh, S., Inoue, K., Igarashi, K., Sugizaki, H., Shirode-Fukuda, Y., Inoue, E., Yu, T., Takeuchi, J. K., Kanno, J., Bonewald, L. F., and Imai, Y. (2013) Estrogen receptor alpha in osteocytes regulates trabecular bone formation in female mice. *Bone* **60**, 68-77
142. Windahl, S. H., Borjesson, A. E., Farman, H. H., Engdahl, C., Moverare-Skrtic, S., Sjogren, K., Lagerquist, M. K., Kindblom, J. M., Koskela, A., Tuukkanen, J., Divieti Pajevic, P., Feng, J. Q., Dahlman-Wright, K., Antonson, P., Gustafsson, J. A., and Ohlsson, C. (2013) Estrogen receptor-alpha in osteocytes is important for trabecular bone formation in male mice. *Proc Natl Acad Sci U S A* **110**(6), 2294-2299
143. Sun, Y. Q., McLeod, K. J., and Rubin, C. T. (1995) Mechanically induced periosteal bone formation is paralleled by the upregulation of collagen type one mRNA in osteocytes as measured by in situ reverse transcript-polymerase chain reaction. *Calcif Tissue Int* **57**(6), 456-462
144. O'Brien, C. A., Nakashima, T., and Takayanagi, H. (2013) Osteocyte control of osteoclastogenesis. *Bone* **54**(2), 258-263
145. Dallas, S. L., Prideaux, M., and Bonewald, L. F. (2013) The osteocyte: an endocrine cell ... and more. *Endocr Rev* **34**(5), 658-690
146. Manolagas, S. C. (1998) Cellular and molecular mechanisms of osteoporosis. *Aging (Milano)* **10**(3), 182-190
147. Notelovitz, M. (2002) Overview of bone mineral density in postmenopausal women. *J Reprod Med* **47**(1 Suppl), 71-81

148. Zarrinkalam, M. R., Mulaibrahimovic, A., Atkins, G. J., and Moore, R. J. (2012) Changes in osteocyte density correspond with changes in osteoblast and osteoclast activity in an osteoporotic sheep model. *Osteoporos Int* **23**(4), 1329-1336

149. Johnson, G. L., and Lapadat, R. (2002) Mitogen-activated protein kinase pathways mediated by ERK, JNK, and p38 protein kinases. *Science* **298**(5600), 1911-1912

150. Bingyu Mao, W. W., Gary Davidson, Joachim Marhold, Mingfa Li, Bernard M. Mechler, Hajo Delius, Dana Hoppe, Peter Stannek, Carmen Walter, Andrei Glinka, Christof Niehrs. (2002) Kremen proteins are Dickkopf receptors that regulate Wnt-beta-catenin signalling. *Nature* **417**(6), 664-667

151. Li, X., Zhang, Y., Kang, H., Liu, W., Liu, P., Zhang, J., Harris, S. E., and Wu, D. (2005) Sclerostin binds to LRP5/6 and antagonizes canonical Wnt signaling. *J Biol Chem* **280**(20), 19883-19887

152. Wang, Y., Li, Y. P., Paulson, C., Shao, J. Z., Zhang, X., Wu, M., and Chen, W. (2014) Wnt and the Wnt signaling pathway in bone development and disease. *Front Biosci (Landmark Ed)* **19**, 379-407

153. Bilic, J., Huang, Y. L., Davidson, G., Zimmermann, T., Cruciat, C. M., Bienz, M., and Niehrs, C. (2007) Wnt induces LRP6 signalosomes and promotes dishevelled-dependent LRP6 phosphorylation. *Science* **316**(5831), 1619-1622

154. MacDonald, B. T., Tamai, K., and He, X. (2009) Wnt/beta-catenin signaling: components, mechanisms, and diseases. *Dev Cell* **17**(1), 9-26

155. Niehrs, C., and Shen, J. (2010) Regulation of Lrp6 phosphorylation. *Cell Mol Life Sci* **67**(15), 2551-2562

156. Zeng, X., Tamai, K., Doble, B., Li, S., Huang, H., Habas, R., Okamura, H., Woodgett, J., and He, X. (2005) A dual-kinase mechanism for Wnt co-receptor phosphorylation and activation. *Nature* **438**(7069), 873-877

157. Lin, K., Wang, S., Julius, M. A., Kitajewski, J., Moos, M., Jr., and Luyten, F. P. (1997) The cysteine-rich frizzled domain of Frzb-1 is required and sufficient for modulation of Wnt signaling. Proc Natl Acad Sci U S A **94**(21), 11196-11200

158. Cong, F., Schweizer, L., and Varmus, H. (2004) Casein kinase Iepsilon modulates the signaling specificities of dishevelled. *Mol Cell Biol* **24**(5), 2000-2011

159. Kikuchi, A. (1999) Roles of Axin in the Wnt signalling pathway. *Cell Signal* **11**(11), 777-788

160. Tamai, K., Semenov, M., Kato, Y., Spokony, R., Liu, C., Katsuyama, Y., Hess, F., Saint-Jeannet, J. P., and He, X. (2000) LDL-receptor-related proteins in Wnt signal transduction. *Nature* **407**(6803), 530-535

APPENDIX A
FIGURES


**Figure 1-1 Photographs and radiographs of patients with hypophosphatemic rickets (left panel) osteomalacia (right panel).** (Adapted from "ASBMR educational materials")

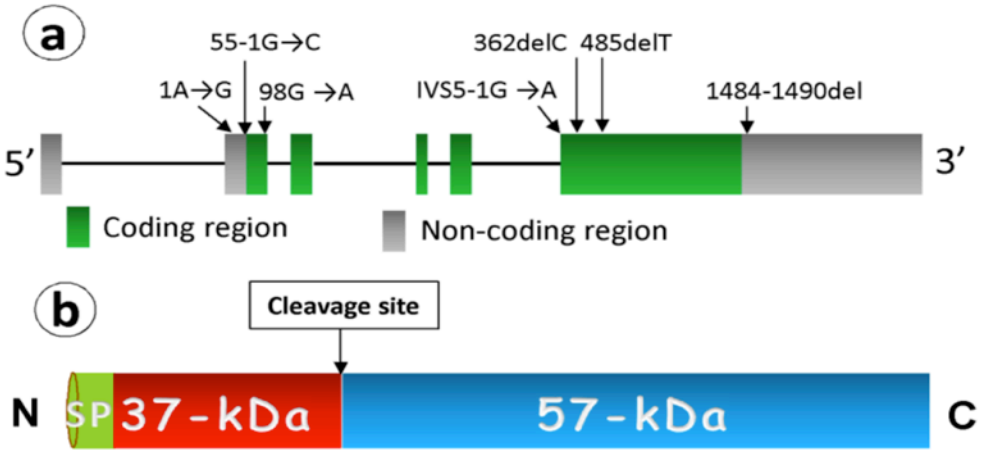


**Figure 1-2 Schematic structure of the human *DMP1* gene and ARHR mutations. (a)** Dmp1 gene contains by 6 exons, and because of the recessive nature of this disease, there are only 7 variable mutations reported in the literature (see text for details). (**b**) DMP1 protein is reported mainly in the extracellular matrix since there is a secretive signal peptide in its N-terminal. Besides, full-length DMP1 protein very likely represents a precursor form, and will be processed into 37-kDa N-terminal and 57-kDa C-terminal fragments.

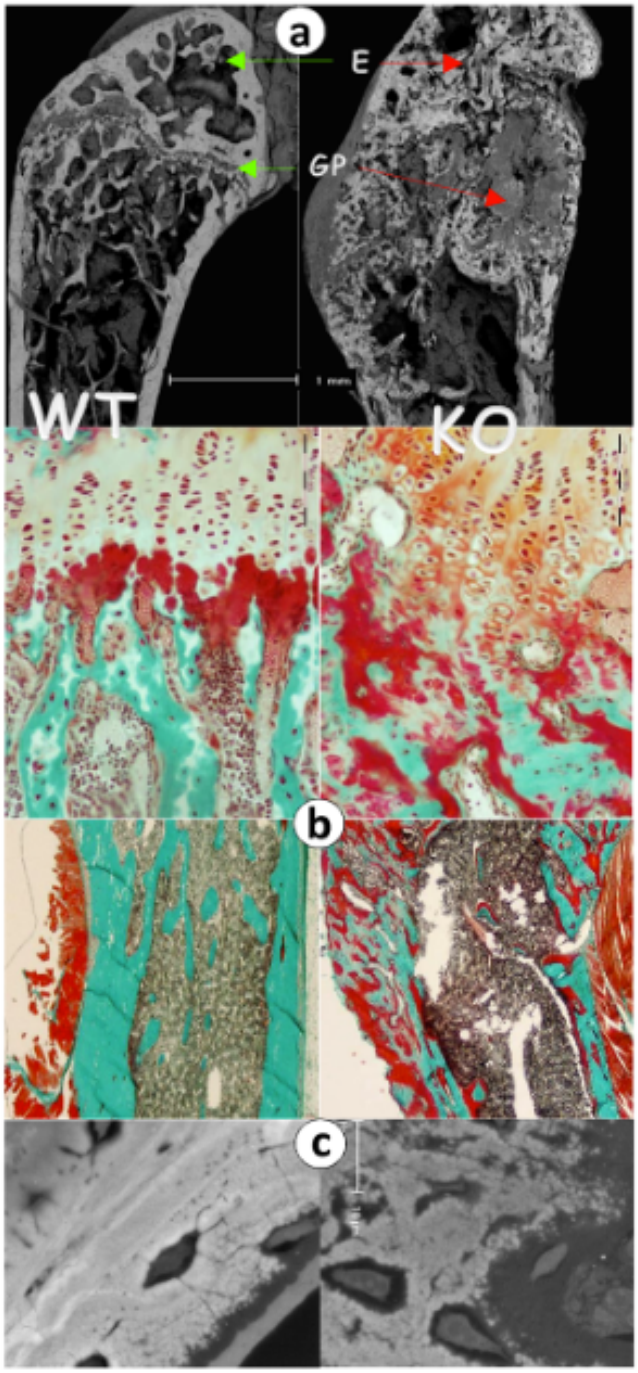


**Figure 1-3 Defective osteocytes are responsible for abnormal bone formation in the *Dmp1* knockout (KO) mice (*right panels*).** (**a**) Backscattered scanning electron microscopic (BSEM) images revealed the expanded and poorly organized growth plate (GP) in the Dmp1 KO femur, and severe defects in mineralization as reflected by discontinuous mineral content in the cortical

bone region; (**b**) The Goldner stain showed sharp increases in osteoid areas (red) but greatly reduced mature bone (green) in the KO bone; and (**c**) BSEM images revealed that the mineral was evenly distributed surrounding the osteocyte lacunae in the control bone (left, white); however, the mineral content was either missing, or sparsely located in regions surrounding the *Dmp1*-KO osteocytes.

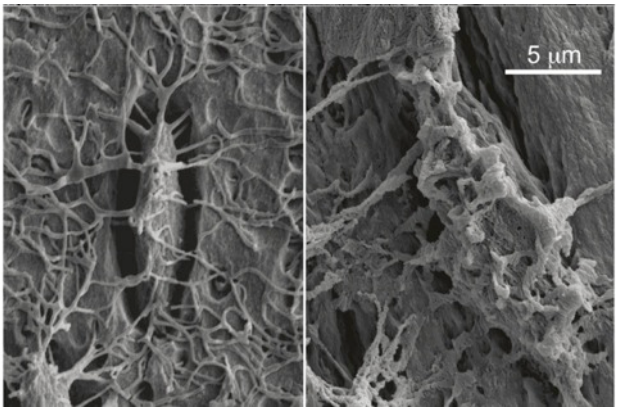


**Figure 1-4 SEM images of the acid-etched, resin-casted osteocyte-canalicular system.** Note the differences between the control (left) and the Dmp1-null (right) in distribution, size and surface of osteocytes. (Adapted from Feng *et al*., 2006)

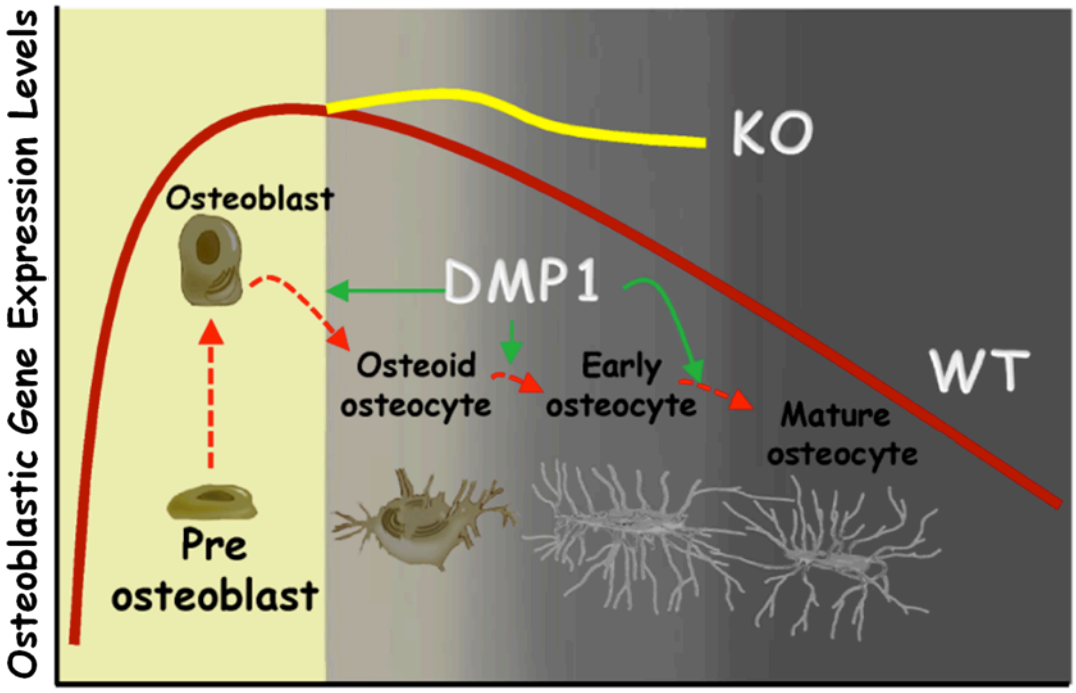


**Figure 1-5 Roles of DMP1 in control of osteocyte maturation.** The gene expression levels are high during differentiation of osteoblasts from preosteoblasts, whereas the gene expression levels are gradually reduced during osteocyte maturation from osteoid osteocyte-early osteocyte and then mature osteocytes. DMP1 is one of the key players during this process. The loss of *Dmp1* in mice or *DMP1* mutations in humans will disrupt normal osteoblast to osteocyte maturation. As a result, these immature osteoblast-like osteocytes express high levels of many osteoblast markers (RunX2, OSX, Col I, ALP, BSP, and OCN) and early osteocyte markers such as E11 in bone matrices.

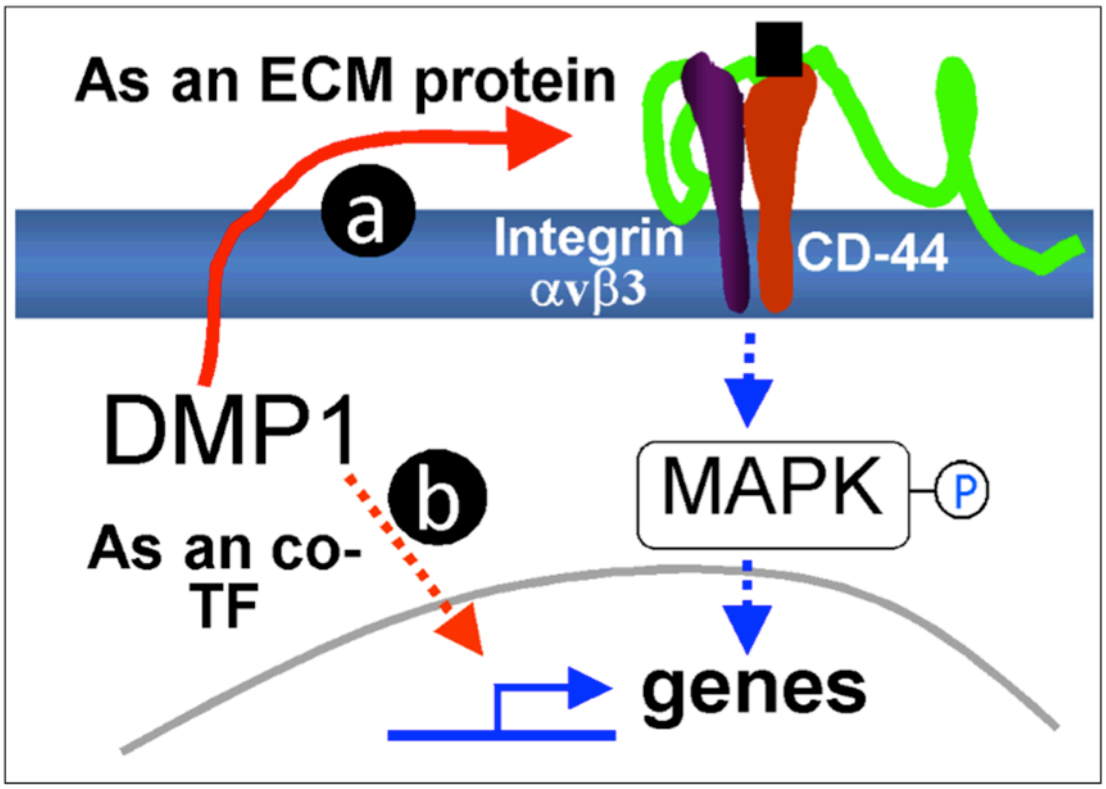


**Figure 1-6 Proposed models for DMP1 control genes critical for osteogenesis.** DMP1 either acts as an extracellular matrix (ECM) protein that binds to integrin αvβ3/CD-44 via its RGD domain and activates the MAPK signaling pathway (**a**), or as a transcriptional factor (TF) that targets the nucleus (**b**). The end results are that the genes critical for mineralization are activated.

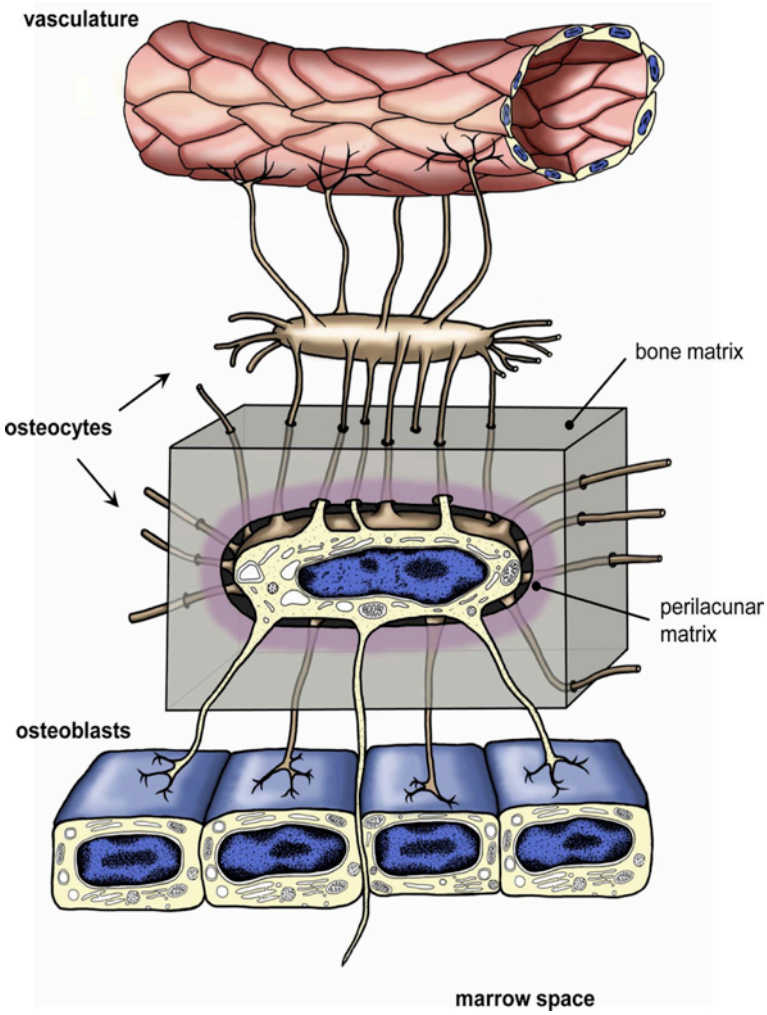


**Figure 1-7 Schematic representation of ostoecytes and their connections.** An embedded osteocyte located within its lacuna, illustrating its dendritic processes passing through the bone matrix (gray shading) within narrow tunnels termed canaliculi. The osteocyte's dendritic processes interconnect with other osteocytes as well as surface osteoblasts. Note that some osteocyte processes may extend beyond the osteoblast layer to potentially interact with cells in the marrow and that osteocyte dendrites are also in intimate contact with the vasculature. The composition of the perilacunar matrix immediately adjacent to the osteocyte (mauve shading) is different from that of the rest of the bone matrix (gray shading), which may influence the magnitude of mechanical strains perceived by the osteocyte. (Adapted from Dallas *et al*., 2013)

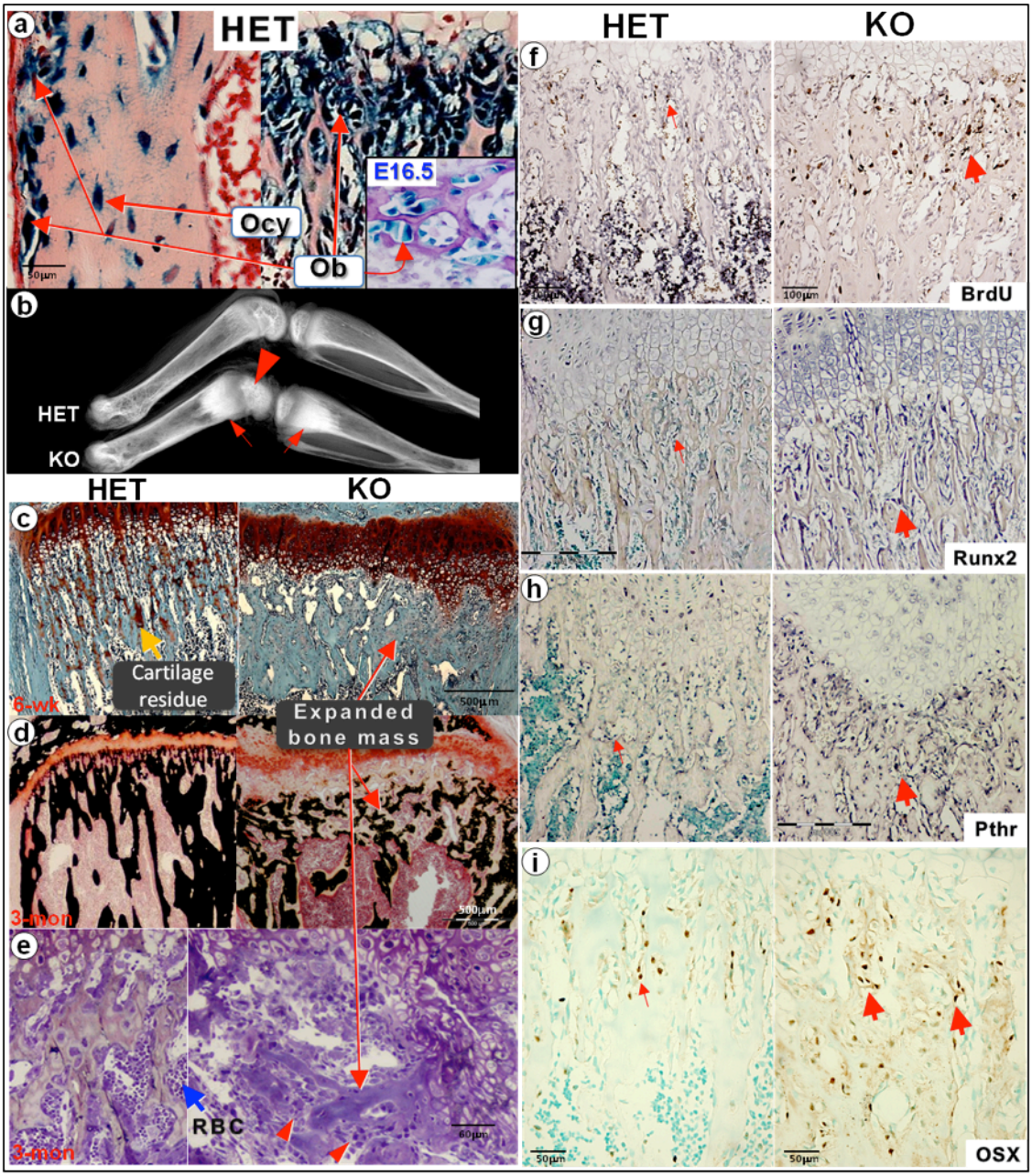


**Figure 2-1** ***Dmp1*** **is expressed in postnatal osteoblasts and responsible for regulating osteoblast proliferation and differentiation.** (**a**) X-gal staining of HET long bone displayed blue positive cells not only in the osteocytes (Ocy) but also in the osteoblasts (Ob) in both the embryonic day 16.5 (insert) and the postnatal 3 weeks, especially in the metaphysis (right image). (**b**) Representative radiographs of the 10-day-old long bones indicate co-exist of the expanded metaphysis and the delay formed epiphysis. *Dmp1*-null long bone shows a delayed formation of epiphysis (arrowhead) and expanded metaphysis (arrows) compared to the age-matched control bone. (**c-e**) Histological images showed that in the *Dmp1*-KO tibia metaphysis (right panels) there was a sharp expansion of bone masses containing little cartilage residue (**c**,

safranin O stain, 6 weeks), which indicated a lack of endochondral bone formation but active intramembranous bone formation. The von Kossa stain (**d**, 3 months) displayed poor mineralization, and the toluidine stain (**e**, 3 months) revealed a large amount of increased osteoblast-like cells (arrowheads) with essentially no red blood cells (RBC) compared to the control (left). (**f-i**) *In situ* and immunohistochemical staining showed that in the KO tibia metaphysis (right images), there were increases in the BrdU positive cells (**f**), *Runx2* mRNA (**g**), *Pthr* mRNA (**h**, Pthr), and OSX protein (**i**).

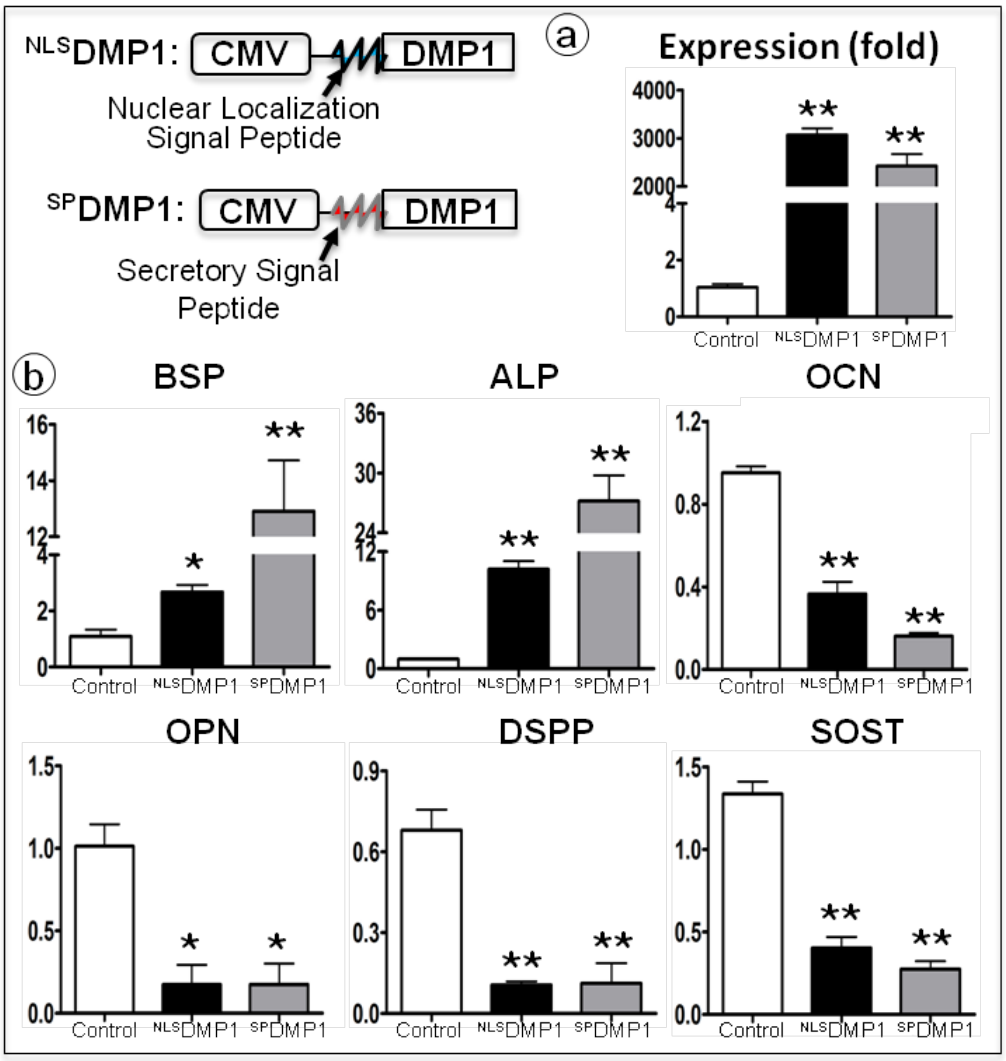


**Figure 2-2 Transfection of Ad-CMV-$^{NLS}$DMP1 or Ad-CMV-$^{SP}$DMP1 greatly changed expressions of bone markers in MC3T3 cells.** **(a)** Left panel: schematic constructs of $^{NLS}$DMP1 and $^{SP}$DMP1, in which the CMV promoter was used to drive the full-length *Dmp1* cDNA. In $^{NLS}$DMP1 the endogenous DMP1 signal peptide aa1-aa16 (MKTVILLVFLWGLSCAL) was replaced by the nuclear localization signal peptide (NLS, PPKKKRKV, upper) in contrast to the $^{SP}$DMP1 with its endogenous signal peptide (lower). Right panel: significantly high mRNA expressions of *Dmp1* were detected after 48-hour transfection. (**b)** Significant changes in mRNA levels of *Bsp*, *Alp, Ocn*, *Opn*, *Dspp*, and *Sost* in both experimental groups with an identical trend. The real-time PCR data, normalized with *Gapdh* (as an internal control), are presented as mean ± SEM; n=4 in each group; *P<0.05; **P<0.01, compared to the control.

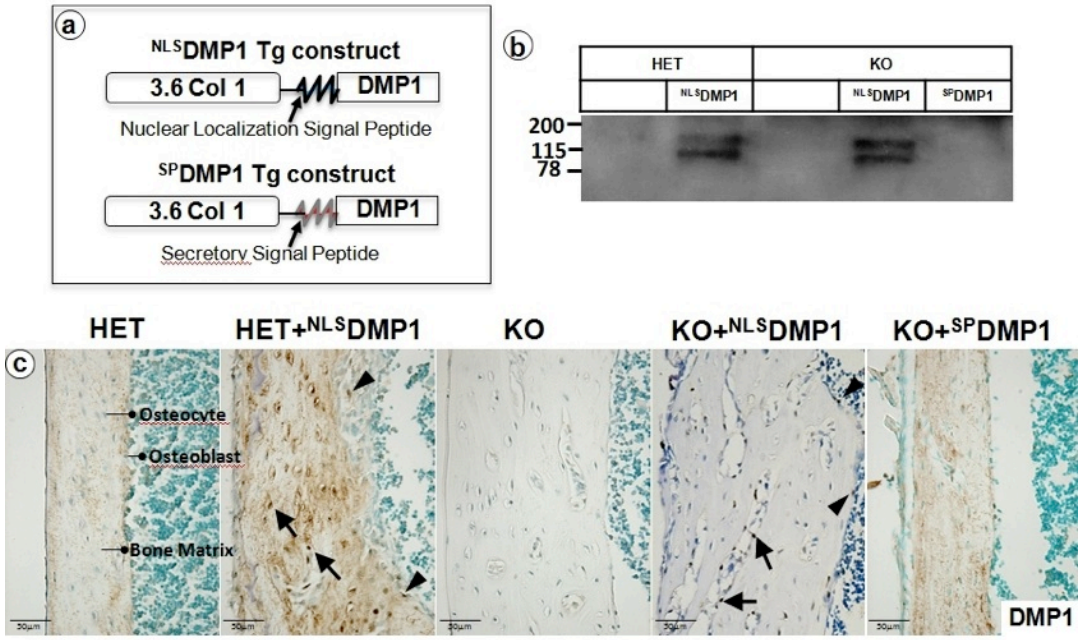


**Figure 2-3 $^{NLS}$DMP1 expressed in the nuclei and $^{SP}$DMP1 mainly secreted in the matrix.** (**a**) Schematic structure of $^{NLS}$DMP1 and $^{SP}$DMP1 transgenes. In the $^{NLS}$DMP1 construct, the full-length *Dmp1* cDNA is driven by the 3.6 kb *Col 1α1* promoter with its endogenous signal peptide replaced by a NLS peptide, while in the $^{SP}$DMP1 construct, the same 3.6 kb *Col 1α1* promoter was used to drive full-length *Dmp1* cDNA with its endogenous secretory signal peptide. (**b**) Non-cleavaged Western bands at the position of ~105 kDa from cell lysates of the primary calvarial osteoblasts with the $^{NLS}$DMP1 transgenes regardless of the HET or KO. (**c**) Immunohistochemistry staining of DMP1 in 3-week-old mouse long bone. DMP1 is mainly expressed in the HET matrix with little signal in the nucleus, compared to no positive signal in the matrix in KO mice. In the $^{NLS}$DMP1 transgenic bone, DMP1 is detected in both the matrix and the nucleus of osteocytes (arrows) and osteoblasts (arrowheads), whereas the $^{SP}$DMP1 is highly expressed in the matrix and the osteoblasts. Data demonstrate that the transgenes is successfully targeted in the nucleus or matrix of the bone cells only.

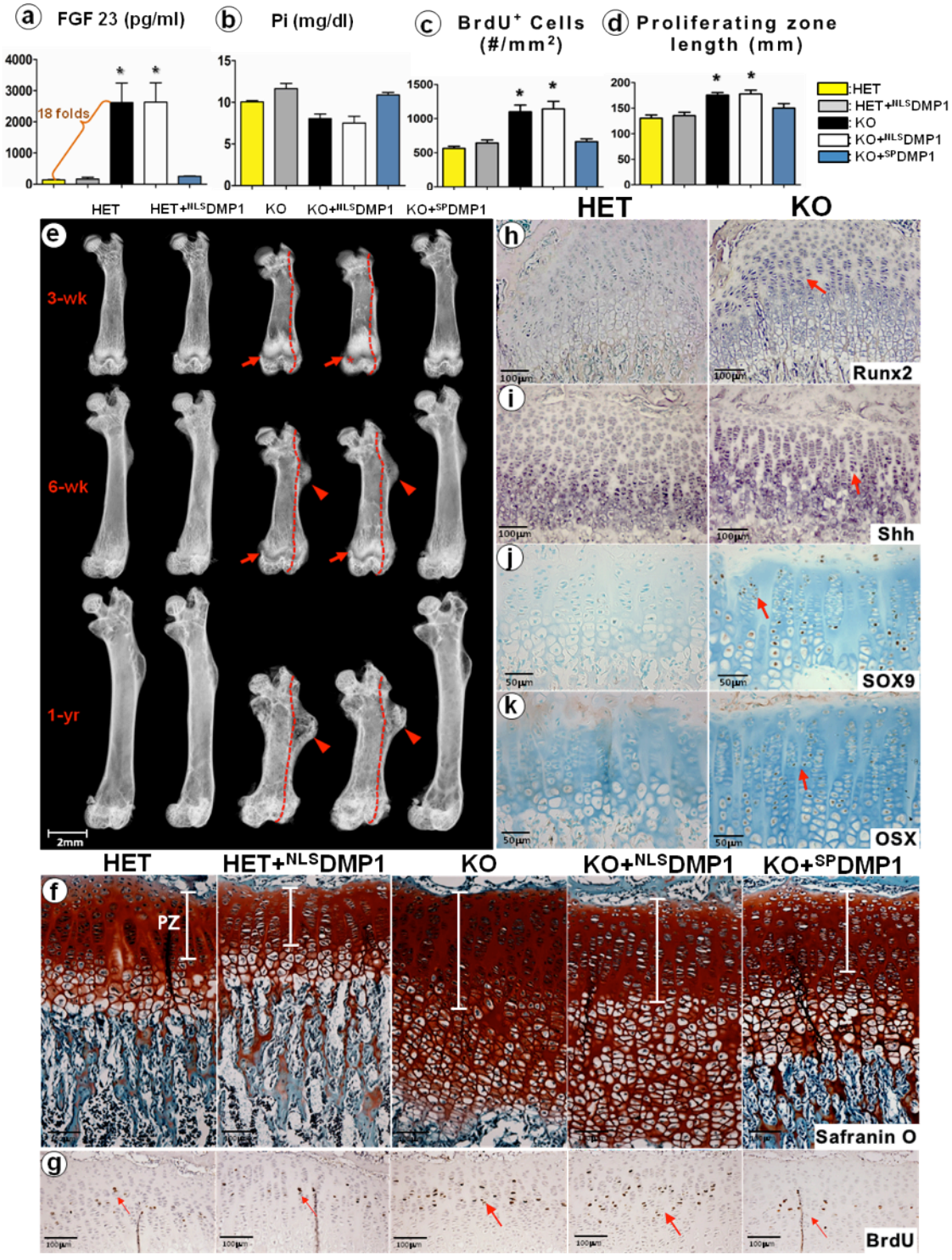


**Figure 2-4 $^{NLS}$DMP1 revealed no cure of rachitic phenotypes in *Dmp1*-null mice, however $^{SP}$DMP1 fully rescued the defects.** (**a-b**) Quantified data displayed a greater than 18-fold up-regulation of serum FGF23 levels, and a decrease of more than 20% of the Pi (phosphorus) in

*Dmp1*-null mice. The overexpression of $^{NLS}$DMP1 had no effect on these parameters in either the HET control or KO groups; however, the $^{SP}$DMP1 fully restored. (**c**) Statistic results demonstrated the above changes in the proliferation zone length and the cell proliferation numbers in the KO groups were significant different from the control groups. Again, the $^{NLS}$DMP1 had no apparent effect on the above changes in either the HET or the KO background, but $^{SP}$DMP1 made functions. (**e**) Representative radiophotography shows short femurs with poor mineral remodeling in all three *Dmp1*-KO groups (3 wk, 6 wk and 1 year). The targeted expression of $^{NLS}$DMP1 had no rescue effects on the length, accumulated bone masses (asterisks), expanded and malformed growth plates (arrows), and distorted tuberosities (arrowheads), all of which were fully rescued by $^{SP}$DMP1. (**f**) Safranin O stain images of 3-week-old tibias, in which there were two expanded regions in the KO growth plate: the proliferation zone (PZ, white lines) and hypertrophic zone. The $^{NLS}$DMP1 transgene had no effect in both regions but $^{SP}$DMP1 recovered this abnormality. (**g**) BrdU stain images indicate increased number of BrdU positive cells in the KO and KO+$^{NLS}$DMP1 groups. (**h-k**) *In situ* and immunohistochemical staining show the molecular changes of the chondrogenic genes in the *Dmp1*-KO background (right images), including *Runx2* mRNA (**i**), sonic hedgehog mRNA (*Shh,* **j**), SOX9 (**k**), and OSX (**l**). Data indicate an increase in cell proliferation and differentiation in the *Dmp1-null* mice, most likely due to hypophosphatemia. (Data are presented as mean ± SEM; n=5; *P<0.05; compared to the control).

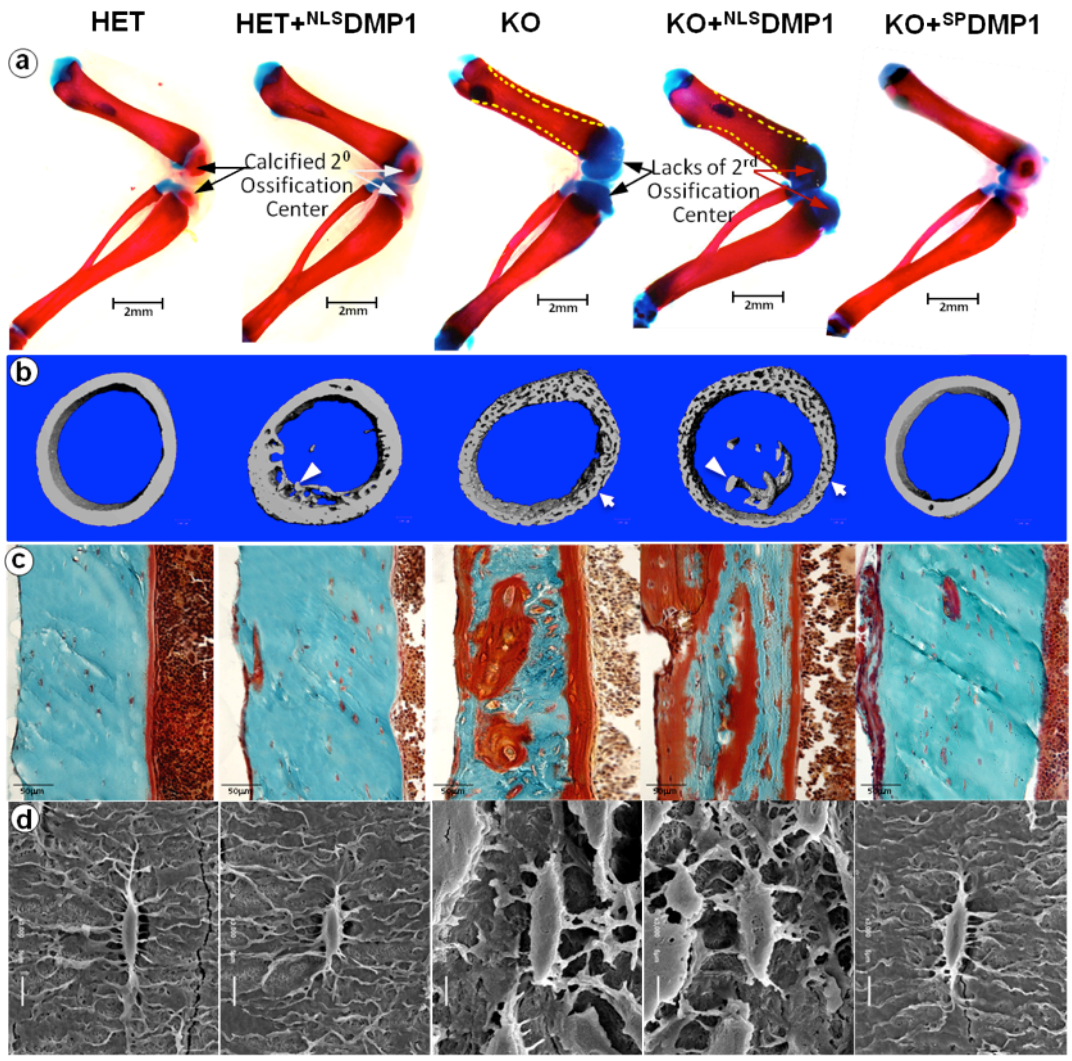


**Figure 2-5 Targeting DMP1 in the *Dmp1*-KO nuclei did not rescue deficiencies of mineralization in *Dmp1*-null mice, however re-expressing DMP1 in the matrix greatly recovered these defects.** (**a-c**) Compared to $^{SP}$DMP1, $^{NLS}$DMP1 had no effect on bone shape and secondary ossification (**a**, alizarin red/alcian blue stains, arrows), bone porosity and mineralization reflected by uCT images (**b**, arrowheads) and Goldner stain (**c**, red indicating a lack of minerals). (**d**) SEM images of the acid-etched, resin-casted osteocyte-canalicular system. Note the KO+$^{NLS}$DMP1 osteocyte shown the same appearance with the KO osteocyte, indicating nuclear activities of DMP1 had no apparent effect on the osteocyte-lacunocanalicular system.

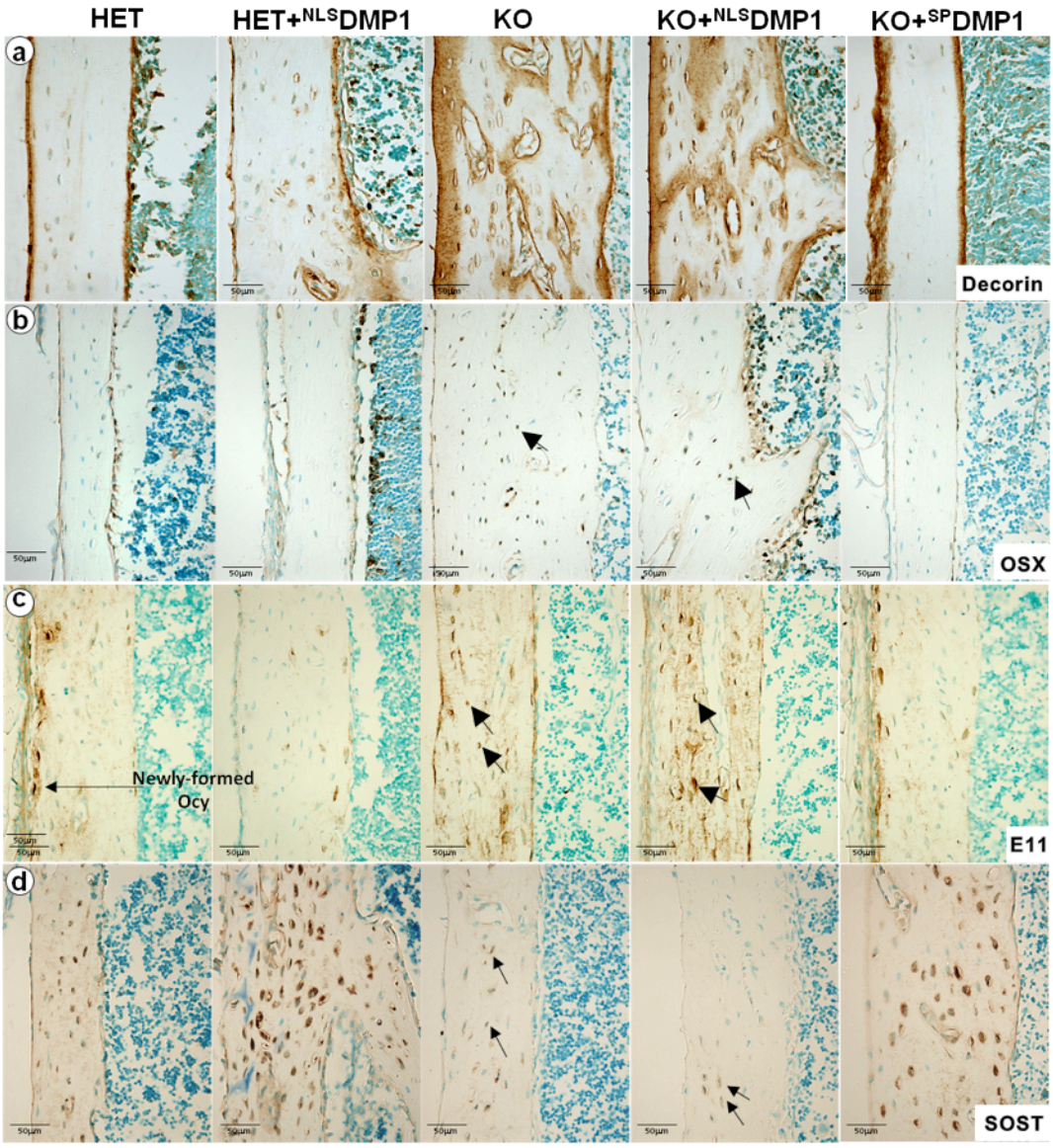


**Figure 2-6 IHC analysis shown the targeted expression of $^{NLS}$DMP1 transgene revealed no rescue of the maturational defects in ostecytes.** (**a**) Immunohistochemistry assay of decorin of 3-week mouse long bones, brown indicates positive staining. (**b**) An increase in the expression of OXS in KO osteocytes and the KO+$^{NLS}$DMP1 osteocytes (arrows). (**c**) Arrows indicate that widely expressed E11 throughout the cortical bone of KO and the KO+$^{NLS}$DMP1 mouse (arrows). (**d**) The staining for SOST shows the osteocytes, in the KO and the KO+$^{NLS}$DMP1 groups, did not express or weakly expressed the SOST (arrows).

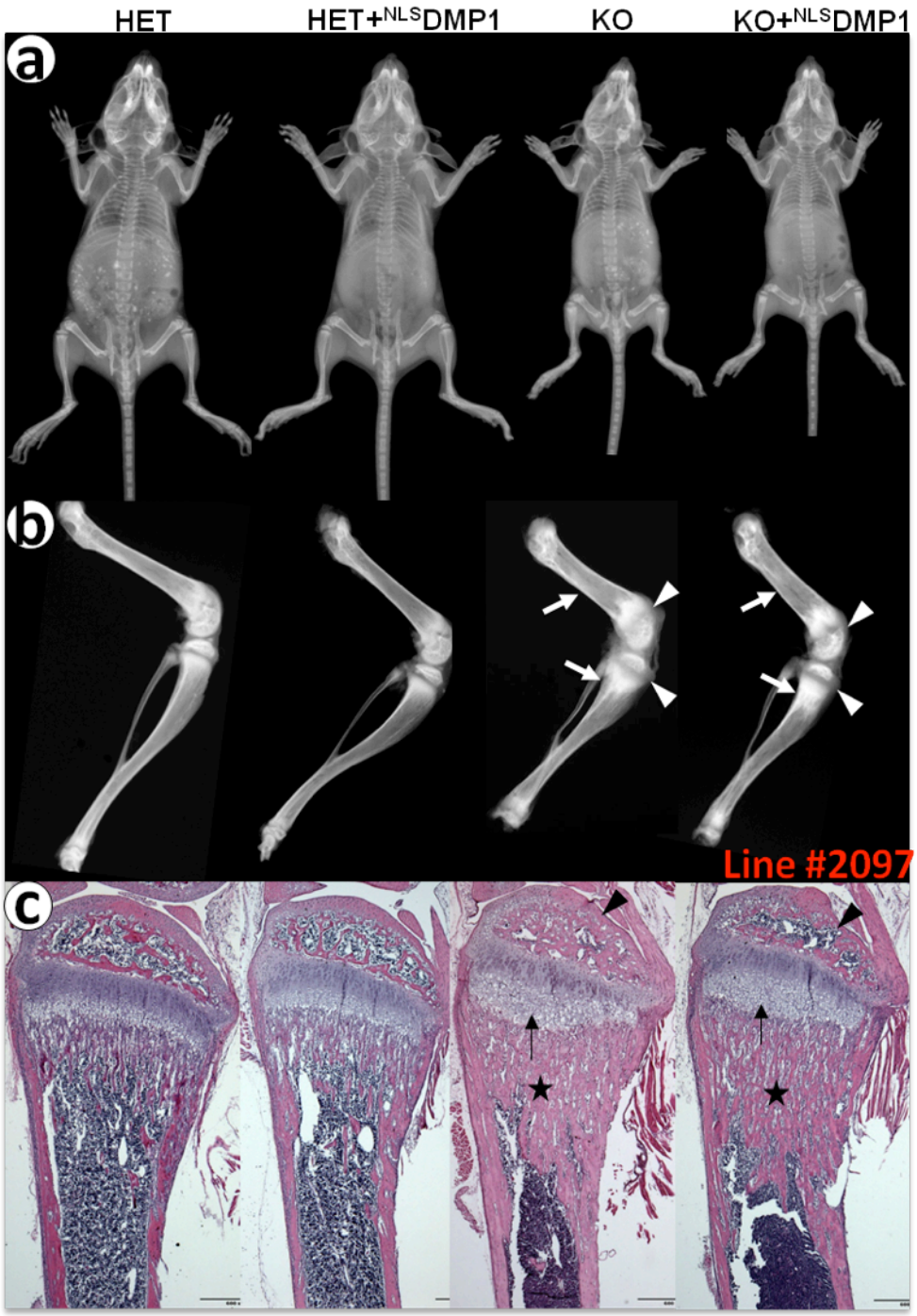


**Figure 2-7 The targeted expression of $^{NLS}$DMP1 transgene (line #2097) in either the *Dmp1* HET or the KO background had no effect.** (**a-b**) Representative radiograph images showed that the $^{NLS}$DMP1 transgene in the HET osteoblast and osteocyte had no apparent effect, and this transgene did not rescue *Dmp1*-KO phenotype. (**c**) H&E staining images, revealed no rescues on

the *Dmp1*-KO skeleton abnormalities, including expanded hypertrophic chondrocyte zone and malformed metaphysis.

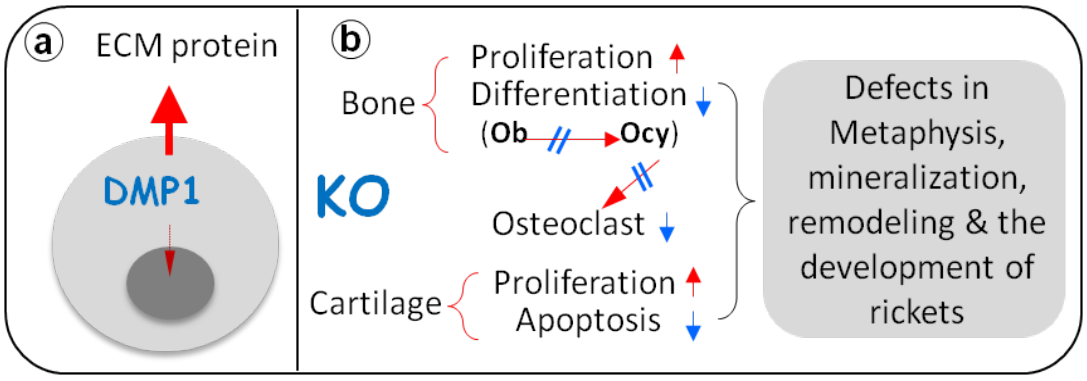


**Figure 2-8 The *in vivo* working model**. (**a**) DMP1, secreted from the cell, binds to integrin via its RGD domain, followed by activation of the MAP kinase signaling pathway (34,35). The targeted expression of DMP1 in the nucleus has no direct role in osteogenesis *in vivo*. (**b**) DMP1, expressed in the osteoblast, facilitates cell proliferation and transformation directly from osteoblasts into osteocytes. Deletion of *Dmp1* leads to an increase in cell proliferation and a reduction in osteoblast cell differentiation. Because of the great increase of FGF23 in *Dmp1*-KO osteocytes, the reduced Pi brings on an increase in cell proliferation and differentiation in chondrocytes (a new indirect role of hypophosphatemia in the growth plate), in addition to the abnormality in the apoptosis process (18).

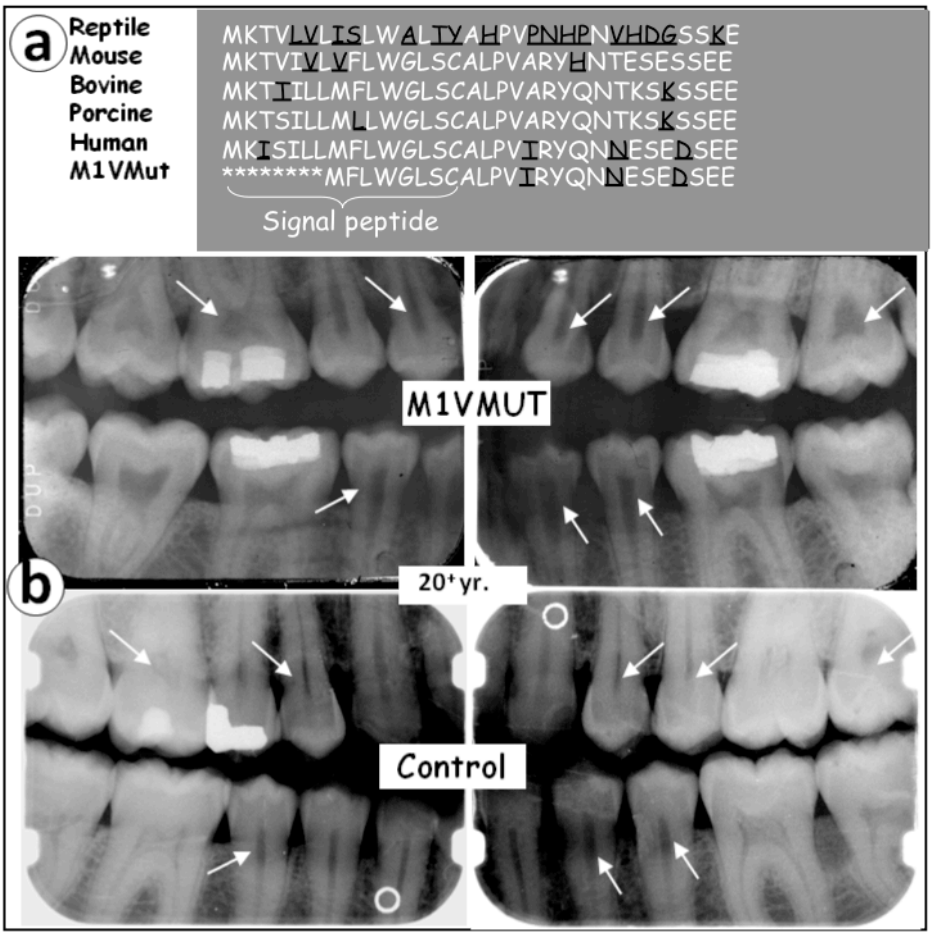


**Figure 3-1 Tooth phenotypes in an M1V Mut ARHR patient.** (**a**) Comparison of the amino acid sequence of the $NH_2$-terminal region of the DMP1 across species, including the M1V mutant human DMP1. (**b**) Radiographs from an adult (20+ years old) ARHR patient (upper panel) and the age-matched control (lower panel). Arrows show the enlarged pulp cavities and root canals and reduced dentin thickness in the patient, compared to the control.

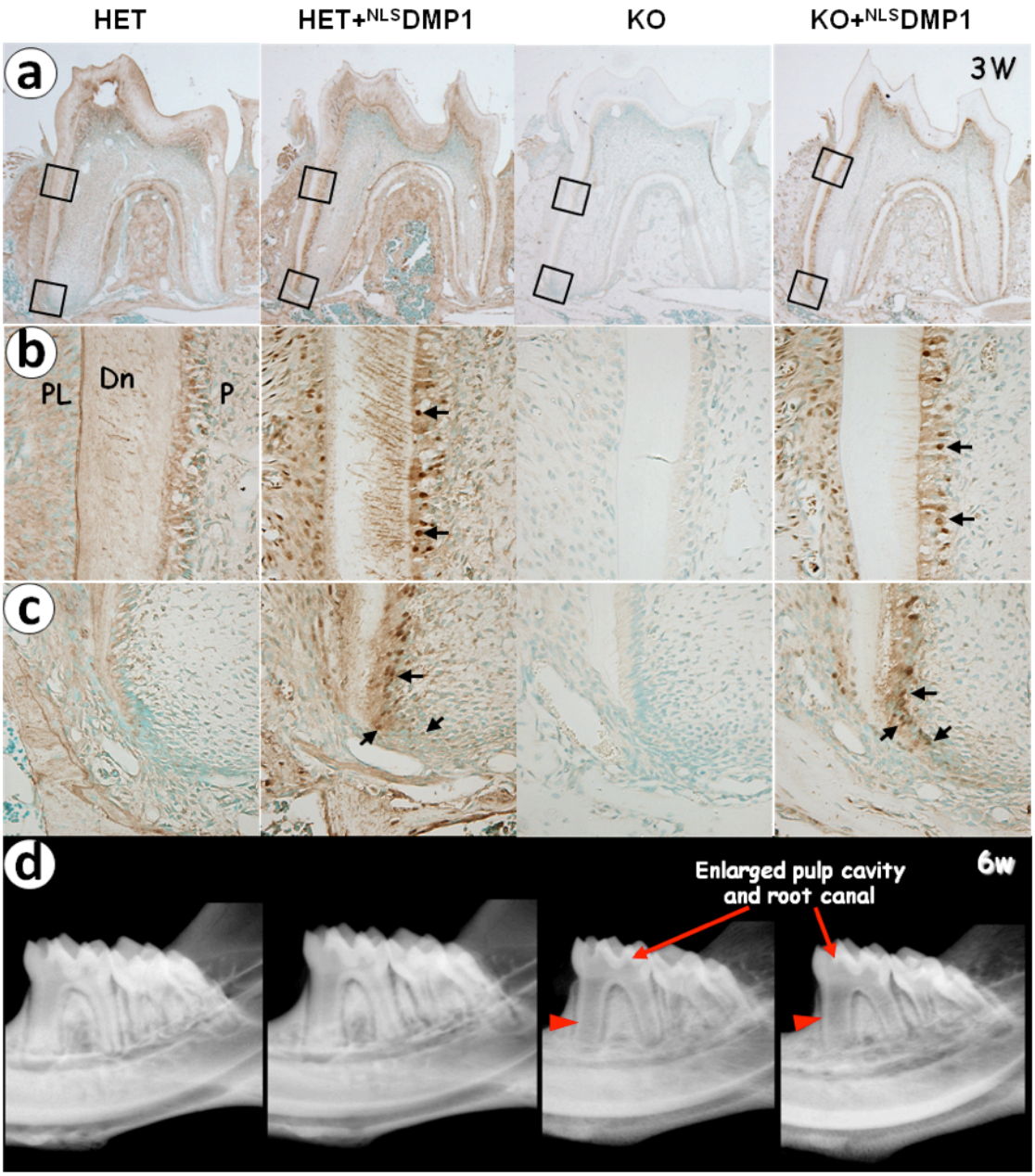


**Figure 3-2 Nucleus-targeted Dmp1 expressed in the pre-odontoblasts and odontoblassts, showing no morphological improvement of *Dmp1*-null tooth.** (**a**) Dmp1 expression was analyzed in the first molars of 3-week-old mice by immunohistochemical staining using anti-Dmp1-C-terminal antibody (signal in brown color). (**b-c**) Higher magnification of the boxed areas in (**a**) demonstrated the presence of Dmp1 in the odonto-lineage and dentinal matrix. (**b**) Localization of $^{NLS}$DMP1 in the nuclei, cytoplasm and dendrites of odontoblasts (arrows). (**c**) Localization of $^{NLS}$DMP1 in the nuclei of pre-odontoblasts (arrows). (**d**) Representative radiographs of 6-week-old mouse mandible. Note the enlarged pulp cavities and root canals (arrows), and the thinner dentin (arrowheads) in both KO and KO+$^{NLS}$DMP1 mice.

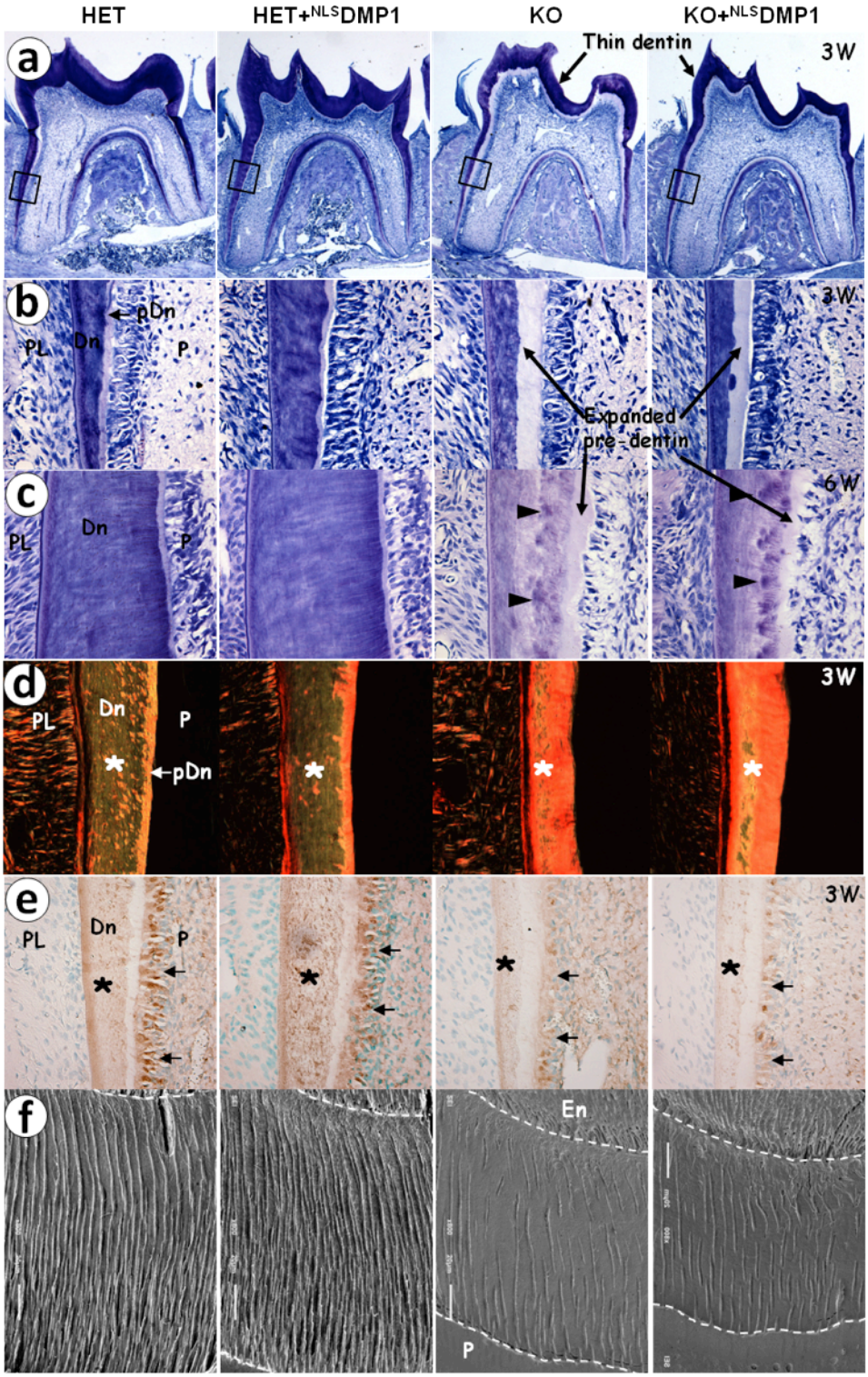


**Figure 3-3 Nucleus-targeted Dmp1 had no rescue of the dental abnormalities of *Dmp1*-null mice.** (**a**) Toluidine Blue staining of the first molars of 3-week-old mice. Note the thinner crown

dentin (arrows) in both KO and KO+$^{NLS}$DMP1 tooth. (**b**) Higher magnification of the boxed area in (**a**). Note the widened predentin (arrows) with thinner dentin in KO and KO+$^{NLS}$DMP1 mice. (**c**) The toluidine blue staining of 6-week-old mouse dentin. Note the widened predentin (arrows) with reduced dentin thickness, as well as the presence of interglobular dentins (arrowheads) in KO and KO+$^{NLS}$DMP1 mice. (**d**) Sirius Red staining sections imaged under polariscope. The orange color indicates larger collagen fibers, whereas the green color means thinner collagen fibers such as reticular fibers. (**e**) Anti-DSP-antibody staining of 3-week-old mice. DSP was down regulated in the odontoblasts (arrows) and dentinal matrix (asterisks) of the KO and KO+$^{NLS}$DMP1 mice. (**f**) Images of dentinal tubular system from resin-casted acid-etched electron microscopy. Note the dendritic branches are fewer and disorganized in the KO and KO+$^{NLS}$DMP1 mice. Notes: PL, periodontal ligament; Dn, dentin; P, pulp; En, enamel; pDn, predentin.

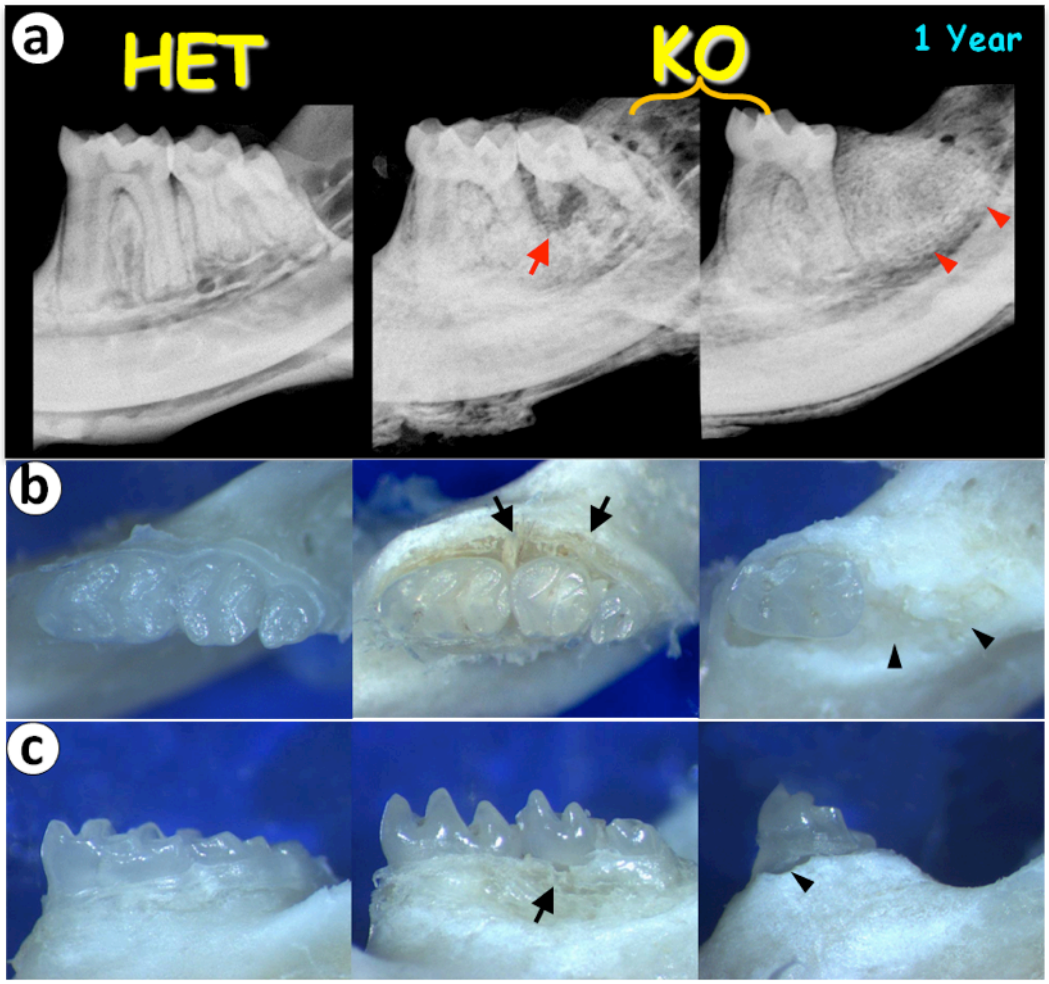


**Figure 3-4** ***Dmp1*-null mice developed typical periodontitis.** (**a**) Radiographs of 1-year-old mouse tooth. Note the periodontal-endodontic combined lesions in the second molar (arrows), and the exfoliation of the second molar (arrowheads). (**b-c**) Occlusal and buccal photographs of 1-year-old mouse tooth. Note the periodontitis with notable loss of periodontal attachment (arrows), and the exfoliation of the second molar with alveolar bone absorption (arrowheads).

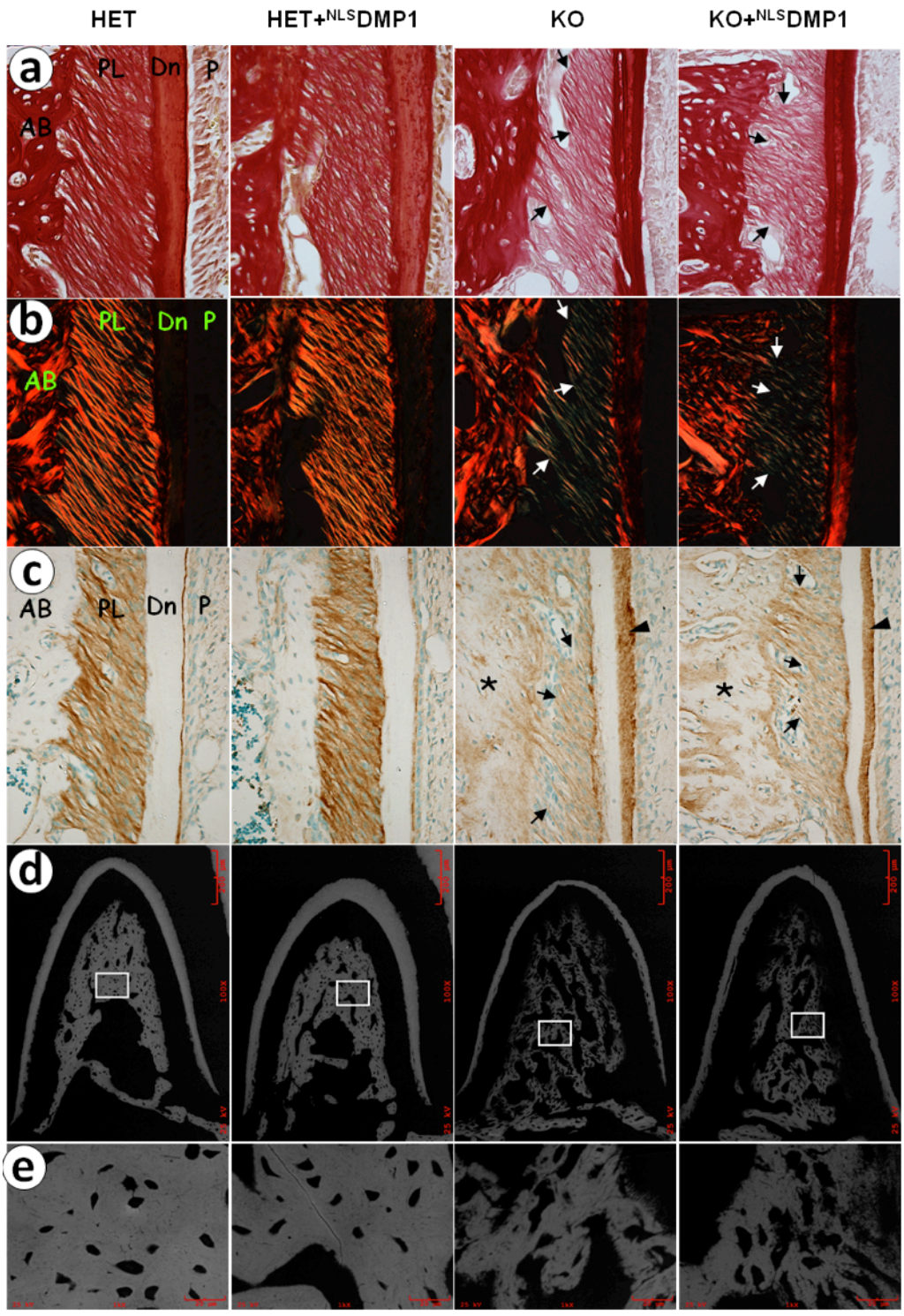


**Figure 3-5 Nucleus-targeted Dmp1 had no improvement of periodontal structures.** (**a**) Sirius Red staining imaged under light microscopy (3-week-old mouse molars). Dark red indicated more collagen contents, light red meant less collagen contents. (**b**) Same sections of (**a**)

but imaged under polarized light (3-week-old mouse molars). (**c**) Anti-biglycan antibody staining of 3-week-old mouse molars. The biglycan was increased in the widened predentin (arrowheads) and the matrix of alveolar bone (asterisks), but was decreased in the PDL (arrows) in KO and KO+$^{NLS}$DMP1 groups. (**d-e**) Back-scatter electron microscopy of alveolar bone. KO and KO+$^{NLS}$DMP1 groups show trabeculae disorganization and hypomineralization. Notes: AB, alveolar bone.

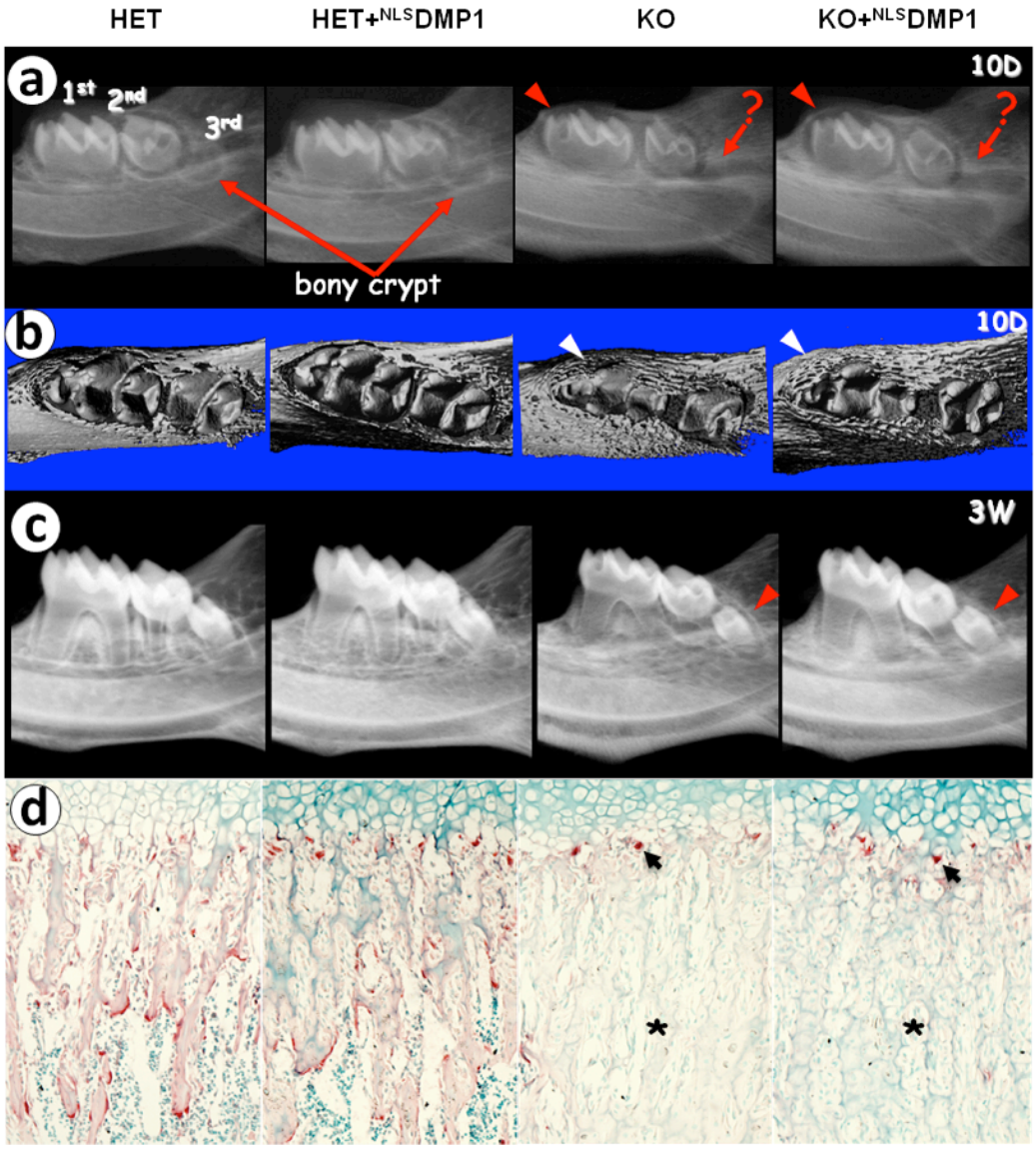


**Figure 3-6 Nucleus-targeted Dmp1 showed no effect on tooth eruptional delay.** (**a-b**) Representative radiographs and micro-CT images of 10-day-old mice mandibles. The bony crypts (arrows) indicate where the third molar will develop in the HET and HET+$^{NLS}$DMP1 mice; whereas they were barely visible in KO and KO+$^{NLS}$DMP1 mice. In addition, the occlusal surface (arrowheads) of the first molars of was partially embedded in the bony crysts in both KO and KO+$^{NLS}$DMP1 mice. (**c**) Representative radiographs of 3-week-old mouse tooth, note the partially eruption of the third molars (arrows). (**d**) TRAP staining of the metaphysis (at 3 weeks). In the primary spongiosa region, the number of TRAP positive cells (red) was significantly reduced in the *Dmp1*-KO and the KO+$^{NLS}$DMP1 mice. Notes: 1$^{st}$, first molar; 2$^{nd}$, second molar, 3$^{rd}$, third molar.

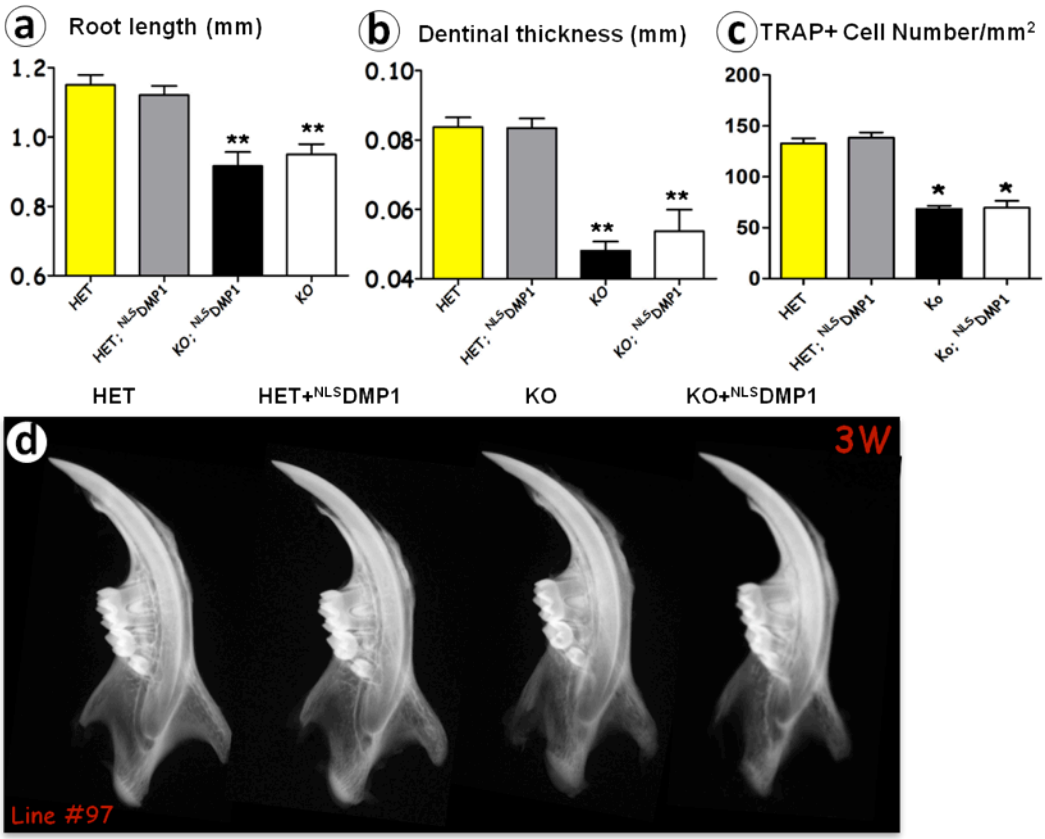


**Figure 3-7** (**a-b**) Shown are the length (mm) of the roots (**a**) and the thickness (mm) of the dentin layer (**b**) from 3-week-old mice. Data are mean ± SEM; n=6 in each group; *P<0.05; **P<0.01, compared to the control (HET). (**c**) Statistic analysis of the number of osteoclasts in 3-week-old mice. Data are mean ± SEM; n=4 in each group; *P<0.05, compared to the control. (**d**) Radiographs of the 3-week-old mandibles of another independent line (line #97). Typical dental and condylar defects can be found in KO and KO+$^{NLS}$DMP1 mice.

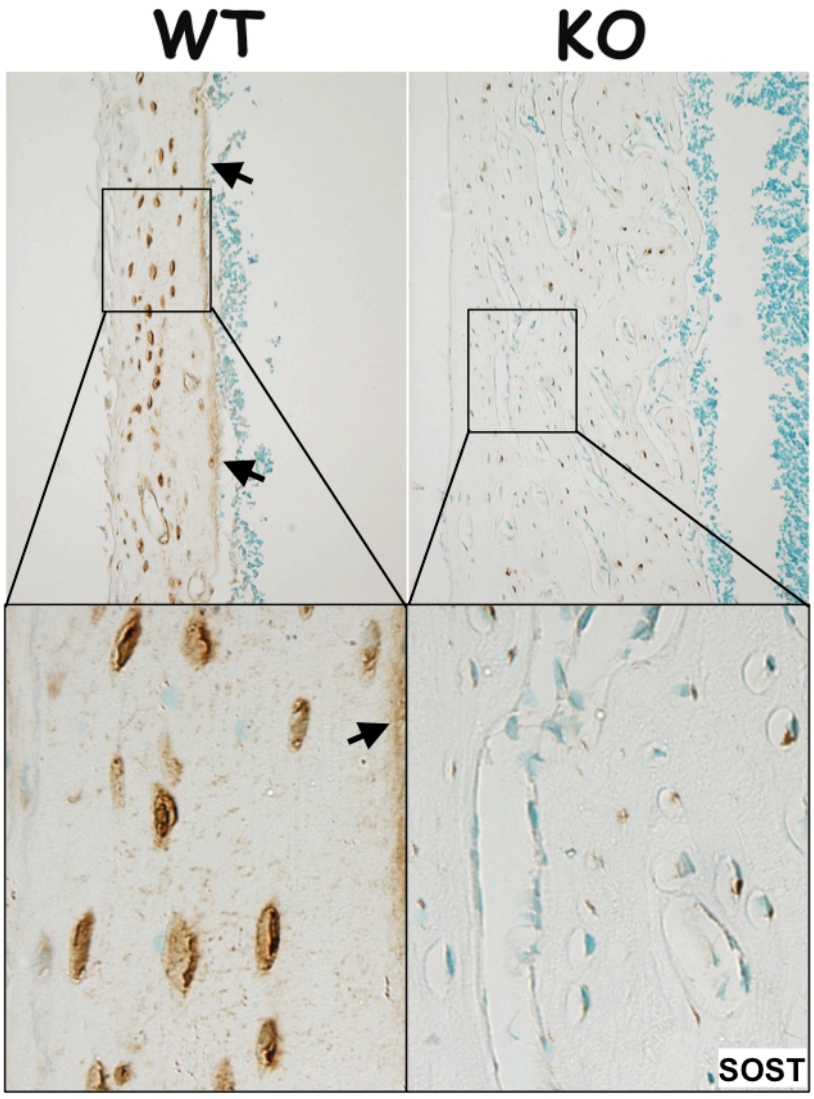


**Figure 4-1 A sharp reduction of SOST expression in the 3-wk-old cortical bone of *Dmp1*-null mice.** The representative immunohistochemistry image displayed a high level of sclerostin in the mature osteocytes and dendrites (left) compared to the age-matched *Dmp1*-KO tibia, where SOST was largely undetectable (right images).

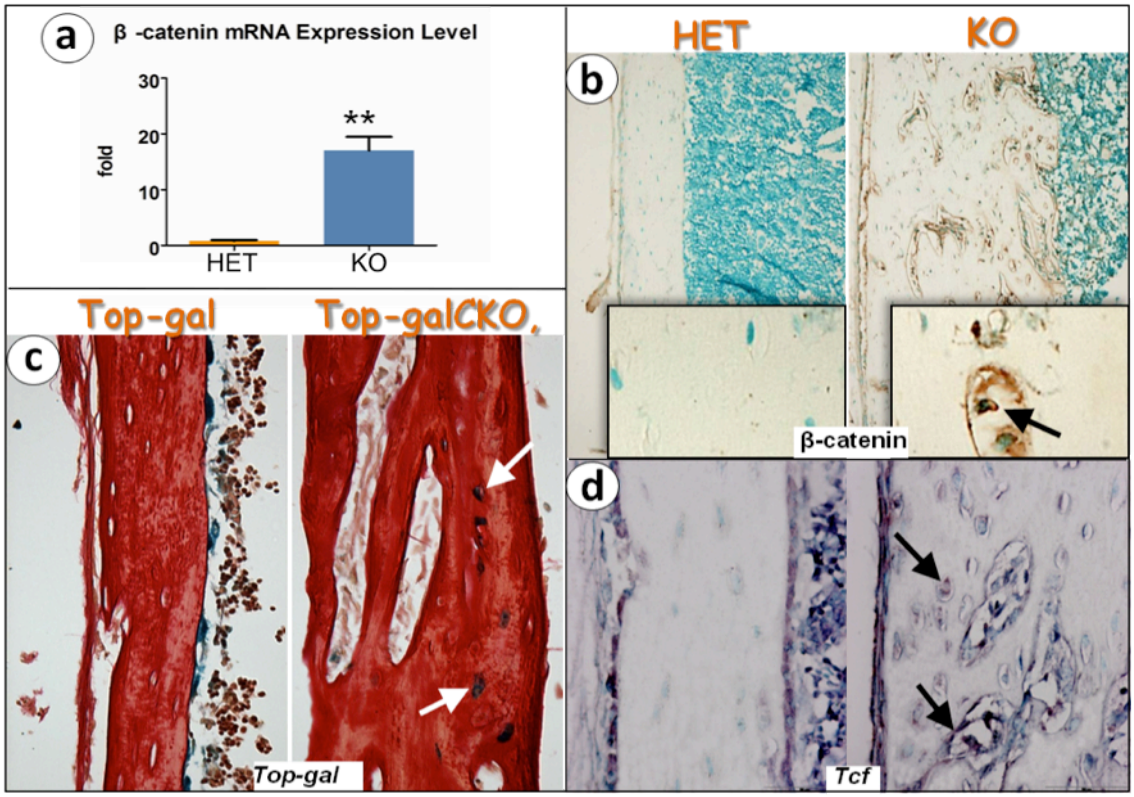


**Figure 4-2 Wnt/β-catenin signaling was up-regulated in the osteocyte of *Dmp1*-null mice.** (**a**) The mRNA expression level of β-catenin showed a more than 15-fold up-regulation in *Dmp1*-null mice compared to the controls. Data are presented as mean ± SEM; n=6 in each group; *P<0.05; **P<0.01. (**b**) Immunohistochemistry staining of β-catenin revealed an increased expression of β-catenin in the osteocytes. The arrow in the magnified box indicated a nuclear localization of β-catenin. (**c**) X-gal positive osteocytes were found in the *Dmp1* conditional knockout (*3.6 kb Col1 Cre; Dmp1*$^{fx/fx}$; Top-gal+) mouse long bones (arrows), compared to few positive osteocytes in the control group (*Dmp1*$^{fx/fx}$; Top-gal+). Note the *β-galactosidase* gene was driven by a TCF-β-catenin responsive promoter in the Top-gal mouse, so canonical Wnt activity was detected by X-gal staining. (**d**) *In situ* hybridization staining demonstrated the *Tcf* expression that was up-regulated in the osteocytes of *Dmp1*-null mice (arrows).

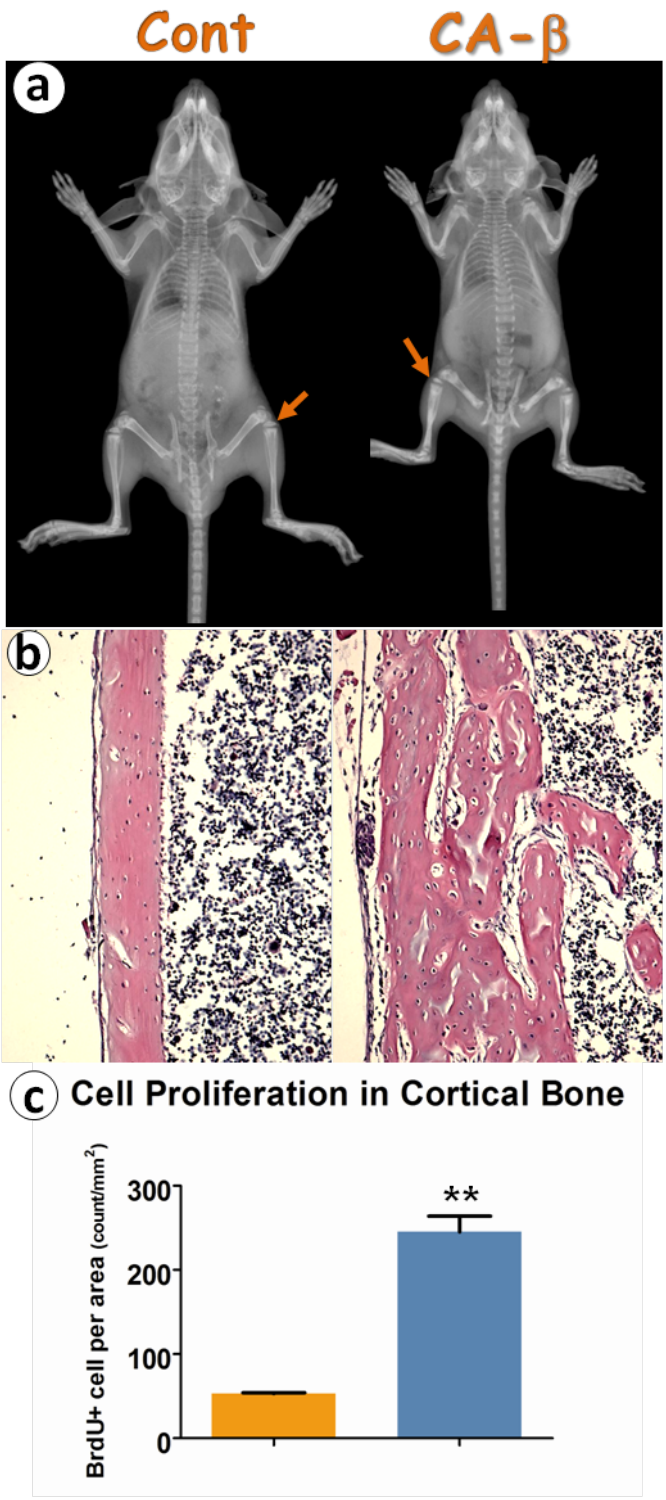


**Figure 4-3 Constitutive stabilization of β-catenin in osteocytes led to abnormal bone structures at age of 3 weeks.** Compared to the control group, CA-β mice display typical

hypophos-phatemic rickets/osteo-ma-lacia phenotype, including short stature and long bone size (**a**), cortical bone porosity (**b**), and osteocyte proliferation (**c**). Data are presented as mean ± SEM; n=4 in each group; *P<0.05; **P<0.01.

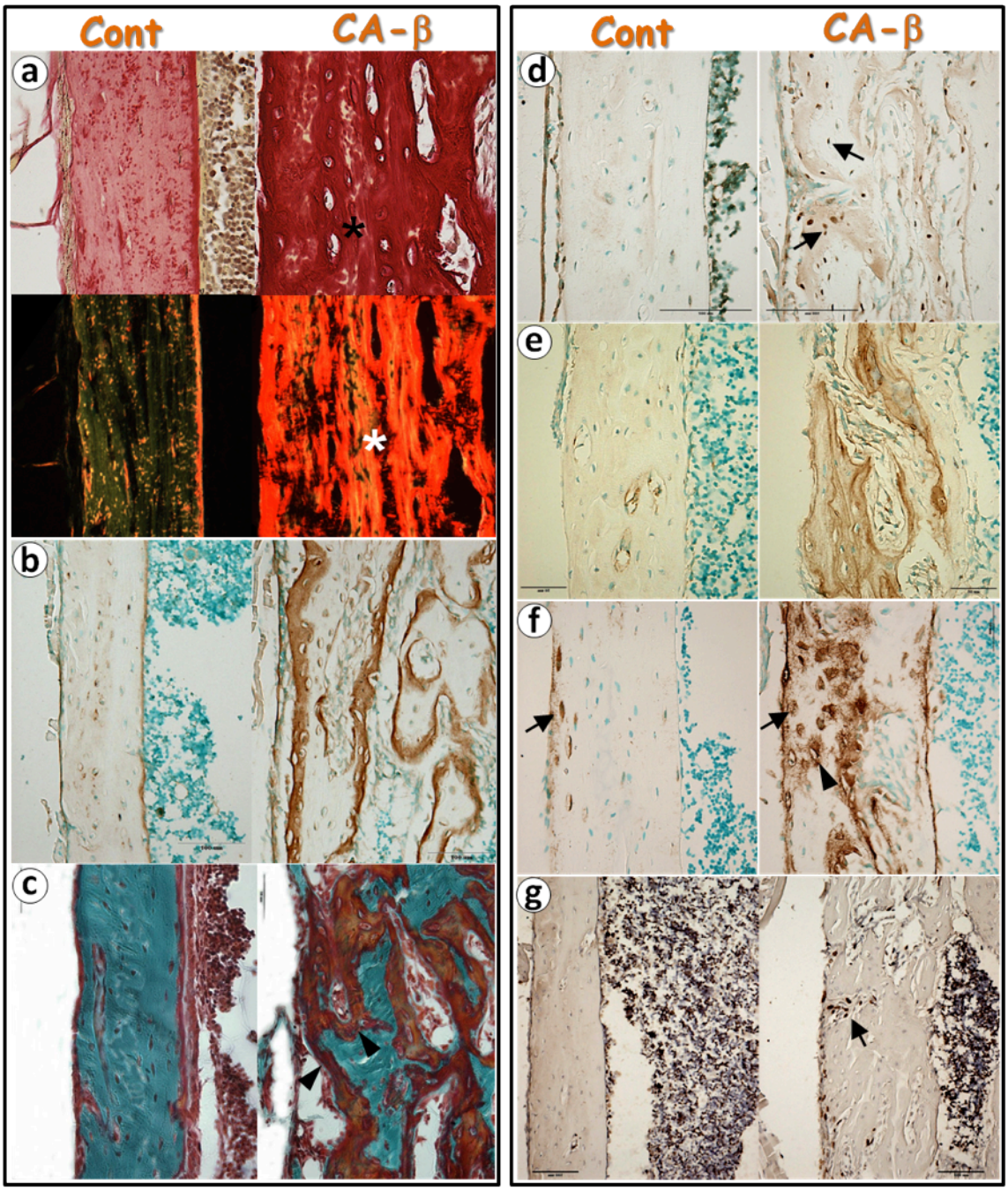


**Figure 4-4 Constitutive stabilization of β-catenin in osteocytes recaptured osteomalacia phenotype and displayed deformed osteocytes.** (**a-c**) Elevated β-catenin levels in offspring of CA-β (*Dmp1-Cre*; β-cat$^{ex3loxP/+}$) mice resulted in osteomalacia indistinguishable from that in *Dmp1*-KO mice, as evidenced by: polarized light images, in which green means thinner collagen fibers such as reticular fibers, whereas red or orange indicates larger collagen fibers such as collagen type I, showing increased disorganized collagen (**a**); Biglycan staining that appeared

more positively stained area (**b**); Goldner-stained sections of bone, which exhibited abundant red-staining osteoid (**c**). (**d-g**) Increased β-catenin levels in osteocytes caused maturation defects, as supported by immunostains of osteoblast and early osteocyte markers, such as OSX (**d**), OPN (**e**), and E11 (**g**) showed apparently elevated expressions; BrdU staining that documented increased proliferation of the immature osteocytes in the osteoid (**g**).

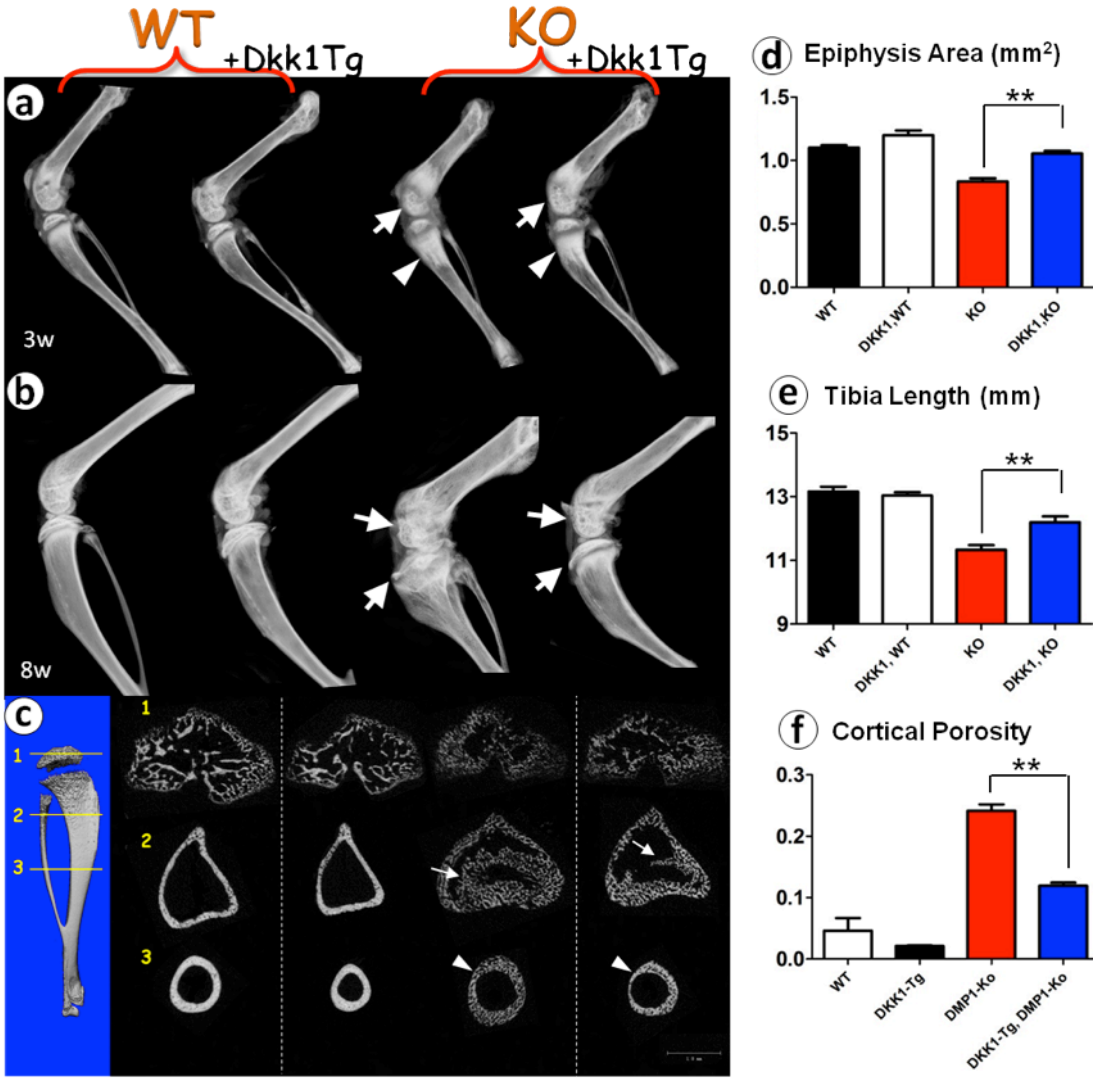


**Figure 4-5 Normalizing the Wnt/β-catenin activity greatly improves the bone morphology.** (**a-b**) Representative radiographs of 3-wk (**a**) and 8-wk (**b**) groups. Note the long bone shape was better formed in the DKK1; KO mice, compared to the KO groups. Also, in the KO mice, the bone accumulation appeared in the metaphysis (arrowhead) and the epiphyseal structures were disorganized and malformed (arrows), but were notably improved by *Dkk1*-Tg. (**c**) μ-CT images of different tibia cross sections indicated malformed epiphysis structure, obvious bone accumulation in the metaphysis (arrow), and porous cortical bone (arrowhead) in the KO mice, which was partially rescued by *Dkk1*-Tg. (**d-f**) Statistical analysis of epiphysis area (**d**), tibia length (**e**), and cortical porosity (**f**) indicated significances between KO and DKK1; KO groups. Data are presented as mean ± SEM; n=5 in each group; *P<0.05; **P<0.01.

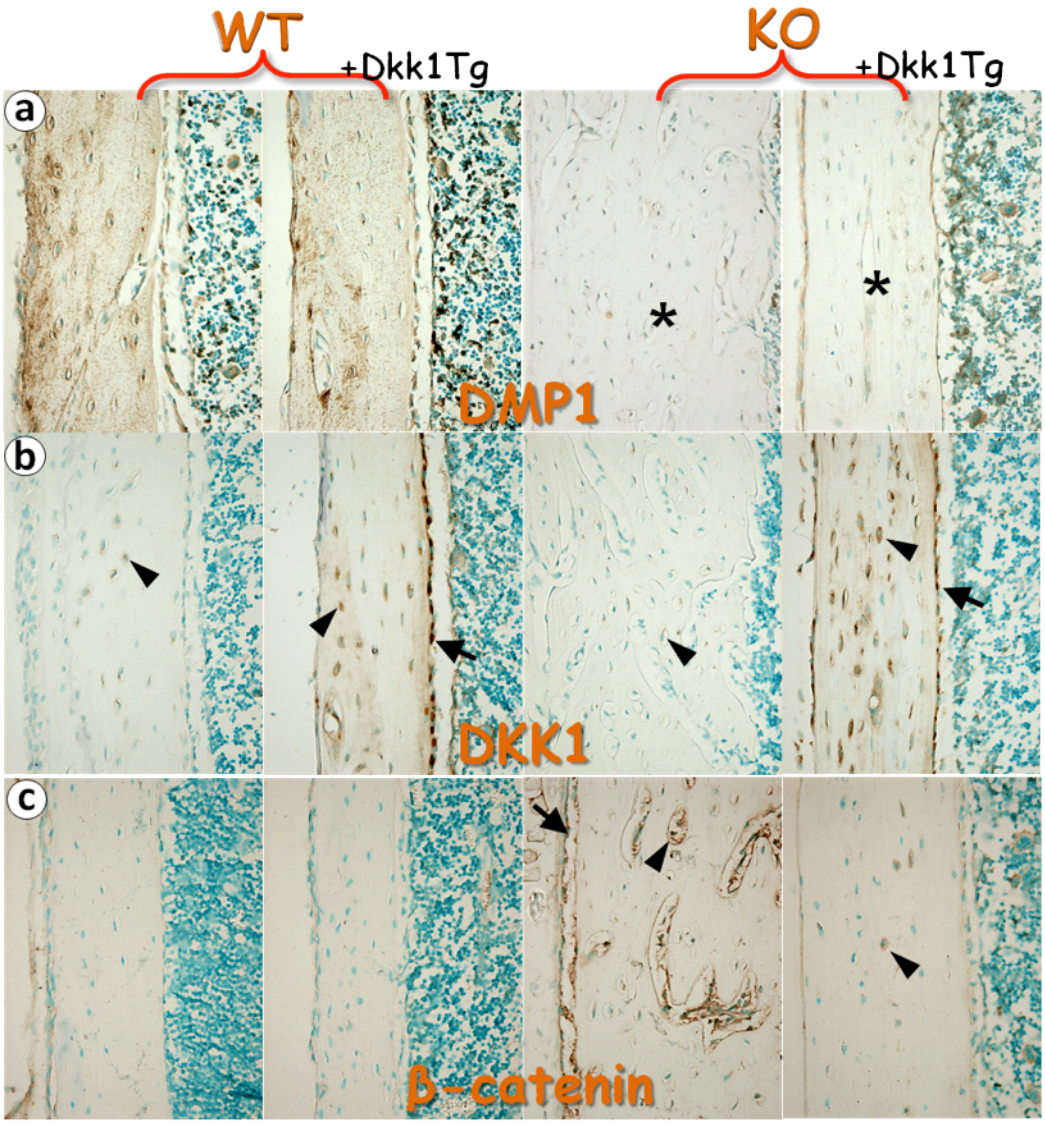


**Figure 4-6 Immunohistochemistry staining of DMP1, DKK1, and β-catenin.** (**a**) In the WT groups, endogenous DMP1 was detected in the bone matrix and osteocytes, compared to no signal in the KO groups (asterisk). (**b**) Endogenous DKK weakly expressed in the osteocytes compared to little signal was detected in the *Dmp1*-null osteocytes (arrowheads). The transgenic DKK1 highly expressed in both osteocytes (arrowheads) and osteoblasts (arrows), consistent with the activity of its 2.3 Col1α1 promoter. (**c**) β-catenin increased in both osteoblasts (arrow) and osteocytes (arrowhead) of *Dmp1*-null mice, which was down-regulated in DKK1; KO group.

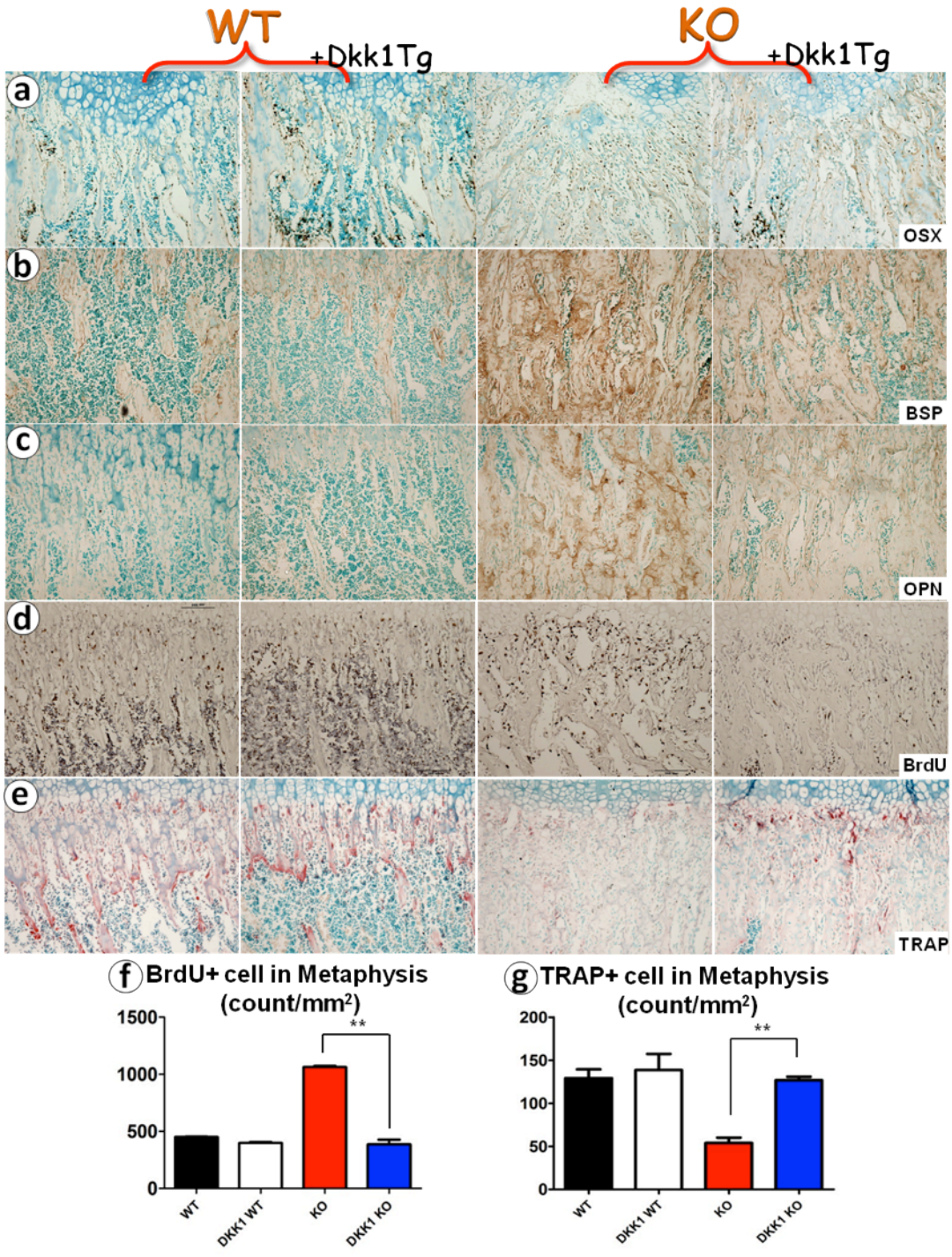


**Figure 4-7 The abnormal bone homeostasis in *Dmp1*-null metaphysis is improved by *Dkk1*-Tg.** (**a-c**) Immunohistochemistry staining of the osteoblastic markers, including OSX (**a**), BSP (**b**) and OPN (**c**), abundantly increased in the KO metaphysis, together with significantly increased cell proliferation activity (**d, f**), suggesting there is an enhanced bone formation in the

*Dmp1*-null metaphysis, which is partially rescued in the DKK1; KO mice. (**e, g**) Analysis of TRAP staining showed a significant restoration of osteoclast numbers in the DKK1; KO groups. Data are presented as mean ± SEM; n=4 in each group; *P<0.05; **P<0.01.

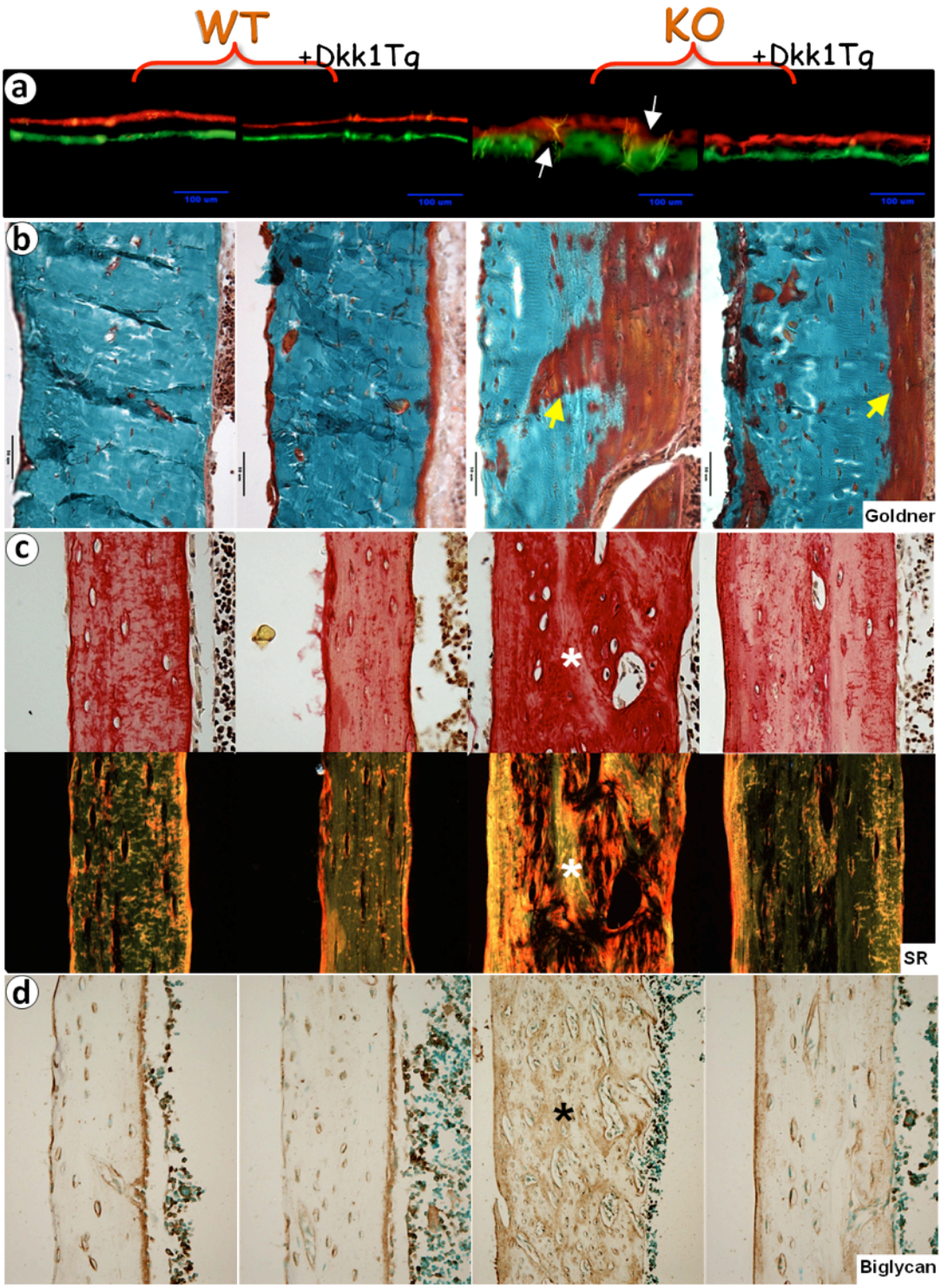


**Figure 4-8 Osteomalacia phenotype in *Dmp1*-null mice was greatly restored by *Dkk1*-Tg.** (**a**) The double fluorochrome labels displayed identical bone-formation rates in WT and DKK1;

WT were similar to the DKK1; KO mice but in contrast to the diffuse label (arrows) in the KO mice at the age of 4 weeks. (**b-d**) Cortical bone mineralization showed an apparent restoration in the DKK1; KO mice, evidenced by: Goldner staining (**b**, arrows); Sirius red-stained sections (**c**, asterisks) imaged under light microscopy (upper panels) and polarizing microscope (lower panels); anti-biglycan staining (**d**, asterisks).

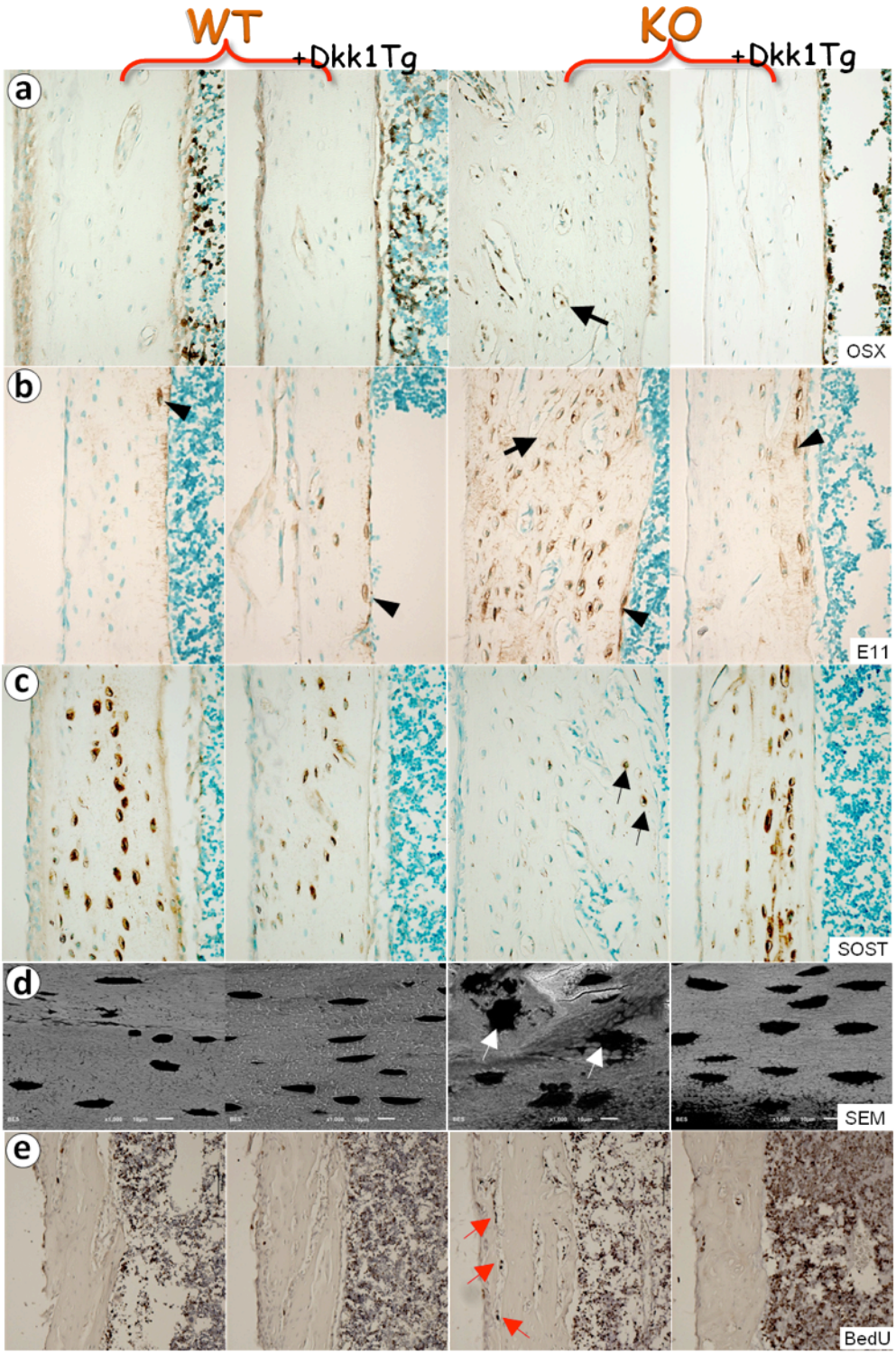


**Figure 4-9 Osteocyte maturation defect in *Dmp1*-null mice is greatly improved by *Dkk1*-Tg.** (**a-c**) Immunohistochemistry staining of the bone cell markers. (**a**) Osteoblastic marker

(OSX) is expressed in *Dmp1*-null osteocytes (arrow) but not in DKK1; KO. (**b**) Early osteocytic marker (E11), which is mainly expressed in the newly formed osteocytes (arrowheads) and widely detected in the KO mice (arrow). (**c**) Mature osteocytic marker SOST broadly expressed in the mature osteocyte but decreased in the *Dmp1*-null osteocyte (arrows). (**d**) Backscattered SEM displayed a notable restoration of osteocyte morphology together with a great improvement in the precellular mineralization in KO; DKK1 sample, compared to the malformation and hypomineralization of the *Dmp1*-null mice (arrows). (**e**) Representative BrdU-stained long bone sections showed that BrdU+ cells increased in number and distribution in the *Dmp1*-null cortical bone (arrows). In contrast, there were fewer BrdU+ cells detected in the DKK1; KO samples.

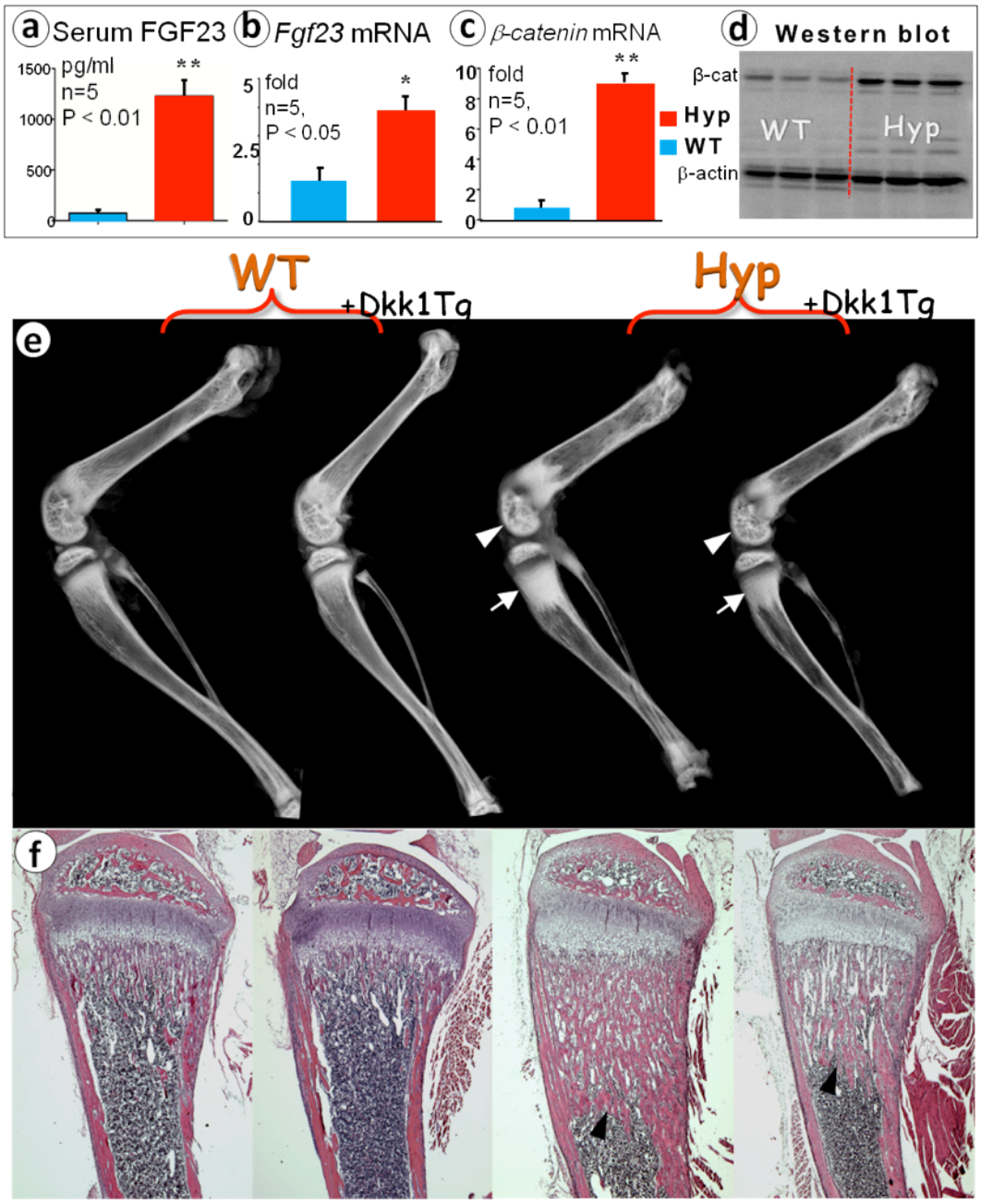


**Figure 4-10** ***Hyp*-mice displayed increased β-catenin level and *Dkk1*-transgene produced a morphological rescue in *Hyp*-mice.** (**a**) Serum FGF23 level in the *Hyp*-mice significantly increased (>1000-fold). (**b-c**) mRNA expression levels of *fgf23* and *β-catenin*. Significant increases can be found in both *fgf23* mRNA (**b**, >2-fold) and *β-catenin* mRNA (**b**, >9-fold). Data are presented as mean ± SEM; n=5 in each group; *P<0.05; **P<0.01. (**d**) Western blot analysis of 3 different pairs confirmed that the protein levels of β-catenin are higher in *Hyp*-mice, compared to the WT control. (**e**) Representative radiographs of mouse long bones. Both epiphyseal structure (arrowheads) and abnormal bone accumulation in metaphysis (arrows) were

partially rescued in DKK1; Hyp mice. (**f**) HE staining further indicates the bone trabeculae in tibia metaphysis is better organized in DKK1; Hyp mice, compared to *Hyp*-mice.

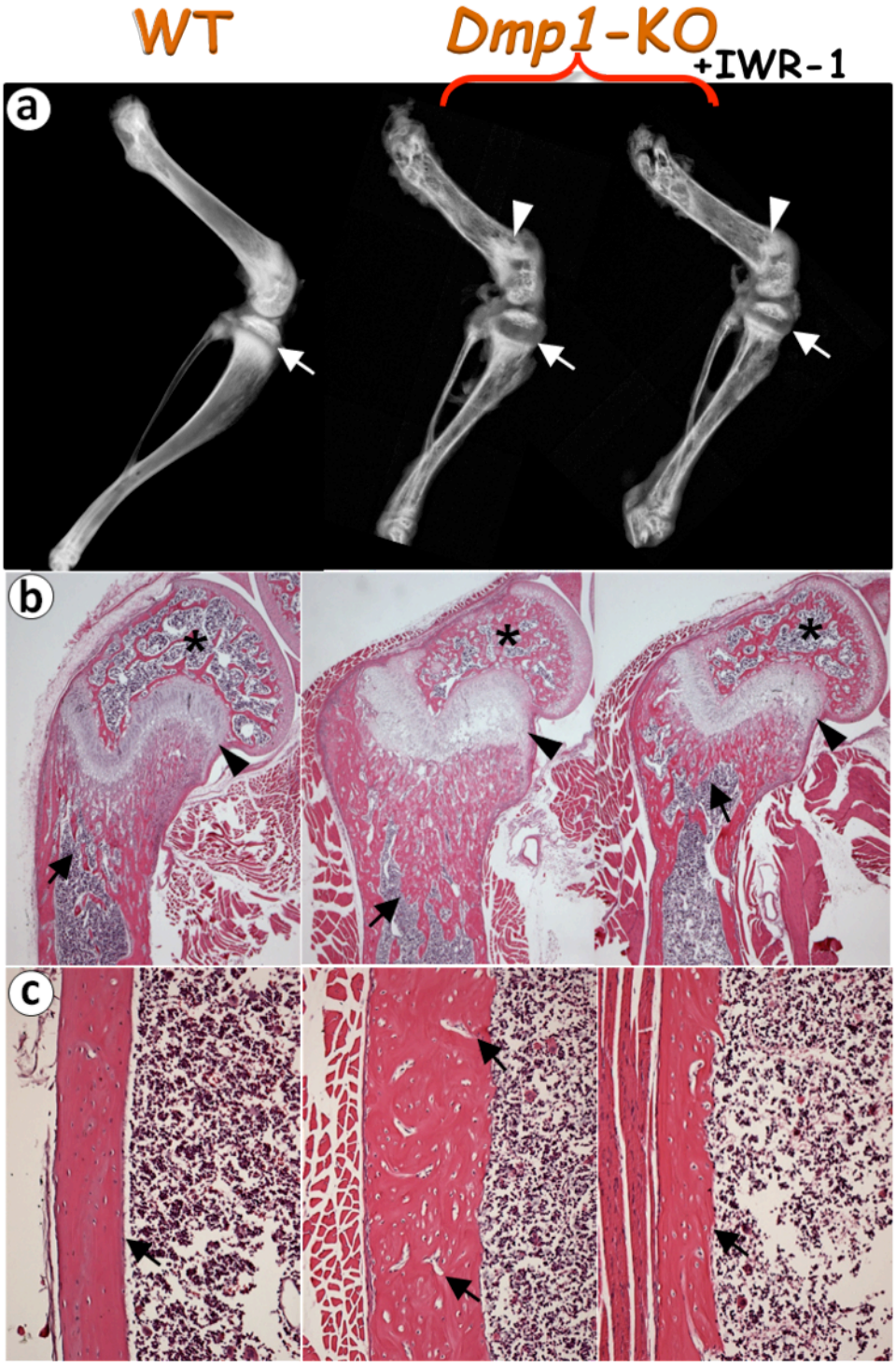


**Figure 4-11 Injection of anti-β-catenin compound drug improved the rickets/osteomalacia deficiency in *Dmp1*-null mice**. (**a**) Representative radiographs of mouse long bones. Both metaphysis (arrowheads) and growth plate (arrows) were partially rescued in the *Dmp1*-null

mice with IWR compound treatment. (**b-c**) Epiphyseal structure (asterisks), growth plate expansion (arrowheads), metaphyseal bone accumulations (arrows), bone porosity (**c**, arrows) are improved in the IWR-1 injected *Dmp1*-null mice.

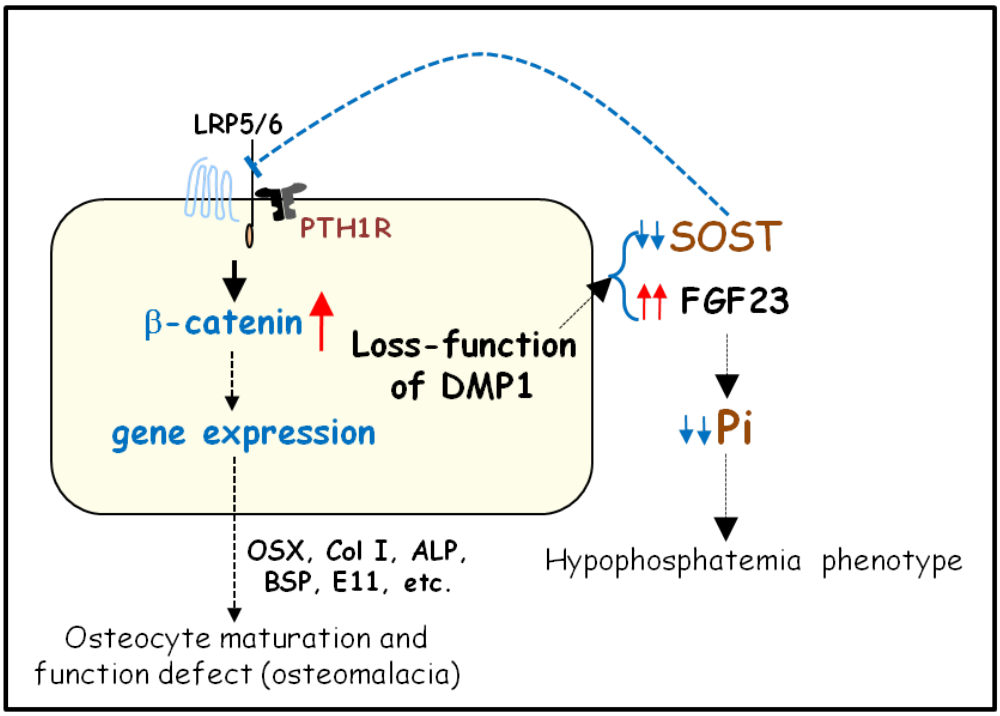


**Figure 4-12 The pathogenesis of the inherited hypophosphatemic rickets/osteomalacia in *Dmp1*-null or Hyp-mice.** The loss-function of DMP1 in *Dmp1*-null mice or *Hyp*-mice caused decreased SOST secretion, which leads to the constitutive stabilization of β-catenin in osteocytes. This ectopic Wnt/β-catenin signaling activity regulated bone-related gene expression, such as *Osx*, *Col I*, *Alp*, *Bsp*, *E11*, etc., affecting osteoblast-osteocyte transition and/or osteocyte maturation and bone mineralization. In contrast, the absence of functional DMP1 also led to the abnormal expression of FGF23, which was secreted from osteocytes and targeted the kidneys, leading to Pi waste and higher serum Pi, a major characteristic of hypophosphatemia.

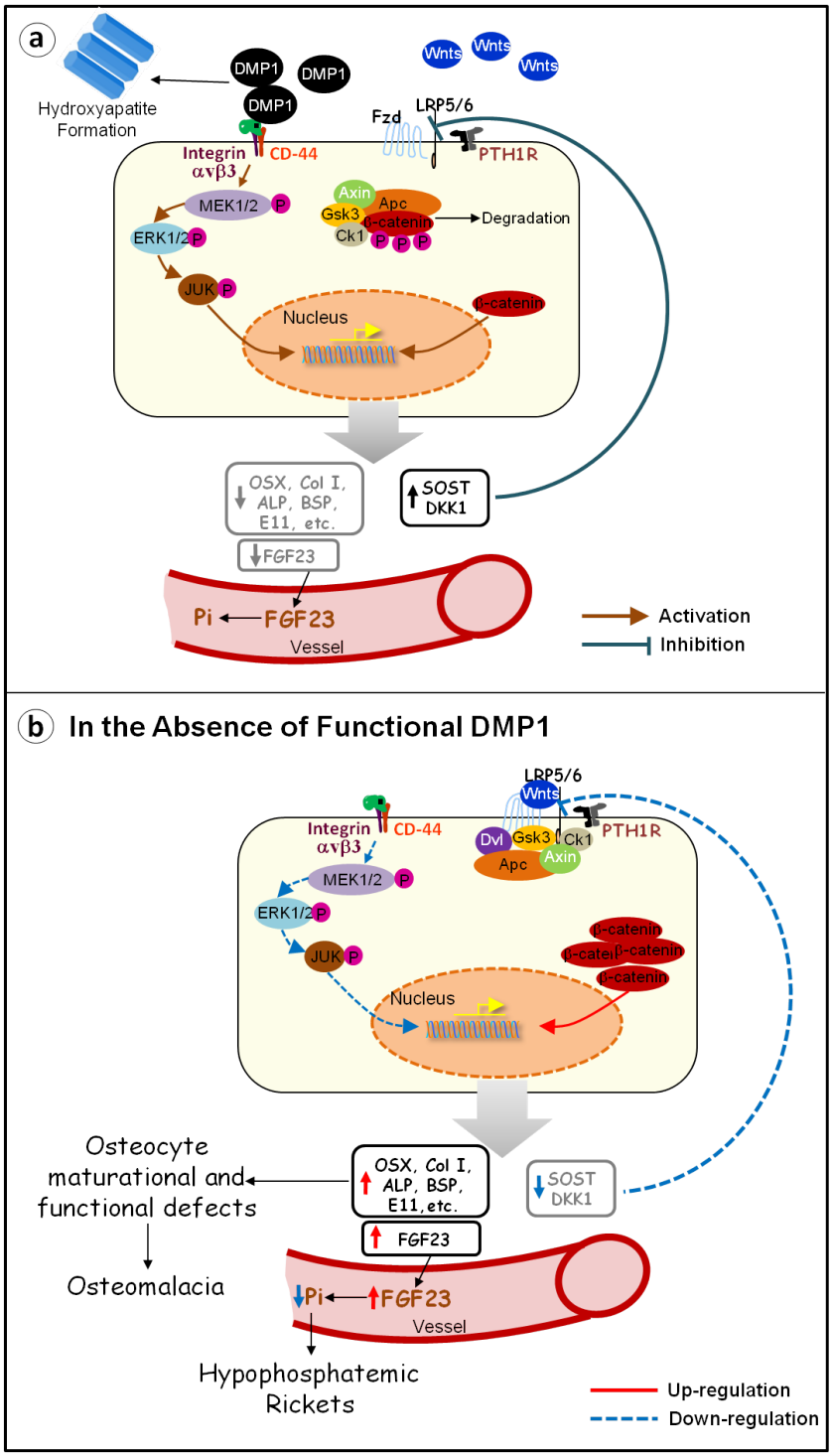


**Figure 5-1 Signaling pathways underlying the osteocyte maturation and function process that was regulated by DMP1.**

APPENDIX B

TABLES

**Table 1-1 Characteristics of ARHR patients and mice models**

| Aspects | | Characteristic Features |
|---|---|---|
| **Clinical manifest** | Figure | short stature or growth retardation |
| | Posture | waddling gait, immobilization of the spine, kyphosis |
| | Craniofacial | facial abnormalities, tooth abscesses or early loss |
| | Limb | genu varum or knock-knees |
| | Symptom | bone and muscle pain, joint pain, contracture, enthesopathy, nerve deafness, learning disabilities |
| **Skeletal dysplasia** | Craniofacial | enlarged dental pulp chambers and thin dentin, thick calvarium and skull base, skeletal malocclusion |
| | Spine | disappearance of intervertebral disks and disk space, ossification of the longitudinal ligament |
| | Jiont | loss of articular cartilage, narrowed joint space, osteophytes |
| | Limb | short, broad, bowing, ossification of tendon attachments, pathological bone fractures |
| | Chest | rachitic rosaries, narrow chest with wide clavicles |
| **Biochemistires** | Increase | FGF23, ALP |
| | Decrease | Pi, TmP/GFR |
| | Inappropriately low/Normal | $1,25(OH)_2D$, Ca, PTH |

**Table 2-1 Three independent lines and their DMP1 expressions**

| Line Number | mRNA Expression of DMP1 | Sex |
|---|---|---|
| 2095 | 6.27 | M |
| 2097 | 118.48 | M |
| 2098 | 4.96 | M |

**Table 2-2 RNA expression levels after transfection**

| | Control | $^{NLS}$DMP1 | $^{SP}$DMP1 | SF between $^{NLS}$DMP1 and $^{SP}$DMP1 |
|---|---|---|---|---|
| DMP1 | 1.046 ± 0.1137 | 3070 ± 137.5** | 2425 ± 248.1** | no |
| BSP | 1.092 ± 0.2434 | 2.677 ± 0.2557* | 12.92 ± 1.806** | P<0.01 |
| ALP | 0.9937 ± 0.01377 | 10.19 ± 0.8495** | 27.18 ± 2.597 ** | P<0.05 |
| OCN | 0.9516 ± 0.03122 | 0.3652 ± 0.05893** | 0.1613 ± 0.01589** | P<0.05 |
| OPN | 1.013 ± 0.1334 | 0.1744 ± 0.1205* | 0.1758 ± 0.1263* | no |
| DSPP | 0.6806 ± 0.07656 | 0.1062 ± 0.01353** | 0.1375 ± 0.09978** | no |
| SOST | 1.337 ± 0.07599 | 0.4026 ± 0.06791** | 0.2758 ± 0.04720** | no |

Values are expressed as mean ± SEM from at least 4 samples per group. Comparisons were performed using one-way ANOVA and post-hoc Fisher test. SP: Significant differences, P<0.05 vs:(*) control; P<0.01 vs:(**) control.

**Table 2-3 Bone Histomorphometry Findings in the femurs of 3-week-old mice**

| | HET | HET + $^{NLS}$DMP1 | KO | KO + $^{NLS}$DMP1 | KO + $^{SP}$DMP1 |
|---|---|---|---|---|---|
| Femur Length | 9.435 ± 0.1480 | 9.590 ± 0.1946 | 8.181 ± 0.1767** | 7.925 ± 0.3497** | 9.491 ± 0.2781 |
| Cross Section Area | 1.028 ± 0.09665 | 1.309 ± 0.08119 | 1.612 ± 0.08318** | 2.225 ± 0.1978** | 1.046 ± 0.09525 |
| TV ($mm^3$) | 0.1202 ± 0.008511 | 0.1984 ± 0.02817 | 0.3079 ± 0.08265 | 0.2834 ± 0.0114 | 0.1301 ± 0.01304 |
| BV ($mm^3$) | 0.1141 ± 0.007430 | 0.1747 ± 0.02520 | 0.1186 ± 0.007385 | 0.1454 ± 0.007223* | 0.1105 ± 0.01078 |
| BV/TV | 0.9507 ± 0.01180 | 0.8807 ± 0.01371 | 0.4625 ± 0.09633** | 0.5128 ± 0.01319** | 0.8512 ± 0.02071 |
| Cortical Porosity | 0.04933 ± 0.01180 | 0.1193 ± 0.01371 | 0.5375 ± 0.09633** | 0.4873 ± 0.01319** | 0.1489 ± 0.02071 |
| Ectopic BV ($mm^3$) | 0.007775 ± 0.0005662 | 0.02748 ± 0.002312** | 0.009975 ± 0.0002462* | 0.04603 ± 0.009238** | 0.0080 ± 0.003395 |

Values are expressed as mean ± SEM from at least 5 mice per group. Comparisons were performed using one-way ANOVA and post-hoc Fisher test. P<0.05 vs:(*) *Dmp1*+/-; P<0.01 vs:(**) *Dmp1*+/- of femur length, cross section area, TV, BV, BV/TV, cortical porosity. P<0.05 vs:(*) DMP1+/-; P<0.01 vs:(**) DMP1+/- of ectopic BV.

**Table 4-1 Hypophosphatemia phenotype in *Dmp1*-null mice was partially rescued by *Dkk1*-Tg.**

| | Phosphorus (mg/dL) | FGF23 (pg/mL) | Calcium (mg/dL) | PTH (pg/mL) |
|---|---|---|---|---|
| Control | 8.664 ± 0.9868 | 155.1 ± 18.55 | 9.820 ± 0.5148 | 42.07 ± 5.664 |
| CA-β | 6.964 ± 0.4852 | 196.1 ± 47.56 | 9.866 ± 0.5095 | 1485 ± 419.3 ** |
| Value are expressed as mean ± SEM from at 7 mouse per group. P<0.05 vs:(*) Control; P<0.01 vs:(**) Control. | | | | |
| WT | 14.43 ± 0.9822 | 160.8 ± 9.387 | 11.03 ± 0.4182 | 61.30 ± 17.72 |
| WT; DKK1-Tg | 15.31 ± 0.7880 | 215.8 ± 13.42 | 10.72 ± 0.5485 | 86.20 ± 21.14 |
| KO | 7.766 ± 0.4509 | 2781 ± 426.7 | 9.580 ± 0.4211 | 313.2 ± 41.46 |
| KO; DKK1-Tg | 9.455 ± 0.6110 | 1840 ± 233.4 | 10.84 ± 0.5536 | 170.7 ± 38.52 |
| Value are expressed as mean ± SEM from at 14 mouse per group. P<0.05 vs:(*) Control; P<0.01 vs:(**) *Dmp1* -KO. | | | | |
| WT | 11.24 ± 0.6448 | 196.1 ± 11.69 | 14.34 ± 1.540 | 34.75 ± 8.138 |
| WT; DKK1-Tg | 13.02 ± 0.4484 | 134.1 ± 19.55 | 15.92 ± 0.5091 | 24.88 ± 6.975 |
| Hyp | 6.197 ± 0.2412 | 1786 ± 264.5 | 12.01 ± 0.9157 | 68.00 ± 12.79 |
| Hyp; DKK1-Tg | 8.584 ± 0.4236 | 2362 ± 767.6 | 11.68 ± 0.7565 | 47.00 ± 16.22 |
| Value are expressed as mean ± SEM from at 5 mouse per group. P<0.05 vs:(*) Control; P<0.01 vs:(**) Hyp | | | | |